A NOVEL ELECTROCHEMICAL PLATFORM BASED ON SCREEN PRINTED CARBON ELECTRODES (SPCES) FOR MOLECULAR DIAGNOSTICS

Nihad Kamal Ibrahim Ahmed

Doctoral thesis

Nihad K.I. Ahmed

A novel electrochemical platform based on screen printed carbon electrodes (SPCEs) for molecular diagnostics

Supervised by Prof. Ioanis Katakis

Universitat Rovira i Virgilli

Nanoscience, materials, and chemical engineering PhD program

Department of chemical engineering

Interfibio research group

Tarragona, 2020

UNIVERSITAT ROVIRA I VIRGILI
A NOVEL ELECTROCHEMICAL PLATFORM BASED ON SCREEN PRINTED CARBON ELECTRODES (SPCES) FOR MOLECULAR DIAGNOSTICS
Nihad Kamal Ibrahim Ahmed

Doctoral thesis

Nihad K.I. Ahmed

A novel electrochemical platform based on screen printed carbon electrodes (SPCEs) for molecular diagnostics

Supervised by Prof. Ioanis Katakis

Universitat Rovira i Virgilli

Nanoscience, materials, and chemical engineering PhD program

Department of chemical engineering

Interfibio research group

Tarragona, 2020

UNIVERSITAT ROVIRA I VIRGILI
A NOVEL ELECTROCHEMICAL PLATFORM BASED ON SCREEN PRINTED CARBON ELECTRODES (SPCES) FOR MOLECULAR DIAGNOSTICS
Nihad Kamal Ibrahim Ahmed

I STATE that the present study, entitled “A novel electrochemical platform based on screen printed carbon electrodes (SPCEs) for molecular diagnostics”, presented by Nihad K. I. Ahmed for the award of the degree of Doctor, has been carried out under my supervision at the Department of chemical engineering of this university.

Tarragona, 2020

Doctoral Thesis Supervisor

Prof. Ioanis Katakis

[signature] [Name]

UNIVERSITAT ROVIRA I VIRGILI
A NOVEL ELECTROCHEMICAL PLATFORM BASED ON SCREEN PRINTED CARBON ELECTRODES (SPCES) FOR MOLECULAR DIAGNOSTICS
Nihad Kamal Ibrahim Ahmed

ACKNOWLEDGEMENT

I would like to express my sincere gratitude to my supervisor prof. Ioanis Katakis for his patience, continuous support, and motivation through the entire period of my PhD. I have learnt a lot through his supervision, I have polished my skills and gained new ones, but mostly I got to acknowledge the contribution of the scientific research to develop the community. It is not easy to become a productive personnel, and it is even difficult to incorporate the scientific research and studies into industrial and economic fields. I am acknowledging his huge capabilities as a researcher and a teacher. He taught me to put my heart and soul into my work to keep moving forward and advancing scientifically and personally.

To prof. Ciara O´Sullivan, the one person without her help and support I got from I wouldn't have this opportunity to have my PhD. To my lab mates and friends, Ivan, Xhensila, Zaida, Julio, Nassif, Sallam and Laura. To the interfibio group members specially Dr. Mayreli Ortiz one of the best people you can ever meet, and to organizers of the nanoscience, materials and chemical engineering PhD program specially Nuria. Thank you for your support and for making this very tough and hard time of my life easier. Special thanks to ministerio de economia industria y competitividad for the schoraship and funds.

Finally, to my mother and father the source of the pure and complete support through all my life, my sisters specially Riham the one who supported me with all what she is going through on her own PhD.

Table of contents

List of abbreviations

Abbreviation	Name
AuNPs	Gold nanoparticles
CA	Chronoamperometry
CDMI	N-cyclohexyl-N-(2-morpholinoethyl)-carbodiimide methyl-p-toluene-Sulfonate
CE	Counter electrode
CV	cyclic voltammetry
DCOOH	4-(N-Carboxymethyl sulfanyl) benzene diazonium hexafluorophosphate salt
DCl	4-chlorophenyl benzene diazonium hexafluorophosphate
DNA	Deoxy ribonucleic acid
DPV	differential pulse voltammetry
GCEs	Glassy carbon electrodes
HRP	Horseradish peroxidase
IUPAC	The International Union of Pure and Applied Chemistry
LOC	Lab on a chip
LOD	Limit of detection
LOQ	Limit of quantification
MD	Molecular diagnostics
PBS	Phosphate buffered saline
PCR	Polymerase chain reaction
PEG	Polyethylene glycol
PEGDE	Polyethylene glycol diglycidyl ether
PLL	Poly (L-Lysine) polymer
RE	Reference electrode
RPA	Recombinase polymerase amplification
SPEs	Screen printed electrodes
TMB	3,3’,5,5’-Tetramethylbenzidine
WE	Working electrode

List of tables

List of figures

SUMMARY

The objective of this work is to develop tools that enable low cost, point-of-use molecular diagnostics. An electrochemical platform based on screen printed microsystems was chosen for this purpose. The first step for the proof of concept of such devices is to ensure that screen printed carbon electrodes (SPCE) can be used as functional elements in the molecular diagnostics assay. This thesis focuses on methods to increase the reliability and reproducibility of screen-printed electrode-based molecular assays. For the proof of concept *Karlodinium armiger*, a toxic microalgae were used as target. Recombinase Polymerase Amplification (RPA), an isothermal amplification method, was chosen because it can be easily incorporated in portable, point-of-use devices. The most important problem encountered when using SPCE is the non-specific interactions of the components of the assay with the porous and irregular surface of the electrodes. Such interactions influence both the assay and the detection in unpredictable manner affecting the reliability of the results. We demonstrate that two methods can remedy to a large degree these problems: in the first approach electro-grafted carboxylated diazonium was linked covalently to the aminated DNA probes (recognition layer) on the SPCE surface. A chloride diazonium salt was used to block the non-specific adsorption of horseradish (HRP) labels that were used for detection. Surface modification was achieved by mixed layer electro-grafting performed for the primary carboxylated diazonium salt (DCOOH) and the back-filler secondary chloride diazonium salt (DCl). DNA hybridization and detection in both solid and liquid phase RPA formats reached detection limits (LOD) of 0.1 fM and 0.3 fM respectively. This approach requires wet chemistry and electrochemical activation of the electrodes during manufacturing, complicating production and increasing its cost.

Electrode surface modification by drop casting is a method more appropriate for large scale production. In the second approach the surface of SPCEs was modified with poly (L-Lysine) polymer crosslinked with polyethylene glycol diglycidyl ether (PEGDE) that also attached the aminated DNA probes (recognition layer). In this approach, treatment with PEG oligomers avoided the HRP non-specific adsorption. DNA hybridization and detection using solid phase RPA achieved LOD of 0.1 fM. The electrochemical detection for the developed system for dsDNA target was un-successful for liquid phase RPA amplification. And in order to be able to calculate the true LOD, a smaller concentration range target and dsDNA target should be performed in order to obtain the true LODs.

In a further refinement of the method, primers incorporating the HRP label were used streamlining the assay and reducing the number of steps requiring user intervention. The resulting biosensors were reproducible and selective allowing amplification and hybridization at the same time and achieving analysis times as short as twenty minutes from sample application to result readout. These approaches can form the basis of integrated screen-printed microsystems if the reagents can be dried and stored in these devices.

OBJECTIVES

Thesis objectives:

General objective:

To develop a generic electrochemical DNA-platform based on screen-printed carbon electrodes (SPCEs) for molecular diagnostics. This platform leads to cheap, available, fast, easy to use sensors, and can be easily adapted to the application.

To achieve this general objective, the following specific technical objectives have been set:

- To survey of methods for screen printed carbon electrodes (SPCEs) surface functionalization to achieve proof-of-concept of control of non-specific adsorption on the surface to allow reliable and reproducible DNA target detection when said target is labeled with horseradish peroxidase (HRP).

- To apply the most reliable configurations of surface modified SPEs for the isothermal amplification and detection of *karlodinium armiger* as an example of validation of the electrochemical platform.

- To advance in the integration of amplification and detection in a single device by demonstrating the feasibility of the on-line reconstitution of dried reagents and temperature control of the device.

CHAPTER I

INTRODUCTION

I. Integrated molecular diagnostic devices for the point-of-need

1.1.1. The need and requirements for integrated molecular diagnostics:

The term molecular diagnostics (MD) as used in this thesis refers to the detection (and ideally, quantification) of specific genetic material sequences or mutations in a complex sample. One might ask why in the era of next generation sequencing and its multiple applications and renditions as powerful and integrated instruments (see for example[1] for a recent comprehensive review) is necessary to investigate point-of-need devices. Although "cost" might come to mind as an answer (and cost is indeed a significant parameter) ease of use and rational utilization of resources is a more plausible answer: most impactful applications of molecular diagnostics do not require full sequencing capability but do require immediate results. Examples include pathogen detection for infectious disease control and treatment, food and water safety and quality assurance, antibiotic resistance detection, diagnosis of some cancers, and even some personalized medicine solutions. These applications comprise more than 80% of the bigger than $(US) 10 billion market of molecular diagnostics, a market that could be much bigger if MD could be applied at the point-of-need [2]. It is therefore desirable to make available MD devices at the point of need, not only because in some environments where resources are limited, but also because the very nature of the applications demand it.

For molecular diagnostics devices to reach the point of need, they must be integrated. For the purposes of this thesis an integrated MD device ideally should be able to carry out as many as possible of the unit operations needed for analysis without or with minimal user intervention: sample pretreatment and extraction of DNA, target amplification, labelling, hybridization, signal amplification, detection, and quality control should all be performed in a seamless sequence producing a result in a reasonable time (usually accepted to be less than 30 minutes). In this definition of "integration" several choices have been made: amplification of target has been assumed necessary as this provides generic applicability, hybridization has been assumed as the method of choice for detection as it is more convenient for miniaturization and detection without gels, labelling has been accepted since it provides signal amplification, more detection method choices and lower limit of detection. In addition, we will limit our discussion to integrated devices based on electrochemical detection because we believe it to provide more flexibility for the resulting configurations, very good detection limits, and simplicity in instrumentation. Many Lab-on-Chip (LOC) devices have been described (see for example[3] for a comprehensive review) that indeed are fully integrated. However, although a LOC device is usually the size of a credit card, normally it requires a more sophisticated, purpose-built instrument that is not only expensive, but also difficult to transport and usually not present when the need arises. Our ambition with this work was to facilitate the reduction to practice of a much more usable device requiring no instrumentation. To achieve this, the very first step of analysis (sample pretreatment and extraction of genetic material) can be excluded from integration since a cost/benefit analysis indicated that for most applications, simple easy to use kits can be applied without the need of any instrumentation providing a sample (a genetic material target) usually dissolved in an aqueous buffer.

To our knowledge, the work by Tsaloglou et al.[4] describes the only fully integrated electrochemical amplification/genosenosr device. It is realized by combining paper fluidics with screen printed carbon electrodes

(SPCE) as detectors of non-retained electrochemically active intercalators (or "electrophores"). Our research team has proposed a different platform that can be used for integrated molecular diagnostic devices. The device is reproduced in Figure (1.1) with the different functional and structural elements explained herein [5],[6]. Briefly, the platform delivers the extracted sample through capillary flow. It lends itself to MD device development due to the possibility to stop the flow using electrochemically activated superhydrophobic "valves" [7]. In a first "chamber" dried reagents are dissolved and amplification is given enough time for enough target copies to be created and labels to be introduced (valve 1 off). When this unit operation is completed, the valve is turned on and the amplified and labelled target (amplicon) enters a second chamber where it is hybridized on the detection surface (a screen-printed electrode) while valve 2 is off for hybridization to complete. Next, valve 2 opens and the sample flows to a third chamber where a second detection surface can be used for quality control of the assay (by capturing for example a control sequence). Finally, the captured amplicon(s) are detected (and ideally quantified) by applying a suitable electrochemical protocol on the detection and control surfaces.

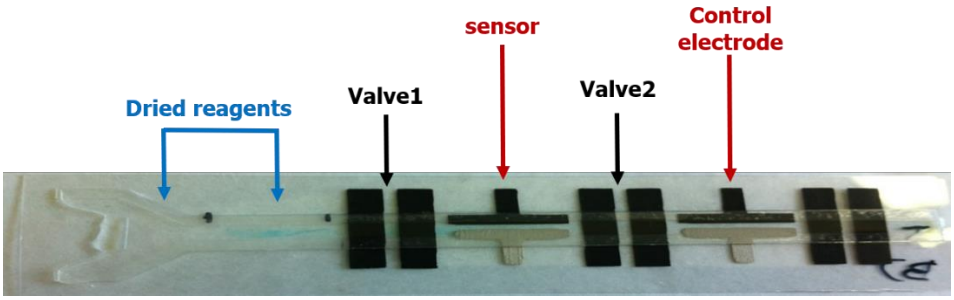

Figure (1.1): *Prototype of electrochemically operated screen-printed platform for integrated molecular diagnostics that is enabled in this thesis. Screen printed electrodes can be used as functional and structural (wall) elements defining a capillary microchannel. In this figure the walls are created by laminating a spacer and a transparent cover. Electrodes (grey as counter/reference and black as working) are printed in pairs. Grey/black pairs are sensing electrodes positioned on the walls of the capillary. Black pairs (traversing the capillary) act as electrochemically activated superhydrophobic valves.*

The important characteristic of this platform (and of interest for this thesis) is the fact that its manufacturing is also integrated: the whole device can be produced using screen printing and lamination, having previously modified electrodes and deposited reagents in the chambers. These processes are well known and optimized since they have been the production methods of choice for electrochemical biosensors in the last 30 years. For this thesis they pose the challenge to make sure that the electrochemical assays and detection can be reliably carried out on screen printed electrodes. For this reason, in the rest of this Introduction we examine in some detail the different components of the device and the unit operations that take place in it.

1.1.2. Screen printed electrodes (SPEs):

Printed electrochemical biosensors have been gaining interest and studied over years[8]. Combining the screen-printing technology with electrochemistry to develop electrochemical detection systems for DNA arrays on low cost

SPEs surfaces has been addressed for different applications. To build an electrochemical genosensors based on SPCEs the procedure has to be divided into different steps: immobilization, hybridization, labeling and detection[9],[10]. Some examples for different applications like environmental monitoring[11] and environmental protection[12],[13], point-of-care analysis[14],[15], food monitoring[16],[17],[18], and chemical and biological warfare protection and monitoring[19],[20]. Through all the electrochemical techniques, chronoamperomtery (CA) using horseradish peroxidase (HRP) and its substrate TMB provides more sensitivity compared with other electrochemical techniques like voltammetry[8].

An electrochemical DNA based senor for DNA damage detection has been developed using screen printed gold electrodes and AuNPs. The AuNPs have been immobilized on the gold surface by electrodeposition, and the thiolated DNA probes then attached[21]. For DNA quantification, different DNA based sensors have been developed. For example, an electrochemical sensor based on using aminated silica nanospheres on SPCEs and AuNPs. The aminated silica used to link the aminated DNA probes by covalent bonding using glutaraldehyde as a cross-linker, and the AuNPs used as a transducer. The developed DNA based sensor shows a linear range of 109–0.5 µM[22]. Another developed electrochemical DNA senor based on aminated silica nanospheres linked to aminated DNA probes and AuNPs and methylene blue as a redox indicator has been developed for carcinogens detection. The developed DNA sensor shows a linear range of 0.0005 to 0.01 ppm for cadmium (Cd) with a LOD of 0.0004 ppm[23]. Using the same described system, a DNA based electrochemical sensor for carcinogens detection in food samples. The LOD achieved was 0.0001 ppm, and a linear range of 0.0001 to 0.1 ppm[24].

A portable label free electrochemical DNA apta-sensor based on gold screen printed electrodes for *B. anthracis* detection has been developed achieving a linear range between 10^4 CFU/mLand 5×10^6 CFU/mL and a detection limit of 3×10^3 CFU/mL[25]. A reagentless electrochemical apta-sensor based on SPCEs was developed for tetracycline (TET) determination in water. The amino aptamer was immobilized on the SPCEs surface through a covalent bond showing a linear range of 0.05 µg/L to 20 µg/L, with a LOD of 0.035 µg/L[26]. A developed electrochemical DNA sensor based on DNA amplification for Ebola virus detection has been introduced. The fabrication steps were followed by the EIS, and the detection was achieved by the DPV achieving a LOD of 4.7 nM[27]. An impedimetric sensor based on SPCEs and AuNPs for *Citrus tristeza virus* quantification and detection has been reported achieving a linear range of 0.1-10 µM[28]. Fully printed system based on graphene oxide and AuNPs for DNA quantification and detection has been described, achieving a linear range of 0.01 to 20 µM[29]

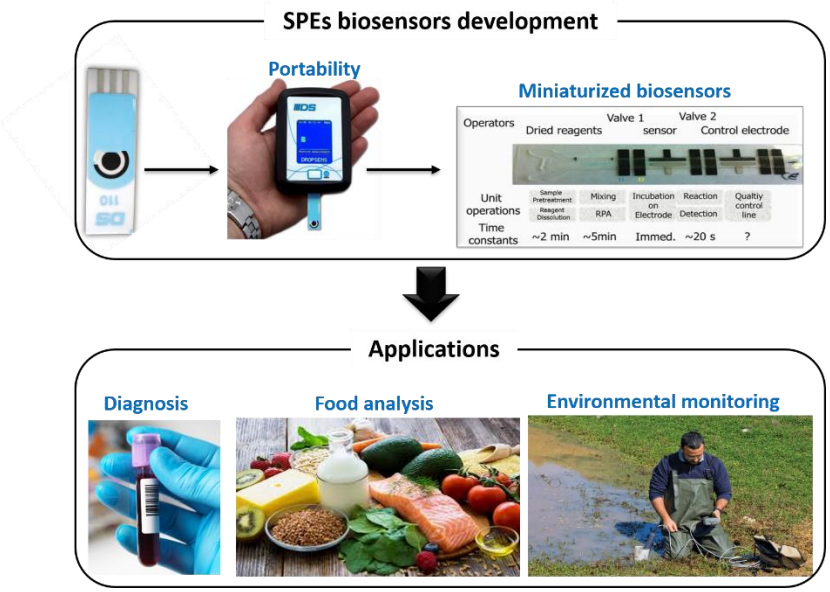

Figure (1.2): *Developed portable SPEs biosensors applications in molecular diagnostics, food industry, and environmental monitoring and protection*

1.1.3 Biosensors:

The International Union of Pure and Applied Chemistry (IUPAC) definition for the biosensor is an integrated analytical device for specific bio-analyte detection and monitoring. The detection of the analyte is through a bio-recognition layer which acts as the biological sensing element specific and selective for the analyte. The biosensor should perform with a reasonable limit of detection (LOD) for the analyte. The concept is to change the biological signal into an electrical signal using a transducer. Depending on the transducer type biosensors are classified as optical, electrochemical, thermal etc. The biological recognition layer is a molecule with high affinity and selectivity for the analyte such as an enzyme, protein, nucleic acid, antibody, ...etc. The type of the recognition layer is another biosensor classification scheme, for example enzyme-based sensors, tissue-based sensors, DNA biosensors. The biosensor as an analytical device can be joined with some separation techniques like high-performance liquid chromatography (HPLC) or sample and reagent injection systems like flow injection analysis (FIA). This HPLC or FIA system are part of the biosensor but are not considered as biosensors even if they contained some reagents reservoirs[30],[31],[32],[33].

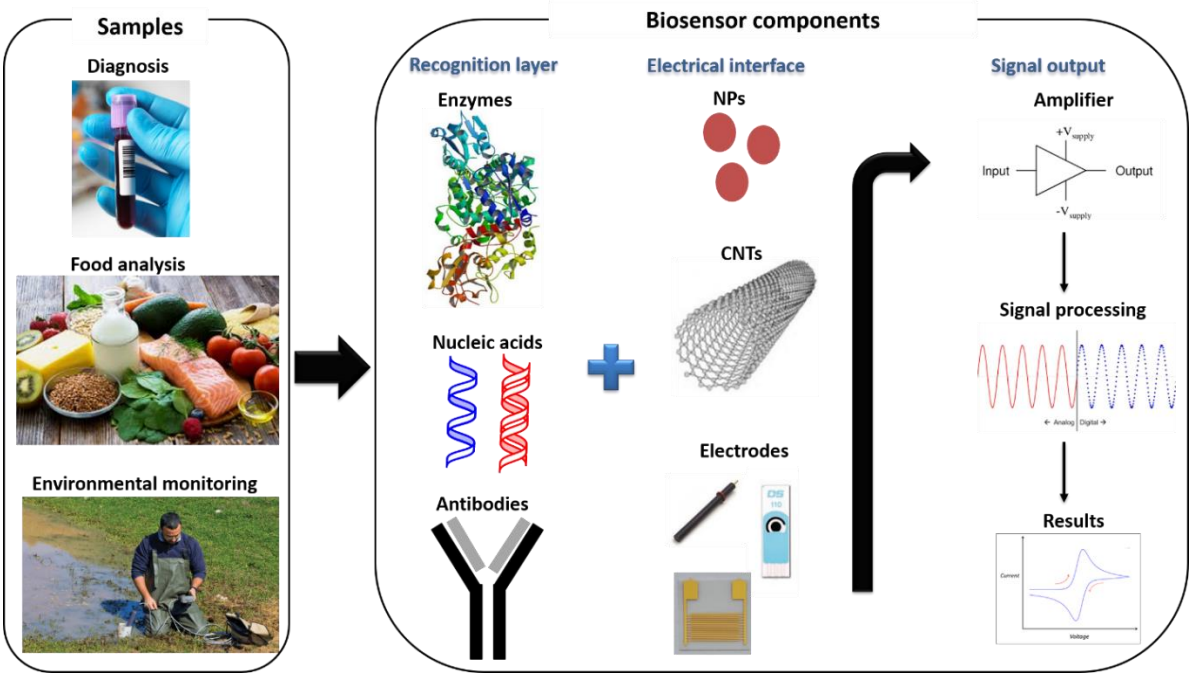

Figure (1.3): *Schematic representation of the biosensor components and signal processing. For different applications or sample types different recognition layers could be used. The electrical interface to transport and detect the changes in the solid-liquid interface where the analyte would be detected by the recognition layer*

- **DNA biosensors:**

The DNA based biosensors rely on the use of a nucleic acid sequence-DNA, RNA, or aptamer- as the recognition layer. The detection is achieved by the binding of the nucleic acid sequence to the complementary strand. The main uses of the DNA biosensors as a molecular diagnostic tool for pathogens infections, genomic disorders and diseases, biological warfare[34]. The DNA biosensor is constructed as any biosensor; immobilization of the recognition layer known as the capture probe. The immobilization achieved by different methods such as physical methods like adsorption, electrostatic interaction, hydrogen bonding etc. or via formation of chemical bonds using a cross-linker. Other modifications might be needed depending on the material of the biosensor, the detection indicator and the application. For instance, an antifouling agent should be used in order to use some electrochemical indicators to reduce the non-specific adsorption of this indicator on the surface[31].

- **Electrochemical biosensors:**

Electrochemical techniques are simple, and can be applied with relatively simple equipment which is the reason why they are extensively used[35]. Electrochemical techniques used for biosensors can be amperometric, potentiometric or impedimetric [34]. Most of the work undertaken in this thesis is based on chronoamperometry (CA).

As mentioned before, especially for affinity biosensors an electrochemical label allows the detection of the biorecognition event. In this thesis especially two electrochemical labels have been used:

1. Gold nanoparticles (AuNPs):

The importance of AuNPs is the ability for different functionalization with different biological molecules such as proteins, antibodies, and oligonucleotides for different biomedical applications. Besides they are stable, non-toxic, and a homogenous particle size profile can be achieved. They can be detected by monitoring changes in surface plasmon resonance (SPR), redox behavior (electrochemical detection), and conductivity when the analyte recognized by the functionalized AuNPs. Functionalization is achieved by using a thiolated biological molecule which is adsorbed on the Au surface to form a stable functionalized particle. AuNPs have been divided into three types: (i) one dimensional NPs like nanowires and nanotubes, (ii) two dimensional NPs like nanoplates, and (iii) three dimensional NPs like nanotadpoles and branched AuNPs like nanostars. The most used form of AuNPs is the spherical shape NPs because they are easy to synthesize. Due to their tunable optical properties with the particle size, AuNPs are widely used in drug delivery and theranostic. Several methods have been developed to synthesize AuNPs like physical method by irradiation, biological method or known as the green chemistry, but the most used method is the chemical method. Depends on the size, shape, and surface functionalization a chemical synthesis protocol can be adopted. For instance, reduction of hydrogen tetrachloroaurate ($HAuCl_4$) with citric acid in boiling water is used to produce AuNPs and by changing the gold/citrate ratio the size can be controlled. One disadvantage of using AuNPs is the irreversible aggregation after functionalization which can be avoided using a surfactant[36],[37],[38].

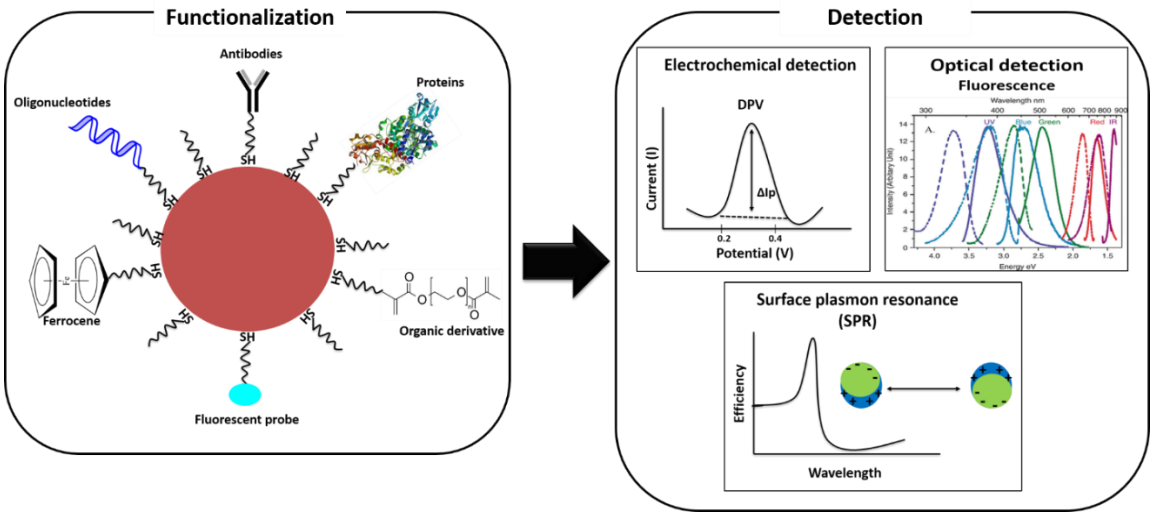

Figure (1.8): *Schematic representations for examples of AuNPs functionalization and detection. Different recognition layers could be attached to the AuNPs surface to detect different analytes*

2. Horseradish peroxidase (HRP):

Horseradish peroxidase is a single polypeptide of 308 amino acid residues originates in the horseradish plant roots. It´s structure contains proteins that contains a heme as a redox cofactor. The importance of the HRP in the biosensors its use as a reporter, where it catalyzes the substrate oxidation and hydrogen peroxide reduction reaction (redox reaction) which could be followed by the change in color. The intensity of the color is proportional to the amount of the analyte. In electrochemical biosensors the detection achieved by the addition and oxidation of a substrate by the HRP and peroxide reduction. 3,3',5,5'-Tetramethylbenzidine (TMB) is a typical substrate for HRP reporter oxidation reduction reaction[39],[40].

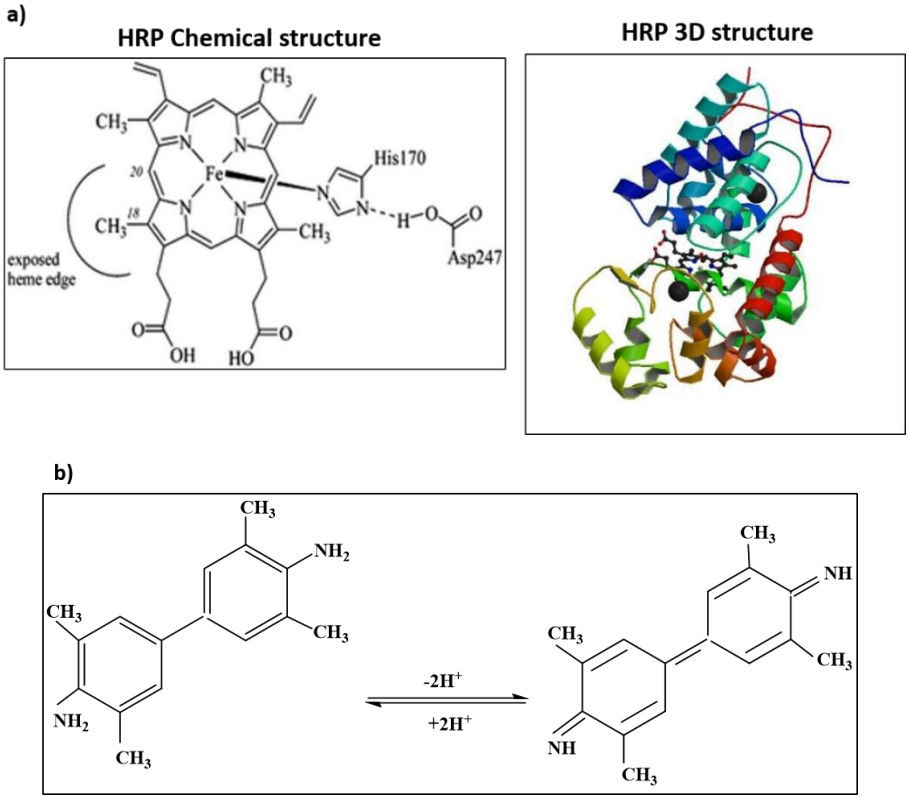

***Figure (1.9):** a)* Horseradish peroxidase chemical and 3D structures[39], b) TMB oxidation by the HRP

1.1.4 Screen printed electrochemical biosensors progress:

Electrochemistry provides rapid, cheap and easy to use technology for detection. Moreover, it could be used directly on fields for simultaneous detection especially at resources-limited environments[41]. Printed electrochemical biosensors have been gaining interest and studied over years[8]. Combining the screen-printing technology with electrochemistry to develop electrochemical detection systems for DNA arrays on low cost SPEs surfaces has been addressed for different applications. To build an electrochemical genosensors based on SPCEs the procedure has to be divided into different steps: immobilization, hybridization, labeling and detection[9],[10]. Some examples for different applications like environmental monitoring[11] and environmental protection[12],[13], point-of-care

analysis[14],[15], food monitoring[16],[17],[18], and chemical and biological warfare protection and monitoring[19],[20]. Through all the electrochemical techniques, chronoamperomtery (CA) using horseradish peroxidase (HRP) and its substrate TMB provides more sensitivity compared with other electrochemical techniques like voltammetry[8].

An electrochemical DNA based senor for DNA damage detection has been developed using screen printed gold electrodes and AuNPs. The AuNPs have been immobilized on the gold surface by electrodeposition, and the thiolated DNA probes then attached[21]. For DNA quantification, different DNA based sensors have been developed. For example, an electrochemical sensor based on using aminated silica nanospheres on SPCEs and AuNPs. The aminated silica used to link the aminated DNA probes by covalent bonding using glutaraldehyde as a cross-linker, and the AuNPs used as a transducer. The developed DNA based sensor shows a linear range of 109–0.5 µM[22]. Another developed electrochemical DNA senor based on aminated silica nanospheres linked to aminated DNA probes and AuNPs and methylene blue as a redox indicator has been developed for carcinogens detection. The developed DNA sensor shows a linear range of 0.0005 to 0.01 ppm for cadmium (Cd) with a LOD of 0.0004 ppm[23]. Using the same described system, a DNA based electrochemical sensor for carcinogens detection in food samples. The LOD achieved was 0.0001 ppm, and a linear range of 0.0001 to 0.1 ppm[24].

A portable label free electrochemical DNA apta-sensor based on gold screen printed electrodes for *B. anthracis* detection has been developed achieving a linear range between 10^4 CFU/mL and 5×10^6 CFU/mL and a detection limit of 3×10^3 CFU/mL[25]. A reagentless electrochemical apta-sensor based on SPEs was developed for tetracycline (TET) determination in water. The amino aptamer was immobilized on the SPEs surface through a covalent bond showing a linear range of 0.05 µg/L to 20 µg/L, with a LOD of 0.035 µg/L[26]. A developed electrochemical DNA sensor based on DNA amplification for Ebola virus detection has been introduced. The fabrication steps were followed by the EIS, and the detection was achieved by the DPV achieving a LOD of 4.7 nM[27]. An impedimetric sensor based on SPEs and AuNPs for *Citrus tristeza virus* quantification and detection has been reported achieving a linear range of 0.1-10 µM[28]. Fully printed system based on graphene oxide and AuNPs for DNA quantification and detection has been described, achieving a linear range of 0.01 to 20 µM[29].

1.1.5. Reagentless electrochemical biosensors devices:

Reagentless electrochemical DNA biosensors for DNA detection have been early described. For example, the reagentless transduction for DNA hybridization and detection using DNA capture probes labelled with ferrocene. The electron transfer changes due to the hybridization on the Au electrode surface, could be monitored and detected electrochemically[42],[43],[29]. Different reagentless electrochemical DNA sensors were described and reported in literature for different analytes such as for glucose determination in diabetes[44], human immunodeficiency virus (HIV)detection[45], genetic biomarkers[46]. Besides nucleic acids, other reagentless DNA biosensors have been developed for protein and small molecules detection for diagnostics and environmental analysis[47],[48]. Paper

based reagentless electrochemical devices for clinical, pharmaceutical, food analysis, and forensic applications were described as low-cost analytical tools[49],[50]. The first reagentless label-free electrochemical device for multiplex DNA amplification and detection has been described by M. Cooper et.al. They have developed a multiplexed assay that can amplify and detect an analyte in the whole blood[51]. A self-powered reagentless electrochemical biosensor has been reported by Wolfgang Schuhmann in 2017[52].

II. DNA amplification methods

As mentioned previously, the first step in the MD assay is the amplification of genetic material, obligatory in most applications due to the low number of target copies present in the sample or the very low LOD obliged by regulations or pathogenicity. Amplification also gives the opportunity to introduce labels in the amplicons and thus facilitate detection. For the platform introduced in Figure (1.1) the preferred amplification method is isothermal, however in what follows we give a general introduction on amplification methods. The polymerase chain reaction (PCR) has been the prevalent amplification method in molecular biology and molecular diagnostics. PCR is a rapid and robust amplification method for a specific DNA sequence, first reported by Mullis in 1990 for DNA amplification and detection. PCR is relying on cycles, where the number of DNA copies is doubled each cycle. Therefore, a thermo-cycler is used to cycle the temperature needed for denaturation of the double strand DNA sequence, annealing, amplification and copying using PCR primers, and then repeat the cycle again. The primers are specific DNA single stranded short sequences that can attach to the strand depending on the complementary sequence. At least one set of primers could be used for amplification, a forward primer and a reverse primer where they attached at the annealing stage[53]. A polymerase enzyme and deoxyribonucleotide triphosphate (dNTP) should be added for the PCR to take place, the polymerase facilitates the primers extension process by adding the dNTP that is complementary to the one in the original strand[54]. There are many different types of polymerases the most common one is the thermostable Taq polymerase[55]. Since then PCR is widely used as a tool for medical diagnosis and warfare diagnosis[56][57], food analysis[58], environmental monitoring[59][60]etc. Due to the need for trained personnel and a thermocycler, PCR is difficult to be envisioned in a point-of-need device as described above.

Due to these limitations of PCR, extensive research has taken place to develop isothermal amplification methods. Recombinase polymerase amplification (RPA) is a single tube isothermal reaction developed as an alternative to polymerase chain reaction (PCR) amplification. The RPA reaction has been firstly reported in 2006 by O. Piepenburg et al. along with a developed assay for amplified DNA detection[61]. The RPA kit is commercially available from TwistDx company (www.twistdx.co.uk), both in solution and dried form. The kit contains a rehydration buffer, magnesium acetate (Mgacet), dNTPs, and polymerase. In the solution form each reagent should be added individually, but for the dried form the polymerase, high molecular weight polyethylene glycol, binding proteins are dried in as a small solid pellet. The process is the same as in the PCR except for the need of a thermocycler, there is no need for temperature cycling since it is an isothermal reaction. The primers should be added, the recombinase protein interacts with the primers which facilitates the attachment to the complementary sequences in the template. Due to this interaction between the recombinase protein and the primers, the reaction is isothermal. The primers used for RPA could be the same for PCR or could be designed specifically for RPA. The optimum primers length is 30-35 bases but shorter primers have been reported to work efficiently [62][63] while longer primers tend to secondary products and primers artifacts[64]. RPA works at temperatures ranging from 22OC to 45OC, and in some cases there is no need for heating element or temperature control system[65]. In other cases different

temperature controlling devices were reported such as body heat[66] and chemical heaters[67]. The high molecular weight polyethylene glycol which is considered as a crowding agent, stabilizes the recombinase-primer complex[64]. The RPA reaction time varies for most of the reported assays, while the optimum time is 25 min to consume all the reagents, reactions as fast as 4 min were reported[68]. RPA reaction can be performed in two different ways:

(i) Solution-phase where the primers and the RPA components are mixed in one tube and incubated for the time needed to reach the amplification saturation (figure 1.10). This is the better approach because lower LOD can be achieved as well as faster reaction time till saturation. The amplification detection and analysis are mainly done by gel electrophoresis, but electrochemistry is widely used due to its sensitivity and time-efficient analysis. The electrochemical approach relies on a tail in the amplified target that is complementary to a capture probe immobilized on a solid support. The interaction between these complementary probes could be detected electrochemically depending on the electrochemical indicator used. Some examples are using chronocoulometry for horseradish peroxidase (HRP), differential pulse voltammetry (DPV) or square wave voltammetry (SWV) for AuNps.

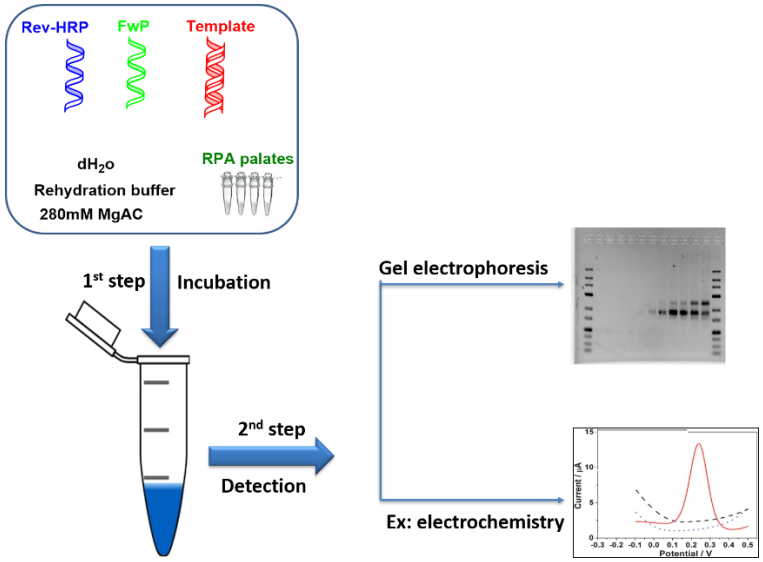

Figure (1.10): *Solution-phase RPA process where the two primers will be added to the RPA mixture and incubated for a specific time to achieve the isothermal amplification*

(ii) Solid phase where one of the primers immobilized on a solid substrate then a mixture of the other primer and the RPA components are incubated for the time needed to reach the amplification saturation. This approach provides the capacity of simultaneous detection and facilitates multiplex assays. The detection techniques can be colorimetry and electrochemistry (figure 1.11).

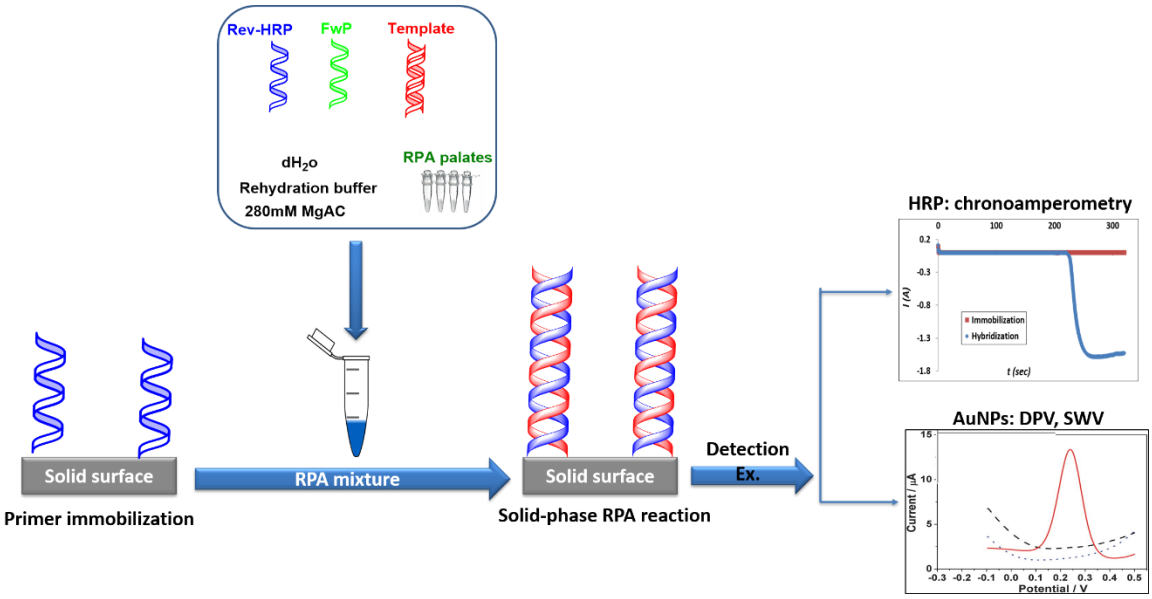

Figure (1.11): *Solid-phase RPA process where one of the primers will be immobilized on a solid support and then incubated with the RPA mixture for a specific time to achieve the isothermal amplification*

Recombinase polymerase amplification (RPA) is a promising tool for multi-pathogen detection in environmental monitoring[69],[70], food safety[71],[72] and clinical testing and diagnostics[73],[74]. RPA is a DNA amplification method at room temperature with no need for a thermo cycler like PCR. It is easy and fast to be performed-one tube reaction- by mixing the primers, pellet which contains the enzymes required for amplification, magnesium acetate, and the target. Solid-phase RPA provides the ease of fabrication of point-of-care devices for molecular diagnostics such as microfluidic devices[75]. The strategy mainly relies on the immobilization of one of the primers on a surface. The RPA mixture is added to the surface where the primer has been immobilized. After the enzymatic reaction the template is amplified on the surface where it could be easily detected[76]. RPA was demonstrated to ease the fabrication of an electrochemical paper-based device[77]. The device is low-cost, portable and was applied in a resource-limited environment. Also, RPA shows the capabilities for multiplex detection as reported[78],[79]. A lap-on-chip device has been developed for target amplification of Neisseria gonorrhoeae, Salmonella enterica and methicillin-resistant Staphylococcus aureus (MRSA) using genomic DNA. The detection achieved by labeling the reverse primer by a fluorophore[78].

Zachary Crannell et.al, introduced the first lateral flow system based on multiplex RPA for Giardia, Cryptosporidium, and Entamoeba at 37^{O}C in 35 min. They used a biotinylated reverse primer with fluorescence labelled DNA probe for the Entamoeba, Alexa Fluor 488 for Giardia, and digoxigenin for Cryptosporidium. These fluorophores chosen because of their low cost and availability to mark the DNA probes. The LOD using genomic DNA for 444, 6, and 9 parasites for Giardia, Cryptosporidium, and Entamoeba respectively. The signal to background ratio was higher by 1.5 order of magnitude than the singlet detection[80].

A centrifugal micro-device based on RPA used for multiplex and real-time detection of three food poisoning bacteria in milk (Salmonella enterica, Escherichia coli and Vibrio parahaemolyticus) is demonstrated by Goro Choi et.al. The multiplexing performed by running twelve RPA reactions simultaneously in four different chambers; at 39^{O}C for 30min. The sensitivity was 4 cells per 3.2 µL of milk sample; and detecting by collecting the fluorescence signals. Some limitations and disadvantageous were incorporate with this device including the complexity of the design. The need for the custom portable genetic analyzer with miniaturized optical detector is essential for the detection, is another drawback which increases the cost. Besides, the temperature and the rotation profiles controlled by a specific software developed in-house[81].

The use of the DVDs-based micro-fluidic device for gene detection has been demonstrated. Microfluidic channels constructed to introduce the RPA reagents and the samples; using immobilized biotinylated primers on streptavidin modified micro-well. The device has the capability to detect five different genomic sequences, by introducing 18 samples in 90 parallel reactions. When the sample was introduced through the inlet, it separated to five different compartments, one compartment per each genomic sequence. The solid phase RPA is bridge amplification approach, takes place in 45 min at 37^{O}C with a LOD of 48.7 fg of DNA. This device shows high multiplexing capability, no cross contamination, no primer interference, and less handling. However, bridge amplification has less analytical performance than the normal solid phase amplification[82].

RPA as a point-of-care tool described by Han Yih Lau at.al, to detect plants pathogens (*Botrytis cinerea*, *Pseudomonas syringae*, and *Fusarium oxysporum*). Multiplex RPA-at 37^{O}C in 20 min- integrated with surface enhanced Raman spectroscopy (SERS) as the detection system. Biotinylated primers for RPA, Raman reporter molecules, AuNPs core and complementary DNA capture probes for the RPA amplicons will form a product composed of biotin/RPA/SERS which will attached to the streptavidin magnetic beads. The LOD reached was as low as 2 copies for B. cinerea, and the method is fast and sensitive[83]. Another SERS detection system example is DNA/RNA biomarkers detection; prostate cancer detection addressed by Jing Wang et.al. They opt to use RT-RPA at 41°C for 15 min. They achieved 39% specificity, 59.3% sensitivity, and 94.2% accuracy[83]. Also, a new method was developed to detect five RNAs biomarkers in tumor and urine. The system is based on RT-RPA and uses SERS as the detection system. The assay takes place in 80 min achieving a sensitivity of 200 ƶmol (100 copies)[84].

Micro RNAs are a new class of biomarkers especially for cancer. Due to the short length of these miRNA-20 bases-, the detection is mainly based on PCR where the length would be manipulated and increased by introduction of some modified PCR reagents. A new method for multiplex detection based on RPA for miRNAs was described. The ligation of the RNA template achieved by PBCV-1 DNA ligase for better performance. The time-to-results is 30 min compare to 2 h when using PCR with portable fluorimeter[85].

A new approach to detect DNA from antibiotic resistant bacteria (Klebsiella pneumoniae NCTC13443 (blaCTX-M-15 positive)) in human urine samples was demonstrated. The method is based on RPA for probes amplification at 39^{O}C

in 40 min with LOD of 1000 bacteria in 1 mL urine. The work presents a new protocol for bacteria lysis, DNA pre-concentration protocol in 3.5 min, and then amplify the extracted DNA using RPA[86].

RPA assay for porcine circovirus 2 (PCV-2) in 20 min at 38^{O}C with 103 copies LOD has been reported[87]. Eid C et.al, integrated RPA with rapid cell lysis and isotachophoresis (ITP) to test the performance of their constructed ITP extraction unit. The procedure used for L. monocytogenes detection in whole blood with 2x10^{4} cells/mL LOD in 40 min at 41^{O}C. An Indium-Tin oxide (ITO) heater used to maintain the temperature profile homogenous for the RPA[88]. Another example for PCV-2 detection is the work presented by Yang Yang et.al. the work is based on RPA at 37^{O}C in less than 20 min integrated with lateral flow dipstick. The sensitivity and the LOD are 102 copies/reaction[89].

RPA as an amplification system for multiple targets for multiple cancer fusion genes RNAs detection in urine samples was demonstrated. The analysis time is 60 min with 2 amoL (1000 copies) LOD for non-invasive multiple variants of TMPRSS2: ERG fusion gene mutations in prostate cancer (PCa), using RPA at 37^{O}C for 15 min[90]. Another one step RNA amplification and detection system were proposed by Bonhan Koo et.al. the system is based on reverse transcriptase RNA amplification and detection using real time RPA-at 43^{O}C- on bio-optical sensor for label-free detection of viral RNA in <20 min; achieving a LOD 10 times lower than the real time reverse transcriptase PCR assay[91].

All above mentioned developed sensors and devices based on RPA isothermal amplification are either laboratory devices, not cost efficient, or not very compatible for resource limited environments. Hence, there is a need for a miniaturized lap-on-chip microfluidic device for molecular diagnostics for resource limited environments. The novelty of the device is the ability for functionalization depends on the needs. By changing the DNA sequence of the recognition layer, different analytes could be detected. This even could be incorporated in one microfluidic device as a multiplex detection.

III. Modification of SPEs surface

The central objective of this thesis is to facilitate the detection of the amplicons on SPEs in the second and third chambers of the MD platform described in Figure (1.1) The problem that all such devices must solve is common: if amplification and hybridization are segregated, the amplicon must be presented to the probe as single stranded DNA (ssDNA) that must be created in the device. We have proposed a "tailed primer" approach that obviates the need for ssDNA production [92] To lower manufacturing costs and simplify the assay SPEs should be used as both functional and detection elements in such devices. This requires that the SPE surface be reproducible, and that non-specific adsorption (of reagents and labels) be avoided. It should be noted, that in the vast majority of applications of SPEs in DNA sensors, the electrode is used simply as a detector and not as a functional part of the assay; for this reason, non-specific phenomena are not critical for other authors, but in our system this aspect is critical. In this sense it is useful to review the most promising methods that have been used to modify and improve the reproducibility of SPEs.

1.3.1. Diazonium salt-based functionalization:

Diazonium salts are a large group of organic compounds with a formula R-N≡N^+-X^- where R is any alkyl or aryl and X is any organic or inorganic anion. The aryl diazoniums are important as intermediates in different organic synthesis for various compounds [93]. They are prepared by the reduction of the corresponding amine in cold (0^OC) solutions using nitrous acid[94]. The elimination of the positively charge N_2^+ is mainly achieved through Meerwein and Sandmeyer reactions[95].

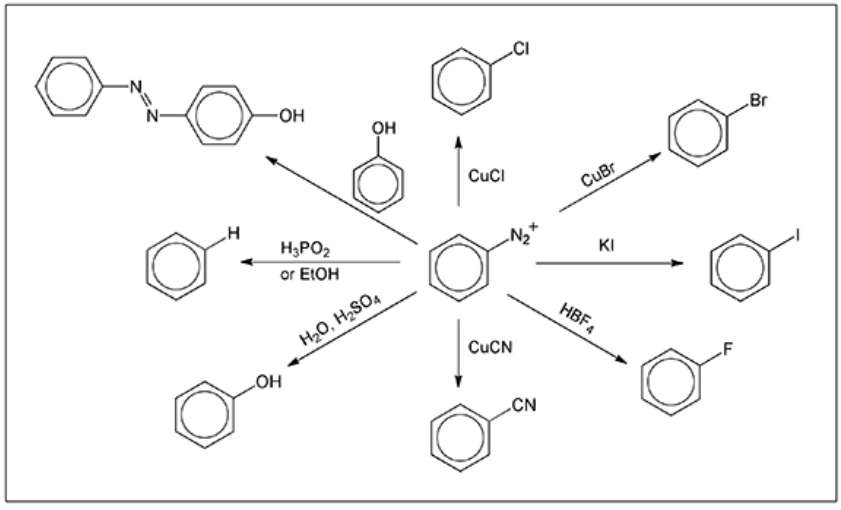

Figure (1.12): *Aryl diazonium salts reactions*[94]

Diazonium grafting and electro-grafting:

The ability of diazonium compounds to be used surface functionalization made them popular. The grafting of these molecules on any solid surface can be done spontaneously[96],[97], electrochemically[98],[99], or though physical methods[100],[101]. This grafting has been widely used in coating by linking bio molecules, polymers, and nano-particles[95]. Figure (1.13) explains the process of diazonium preparation, reduction, and grafting on a solid support. The reduction step which is the pre-grafting step could be done through wet chemistry or electrochemically by applying the reduction potential for the $-N_2^+$ using electrochemical polarization, or by scanning the potential using cyclic voltammetry (CV). The reduction forms a free radical that is highly reactive to another free radical, which is the solid surface.

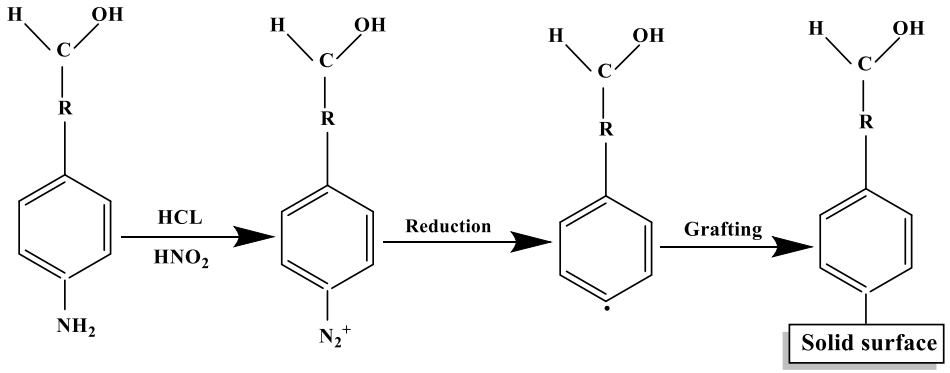

Figure (1.13): *Diazonium reduction and grafting on solid support, R is any functional group*

In-situ generation and electro-grafting for diazonium salts on SPEs for trace Pb (II) detection for environmental monitoring has been described by S. Bouden et.al. The interference studies show no major effect from Cu (II), Hg (II), Al (III), Mn (II), Zn (II), and Cd (II); with LOD $1.2x10^{-9}$ M and a LOQ $4.1x10^{-9}$ M[12].

The electrochemical and chemical parameters for diazonium electro-grafting on SPEs surface for Cu (II) detection has been investigated and reported by S. Bouden et.al. They concluded that the optimum conditions for Cu (II) detection are 5mM diazonium salt concentration, the applied potential is -0.6V/SCE for 300 s at 20^{O}C; with LOD 1.4 nM and LOQ 4.7 nM. the conditions reported produce multilayers not a mono layer on the surface, and the authors claim that as more layers being grafted as less signal-reduced signal-recorded for Cu (II). They explain this by the blocking of the pinholes that facilitate the Cu (II) to diffuse to the immobilized carboxylic groups[102].

Another example is the impedimetric apta sensor for on-site Orchratoxin A in cocoa beans detection has been developed by R.K. Mishra, et.al. The system is based on electro-grafting the diazonium on the SPEs surface, and then coupling the aminated ssDNA via EDC/NHS reaction. The diazotation achieved in-situ to electro-graft 4-carboxyphenyl diazonium salt. The sensor is stable, reproducible, and selective with a LOD of 0.15 ng/mL[16]. An electrochemical

apta sensor based on diazonium electro-grafting has been developed for ubiquitous protein Lysozyme (Lys). Two aptamers have been used for comparison, COX and TRAN; the linear ranges obtained 0.1-0.8 µM for Apt COX and 0.025-0.8 µM for Apt TRANS[103].

Aryl diazonium and aryl diazonium derivatives have been widely used due to versatility for functional groups moieties[41]. The diazonium could be generated in-situ for mono or mixed layers, and the surface functionalization could be achieved via spontaneous grafting[104]. Another approach is to use electro-grafting which is faster and easier, besides it provides uniform layers[104],[105]. The ability of the SPEs to be functionalized with the diazonium and link the DNA to generate a geno-sensor has been demonstrated[106]. Different parameters should be optimized like the density of the aryl diazonium layer and time for deposition[102],[107].

A label free electrochemical immunosensor was described by S. A. Lim et.al, the sensor is built for porcine serum albumin detection (PSA). 4-carboxyphenyl diazonium salt reduced electrochemically on carbon nano-fiber modified electrode SPCEs; and EDC/NHS chemistry to link the antibody. The sensor shows reproducibility and specificity; and a linear dynamic range from 0.5-500 pg/mL, with a LOD 0.5 pg/mL [14]. Another label free impedimetric electrochemical sensor for Aflatoxin B1 (AFB1) detection in alcoholic beverages has been introduced. Two aptamer sequences were used to identify and detect the AFB1 by diazonium salt electro-grafting on the surface of the SPCEs. EDC/NHS chemistry was used to attach the two aptamer sequences to the immobilized diazonium layer; then the incubation with the AFB1 for detection and quantification. The quantification range for the two sequences is from 0.125-16 ng/mL; with a LOD 0.12 and 0.25 ng/mL [17]. For Aflatoxin M1 (AFM1) detection in milk another apta sensor impedimetric electrochemical sensor introduced by G. Istmboulie. The immobilization of the aptamer on the SPCEs surface achieved after diazonium salt electro-grafted and activated by EDC/NHS chemistry. The LOD 1.15 ng/L with a linear range from 2-150 ng/L; using milk concentrations from 20 up to 1000 ng/kg[18]. Binding a macrocyclic ligand on the SPCEs surface has been achieved by J.P. Jasmin et.al, by the electro-grafting of in-situ generated diazonium salt on the surface. The macrocyclic ligand used is 1,4,8,11-tetraazacyclotetradecane (cyclam), for electrochemical detection of trace Cu (II) with a LOD $1.3x10^{-8}$ M, and a LOQ $4.0x10^{-8}$ M[108]. An electrochemical apta sensor for anti-Ochratoxin A (OTA) detection in cocoa samples has been described; the anti-Ochratoxin A (OTA) tagged with methylene Blue (MB). Diazonium salts electro-grafting propose as one of the several methods for aptamer immobilization. The sensor shows a linear range from 0.01-5 ng/mL, with a LOD 0.01ng/mL and a LOQ 0.03 ng/mL[109]. Modified SPEs with reduced graphene oxide (rGO) demonstrated as an electrochemical immunosensor for multiplex detection of gherlin (GHRL) and peptide (PYY) hormones. The method is based on electro-grafting the diazonium salt, and then coupling the corresponding anti-body using EDC/NHS. The linear current vs the log of the hormone concentration is from 10^{-3}- 100 ng/mL for the GHRL and for PYY from 10^{-4}-10 ng/mL. the LODs obtained are for RHL 1.0 pg.ml and 0.02 pg/mL for PYY[15].

A sensor for Pb detection based on AgNPs was introduced by J.P. Jasmin et.al, the surface of the SPEs was functionalized through multiple steps to detect the Pb (II). The use of the electro-grafted diazonium layer is crucial to bond AuNPs, then another electro-grafting step for carboxylic moieties to capture the Pb (II)[13]. In-situ generation

of aryl diazonium salt and electro-grafting on the surface of SPEs modified with selenocystine (SeCyst-SPCNFE) for Pb (II) and Cd (II) electrochemical detection. The coupling between the aryl diazonium and the selenocystine has been achieved by the EDC/NHS reaction. The SeCyst-SPCNFE system compared to the previously develop system for the same purpose i.e. SPEs modified with L-Cystine (Cyst-SPCNFE); and SeCyst-SPCNFE shows better response; i.e. less LODs obtained by using SeCyst-SPCNFE compare to Cyst-SPCNFE[110]. The first electrochemical sensor for Mucin 4 (MUC 4) detection-a biomarker for pancreas, esophagus and breast cancers-has been described by O. Hosu et.al. The system is based on in-situ generation and electro-chemical grafting of aryl diazonium salt, and by EDC/NHS chemistry the corresponding antibody attached to the modified SPCEs surface. The method showed a linear range from 1-15 µg/mL and a LOD 0.33 µg/mL[111].

1.3.2. Poly (L-Lysine) polymer (PLL)-based functionalization:

Poly lysine is a very interesting molecule due to its biocompatibility, thus it has been used for gene and drug delivery[112] and coatings[113]. Two methods for poly lysine synthesis have been described by Aesculap AG et.al, because it cannot be prepared from direct polymerization of lysine[114], or it can be produced by basic polycondensation reaction[115]. PLL is a cationic polymer, i.e. positively charged contains one primary and one secondary amine. It can be produced naturally by a specific bacterial strain that belongs to *Streptomyces* and *Streptomyces albulus.*

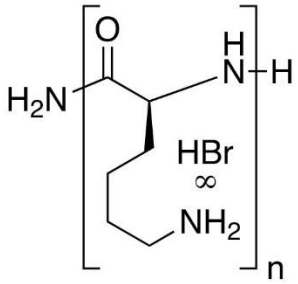

Figure (1.14): *Poly(L-Lysine) polymer (PLL) chemical structure*

PLL is widely used through past years for different biomedical and biotechnological applications. Besides, the adherence of the PLL has been confirmed to be better on rough surfaces compared to polished ones[116]. PLL positive charge was used to electrostatically and covalently link the negatively charged DNA probes[117] Lorenzo Berti et al. reported the increase in loading capacity and stability of ssDNA through electrostatic interaction by using PEGylated PLL[118].

A developed sensor for Au (III) detection based on PLL and screen printed electrodes using voltammetry analysis methods was reported[119]. An electrochemical biosensor for transgenic plants gene fragment detection using impedance spectroscopy has been developed using PLL+SWCNTs composite[120]. It has been reported that PLL conjugated with PEG enhances the single molecule detection and stability in microarray system[121]. PLL as a coating

material to improve the stability of a developed sensors and detection systems has been described[122],[123],[124]. An electrochemical sensor for bovine papillomavirus (BPV) detection on screen printed electrodes based on PLL and chitosan has been developed[125]. An impedimetric biosensor for real-time monitoring of dengue virus (DENV) infection based on PLL and screen printed electrodes has been described[126]. A reported multiplex detection platform for miRNA detection based on PLL and screen printed electrode has been described[127]. Another electrochemical sensor based on MWCNTs/Au/PLL composite has been used for pharmacokinetic of theophylline in rats using square wave voltammetry (SWV) detection system[128]. Another reported platform based on PLL/MWCNTs for femto-molar level cholesterol detection using cantilever has been reported[129]. A DNA-directed antibody immobilization sensing platform has been described using PLL and magnetic nanoparticles[130]. Another example is the developed biosensor using PLL and ethylene glycol composite (PLL-EOG) to link peptide nucleic acid (PNA) probes[131]. A label free electrochemical sensor for haptoglobin (Hp) biomarker base on black phosphorous nanosheets, PLL, and antibodies on screen printed electrodes has been demonstrated[132].

The single base mismatch or point mutations in 12-mer length oligonucleotides have been detected by a label-free approach which detect nM concentrations within minutes[133]. Another example for mismatch detection the use of a fluorescent single-labeled DNA probe and graphene oxide (GO) to develop fast and cost-effective strategy[134]. The cationic polymer poly(L-lysine)-graft-dextran (PLL-g-Dex) enhances the kinetics of hybridization and amplification. Also, the graphene oxide (GO) prefers to link to ssDNA than dsDNA which makes it a rigid amplification platform for rapid real time DNA amplification and detection for real genomic samples. Modified poly (L-Lysine) with oligo (ethylene glycol) (OEG) and thiolated maleimide has been linked to thiolated peptide nucleic acid (PNA) probes. The study concluded that there is a linear relationship between the amount of grafted PLL and the PNA probes density[135]. A label free DNA biosensor based on thin-core fiber (TCF) modified with PLL and ssDNA capture probe has been reported using transmission spectroscopy as a detection system[136].

Large number of developed point of care electrochemical biosensors based on screen printed electrodes (SPEs) were described in literature. For example the impedimetric biosensor based on PLL and SPCEs for real time monitoring of dengue virus (DENV) infection has been described by Cheng, et.al[126]. Another example is the electrochemical sensor based on PLL on screen printed carbon electrodes (SPEs) for bovine papillomavirus (BPV) detection in cattle was addressed. The surface of the SPEs was modified with PLL and chitosan to link the BVP DNA probe[125]. Black phosphorous nanosheets were used to develop a label-free electrochemical immunosensor for haptoglobin (Hp) biomarker based on SPCEs; where the interaction between the PLL and antibodies via electrostatic interaction [132]. Positively charged PLL was used to capture the negatively charged glucose oxidase (GO_x) and ferricyanide on SPEs surface. The developed glucose sensor showed better sensitivity for glucose due to the electron transfer facilitated by the positively charged PLL and negatively charged glucose oxidase (GO_x) and ferricyanide[137]. PLL for surface modification has been used for multiplex detection for microRNA using electrochemiluminescence (ECL) coupled with cyclic voltammetry (CV) as detection systems. The ECL and CV were used for signal on and off for dual signal ratio[138].

PEGDE is a PEG derivative which acts as a cross-linker for amine group to an amine group, it has been used to cross-link proteins as hemoglobin. It´s very soluble in water and contains two very reactive epoxy groups. These epoxy groups will undergo hydrolysis and ring opening to form hydroxyls in aqueous medium, that's why It cross-links amine to amine in dry conditions. The cross-linking is through inter and intra molecular interactions to form the final cross-linked amine groups products[139]. Biodegradable hydrogels for drug delivery and monitoring systems have been synthesized by using PEGDE as a cross-linker for amines. We have used PEGDE in this work to crosslink PLL on SPE surfaces and to increase their biocompatibility (lack of adsorption of proteins).

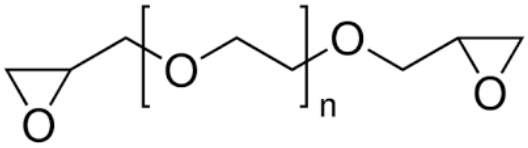

Figure (1.15): *Polyethylene glycol diglycidyl ether (PEGDE) chemical structure*

CHAPTER II

GENERIC PLATFORMS (PROOF-OF-CONCEPT)

Introduction

Screen printed carbon electrodes (SPCES) surface is one of the most difficult and challenging surface for modification. SPCEs have an irregular and rough surface with several additives and polymers that do not totally disappear especially when the treatment is not done at high temperature. This has an impact on the reproducibility and the reliability of the SPCEs performance as electrodes. Very high non-specific adsorption is a problem when the electrodes are used as functional components of the assay instead of as mere detectors. This is avoidable with the use of the appropriate blocking agent, but the blocking agent could also affect the specific signal or increase the number of assay steps. In order to find the appropriate blocking agent, a long optimization process should be performed against the non-specific control. Among long list of tested blocking agents, one or two would show the best blocking behavior by comparing the ratio between the specific signal with the non-specific control.

These non-specific phenomena are especially grave when HRP is used as a label. And we have succeeded to control the HRP non-specific adsorption and we were able to develop a platform for DNA immobilization and detection based on SPCEs. We used a simple model system to search for appropriate blocking of the electrodes that does not depend on the other assay steps (for example amplification or labeling). This model system comprises poly 15T as a capture probe and poly 15A as the complementary sequence (emulating the amplicon).

Two surface chemistry strategies have been tested and validated, diazonium salts electro-grafting and PLL polymer drop-casting. We considered the polymer drop-casting because it is the most appropriate approach for large scale production and manufacturing. Multiple steps and the use of wet chemistry during manufacturing are the undesirable characteristics of the diazonium salts electro-grafting approach for mass production.

I. Diazonium electro-grafting on screen printed electrodes

2.1.1. Problem:

Modification of SPCEs surface using diazonium electro-grafting for DNA probes immobilization and detection to avoid non-specific response.

2.1.2. Solution:

Herein we are demonstrating an electrochemical genosensor for DNA detection based on SPCEs and aryl diazonium electro-grafting and comparing the efficiency to glassy carbon electrodes (GCEs). The diazonium has been synthesized, characterized and then electro-grafted on SPCEs and GCEs surfaces. We used N-cyclohexyl-N-(2-morpholinoethyl)-carbodiimide methyl-p-toluene-Sulfonate (CDMI) as a cross-linker to cross-link carboxylate groups to amine groups in order to avoid the large molecules and different by-products using regular EDC/NHS reaction for cross-linking, i.e. avoid the steric hindrance. The concentration of the diazonium, electro-grafting parameters, and immobilization and hybridization parameters has been optimized achieving a LOD 2.6 nM with a linear range from 10 to 100 nM and 9.5 nM with a linear range from 20 to 200 nM for GCEs and for SPCEs respectively. Although the performance is acceptable, wet chemistry where many reagents are involved and multiple steps for surface functionalization are the limitations for this approach to be used for any POC device or sensor manufacturing. Then for the large-scale production we should consider an easier, faster, and reagentless strategy.

2.1.3. Materials and method:

All reagents were used as received.N-cyclohexyl-N-(2-morpholinoethyl)-carbodiimide methyl-p-toluene-Sulfonate (CDMI), Phosphate buffered saline (PBS), Strontium Nitrate (Sr (NO3)2), Potassium Chloride (KCl), Sodium acetate, Potassium hexacyanoferrate(III) ($K_3Fe(CN)_6$, 99+%), ruthenium hexamine (III) chloride, and ethanolamine hydrochloride were purchased from Sigma-Aldrich. The 4-(N-Carboxymethyl sulfanyl) benzene diazonium hexafluorophosphate salt (DCOOH) was prepared as previously reported[105]. SPCEs (DRP-110) were purchased from DropSens with a diameter of 4mm. Synthetic HPLC-grade oligonucleotides DNA probes were purchased from Biomers.net (Ulm, Germany):

Capture probe: NH2-5-ttt ttt ttt ttt ttt

Complementary probe: HRP-5-aaa aaa aaa aaa aaa

Non-specific probe (NSC): aca cac atc caa cca tyt cac tg-5-HRP

All the electrochemical measurements were performed with a PC controlled PGSTAT12 Autolab potentiostat (EcoChemie, The Netherlands) using screen printed carbon (DRP-110) and standard glassy carbon electrodes (GCEs). The electrode configuration for SPCEs: working electrode: carbon disk (ϕ=4 mm), reference electrode: silver, counter electrode: carbon. The electrode configuration for GCEs: working electrode: carbon bar (ϕ=3 mm), reference electrode: silver/silver chloride, counter electrode: platinum wire.

The GCEs were polished by water-based diamond suspension with size of 15, 6, 3, and 1 µm. Then, the electrodes polished by the 0.3 and 0.05 µm polishing powder. The electrodes were sonicated in milliQ, 2M nitric acid and ethanol after each polishing step for 5min.

Electrode activating:

The electrodes were activated by 0.1 M H_2SO_4 for 5 cycles from 0.1 to -1V at 200 mV/s using Ag/AgCl reference electrode and Pt wire as a counter electrode.

Diazonium grafting:

5 mM N-methylcarboxyamino-4-silcondioxyphenyl hexafluorophosphate diazonium salt (NM-4-HD) in MilliQ grafted electrochemically by applying 2 cycles from +0.1 to -0.6 V at 50 mV/s for GCEs and from +0.1 to -1 V for SPCEs using Ag/AgCl reference electrode and Pt wire as a counter electrode. Grafted electrodes washed with acetate buffer PH 5.0 for 30 min, dried with nitrogen. The electrodes could be stored dry for use.

ssDNA immobilization:

The surface has been activated by N-cyclohexyl-N-(2-morpholinoethyl)-carbodiimide methyl-p-toluene-Sulfonate CMC-(24 mg of in 250 µL milliQ)-incubated for 30 min. 100 µL of 5 µM aminated ssDNA (Poly T) in 0.05 M PBS buffer PH 7.4 drop-casted on the surface for 2 h; washed with a stream of milliQ. 1 M of ethanolamine in milliQ at PH 8.0 drop-casted for 30min, to block all non-linked diazonium carboxylic groups on the surface, washed with milliQ by stirring for 10min and dried with nitrogen. The electrodes could be stored until used.

DNA hybridization and detection:

Functionalized electrodes were incubated with 20 nM complementary probe (poly A-HRP) in 10 mM tris buffer in 0.5 M NaCl for 30 min at 37^{O}C in thermo-mixer for GCEs and at room temperature under controlled humidity chamber for SPCEs. For the non-specific control, different reporter-other than the poly A-HRP- has been used *(aca cac atc caa cca tyt cac tg-HRP)*. The response of the hybridized probes was followed by chronoamperometry (CA) using Ag/AgCl reference electrode and Pt wire as a counter electrode in a 2 mL vial. For CA measurements, the electrode immersed in the 0.05 M PBS, using Ag/AgCl reference electrode and a Pt wire as a counter electrode. A potential of -0.2 V has been applied for 100 sec. At t = 100 s, 1 mL of TMB added to the PBS solution while the measurement was being recorded. At the end of the 250 seconds, the difference between the readings before and after TMB addition has been recorded for each electrode.

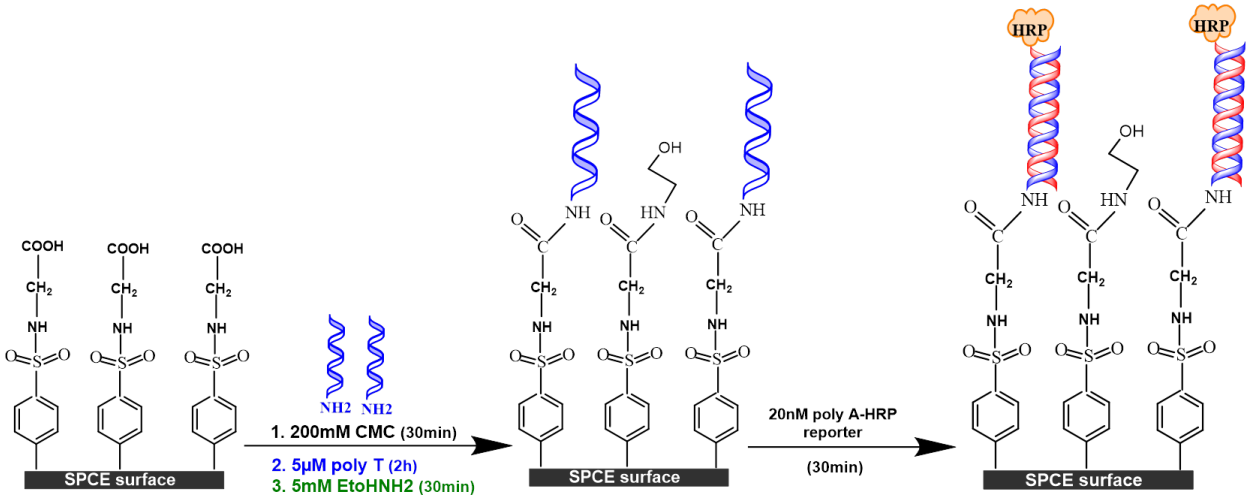

Figure (2.1): *Schematic representation for surface functionalization with NH_2-poly15T after DCOOH diazonium salt electro-grafting*

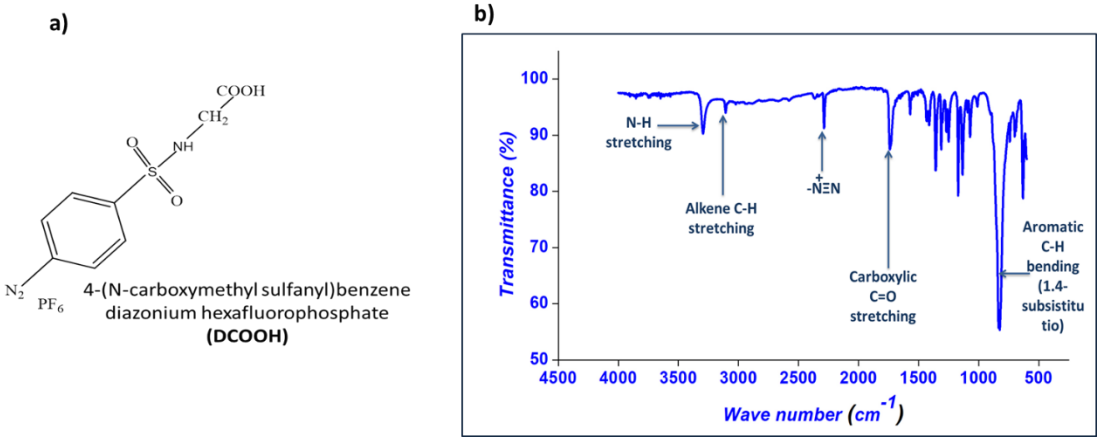

Figure (2.2): a) *Chemical structure of:* ***a)*** *the DCOOH, and* ***b)*** *IR characterization for DCOOH*

2.1.4. Results and discussion:

<u>System validation on glassy carbon electrodes (GCEs):</u>

Before applying the diazonium on SPCEs surface we need to ensure it is working on a well characterized carbon surface, i.e. GCEs. To immobilize the DNA probe, a covalent interaction between the amine poly T and carboxylate group in the diazonium to form the amide bond should take place. The electrodes were characterized by CV before proceeding as in figure (2.3). After electro-grafting the surface becomes compact and the $[Fe(CN)_6]^{-2/-3}$ cannot easily reach the surface through diffusion.

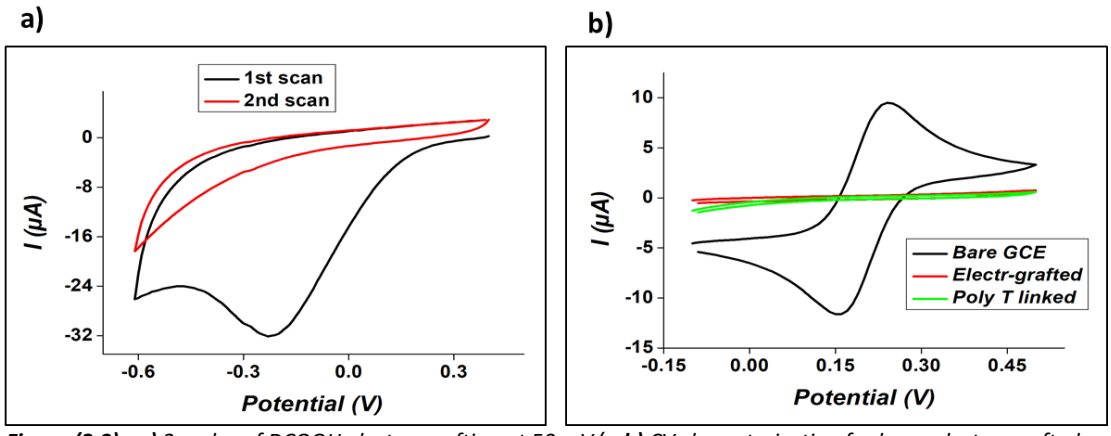

Figure (2.3): ***a)*** *2 cycles of DCOOH electro-grafting at 50 mV/s,* ***b)*** *CV characterization for bare, electro-grafted, and poly T modified GCEs*

The hybridization with the complementary poly A-HRP is producing a signal that confirming poly T immobilization. The non-specific control which is a poly A is confirming the selectivity and specificity of the strategy, as well as the reproducibility (figure (2.4)).

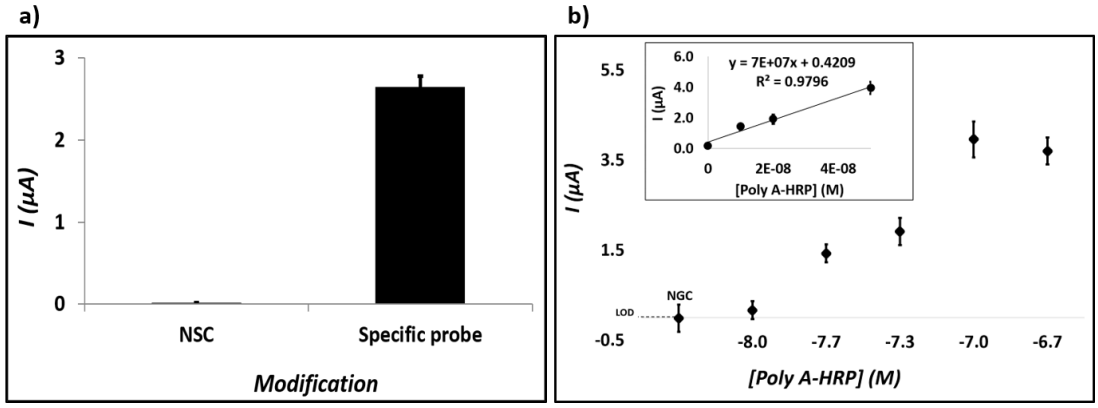

Figure (2.4): *Chronoamperometric measurements for* ***a)*** *selectivity and reproducibility of the strategy, and* ***b)*** *A calibration curve from 0 nM to 200 nM poly A-HRP showing a linear range from 10 nM to 100 nM*

<u>System optimization on screen printed carbon electrodes (SPCEs):</u>

Now the system is verified and validated and is ready to be tested on the SPCEs surface. Although there is a six times difference between the specific and non-specific control, there is a very big HRP non-specific adsorption on SPCEs surface as expected and high background current. Then a study to test different blocking reagents in order to reduce HRP non-specific adsorption is essential, this is shown in table (2.1) and figure (2.5).

Blocking agent	Non-specific control	Specific probe	Ratio	Reproducibility
BSA 5%	-1.54	-1.57	1.02	x
BSA 3%	-0.51	-2.66	5.25	x
ssDNA	-0.35	-0.48	1.37	Yes
Glycine	-1.47	-10.74	7.31	x
PEG400	**-0.39**	**-3.15**	**8.08**	**Yes**
0.1% Tween	-0.30	-1.85	6.17	x
5x denhardt	-0.21	-1.24	5.90	Yes
1x denhardt's	**-0.21**	**-1.90**	**9.05**	**Yes**

Table (2.1): *Non-specific control, specific probe, ratio between the non-specific control and specific probe, and the reproducibility for different blocking agents on SPCEs surface*

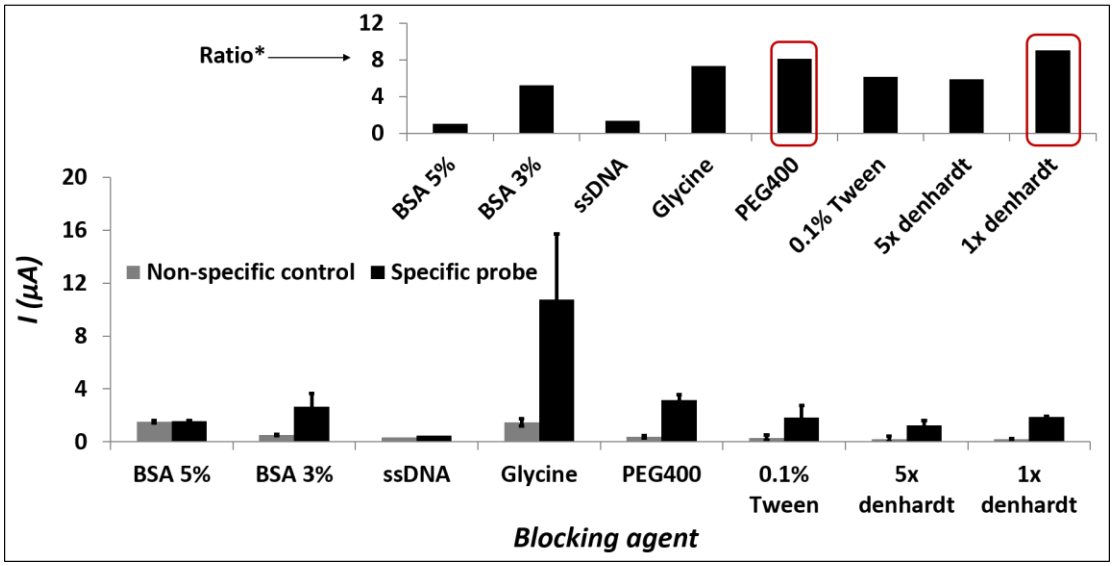

Figure (2.5): *CA measurements for the non-specific control and specific probe CA measurements, Ratio* is the ratio between the non-specific control and the specific probe*

Surface characterization:

CV surface characterization for bare and electro-grafted SPCEs surfaces are shown in figure (2.6). The electro-grafting has been confirmed by the reduction in the peak currents VS (scan rate)$^{1/2}$ compared with the bare electrode.

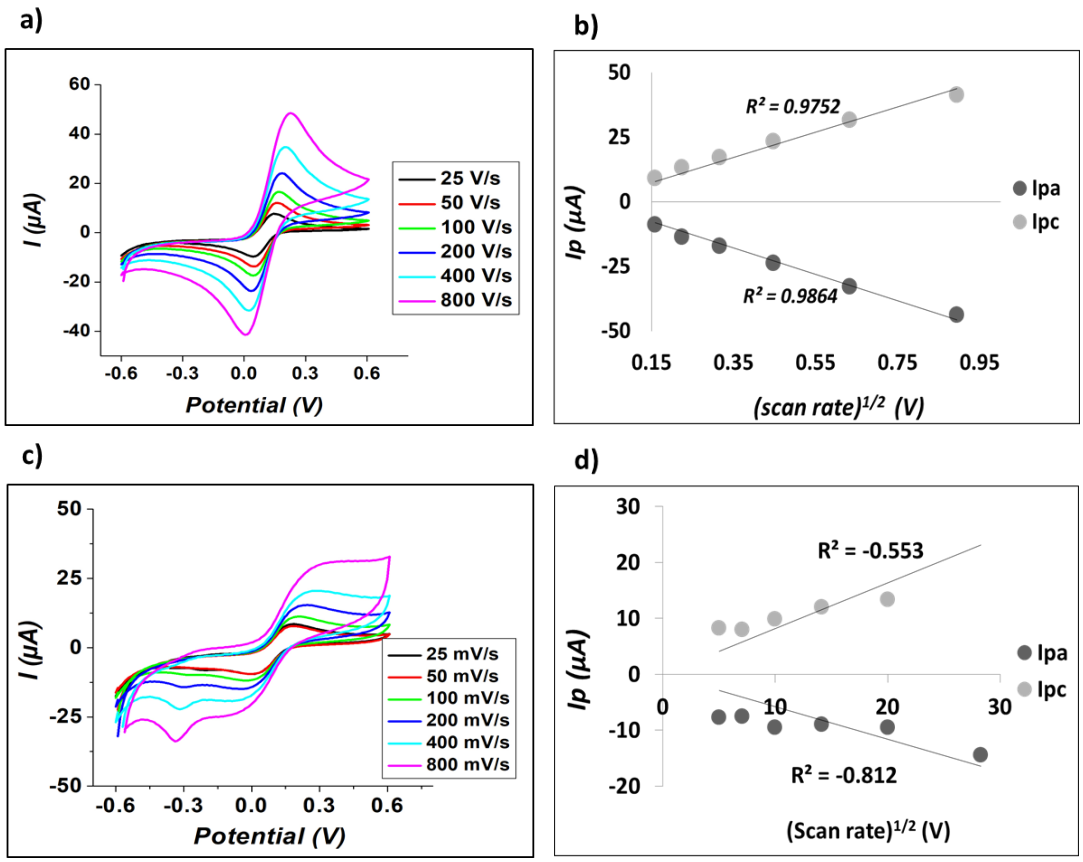

Figure (2.6): *Cyclic voltammetry characterization using 1 mM $[Fe(CN)_6]^{-3/-2}$ containing 50 mM Sr (NO_3) electrolyte for:* ***a)*** *and* ***b)*** *bare SPCEs,* ***c)*** *and* ***d)*** *electro-grafted SPCE with 2 cycles DCOOH*

The CV after electro-grafting shape compared with the bare SPCEs electrode sows less diffusion of the *$[Fe(CN)_6]^{-3/-2}$ ions* which indicates the formation of a dense layer on the SPCE surface. After poly T immobilization the CV shows a more reversible wave on the grafted layer (figure (2.7a). The EIS measurements as in figure (2.7b), appear to suggest that the electro-grafted layer inhibits the electron diffusion through the surface. But after poly T immobilization, penetration of the electrochemical indicator is facilitated.

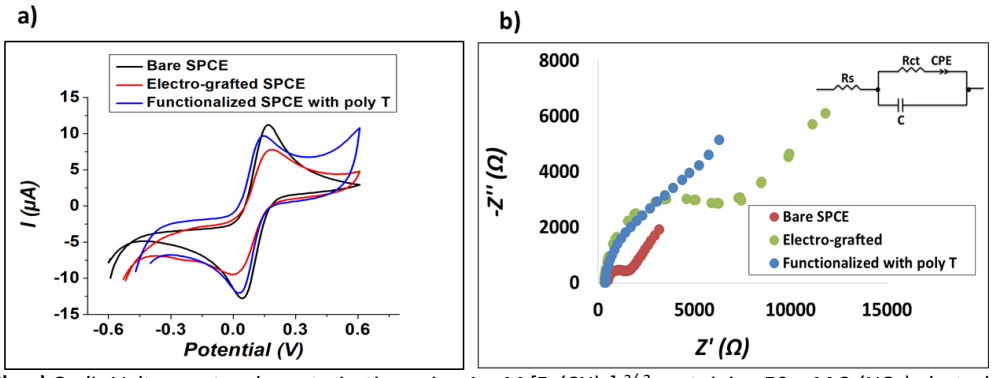

Figure (2.7): ***a)*** *Cyclic Voltammetry characterization using 1 mM $[Fe(CN)_6]^{-3/-2}$ containing 50 mM $Sr(NO_3)$ electrolyte for bare SPCE, electro-grafted, and modified SPCE with poly T.* ***b)*** *Electrochemical impedance spectroscopy at 0.1 V, frequency range from 1000 to 0.01 HZ, and 10 mV points per decade for bare SPCE, electro-grafted, and fictionalized with poly T*

CA detection:

After optimization study for different blocking agents on SPCEs surface, the 1x Denhardt's is showing the highest ratio between the non-specific control and specific probe, as well as the most reproducibility obtained. It also results in the lowest background current. PEG 400 is a good candidate and it performs same as 1x Denhardt's; but we opt to choose the 1x Denhardt's solution. The specific responses and poly A-HRP reporter concentration logarithmic calibration curve (figure (2.8)), with good sensitivity. The linear range is from 20nM to 200nM, the LOD is calculated to be 9.5 nM.

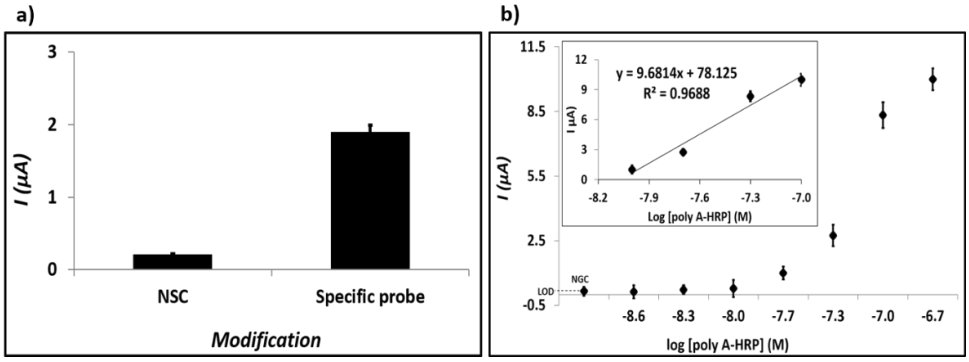

Figure (2.8): *CA measurements for* ***a)*** *Specific response of the system,* ***b)*** *Poly A-HRP reporter concentration calibration curve, the linear range is from 20 nM to 200 nM and the LOD is 9.5 nM. measurements were performed at -0.2V potential for 250 s using 100 µL PBS 0.5 M for the first 100 s and 100 µL TMB substrate was added after 100 s for 30 min hybridization*

2.1.5. Conclusion:

5 mM of 4-(N-Carboxymethyl sulfanyl) benzene diazonium hexafluorophosphate salt (DCOOH) was electro-grafted on GCEs and SPCEs surface using general sequences (poly T complementary to poly A-HRP, and poly A as the non-specific control). The LOD achieved were 2.6 nM with a linear range from 10 to 100 nM and 9.5 nM with a linear range from 20 to 200 nM for GCEs and for SPCEs respectively. But this strategy is not compatible for the large-scale production due to multiple steps and wet chemistry used.

II. Poly (L-Lysine) polymer drop-casting on screen printed electrodes

2.2.1. Problem:

Modification of SPCEs surface using poly (L-Lysine) drop-casting on the SPCEs surface for DNA probes immobilization and detection to avoid non-specific response.

2.2.2. Solution:

We are demonstrating a fast, easy and direct approach for DNA immobilization and detection based on PLL, PEGDE cross-linker and screen-printed electrodes. The polycationic PLL is electrostatically interacts with the polyanionic DNA backbone. The presence of the PEGDE seems to enhance the reproducibility presumably due to covalent bonding. The method shows a one order of magnitude difference between the specific signal and non-specific control. And the linear range for detection of the model sequence is from 2.5 to 50 nM with a LOD of 1.2 nM. The approach is easy, direct, fast, and reagentless which makes it the proper strategy for large scale production and manufacturing.

2.2.3. Materials and methods:

All reagents were used as received, poly(L-lysine hydrobromide) PLKB 20 average Mw 4200, 50 KDa, and 120 KDa, polyethyleneimine hydrobromide (PEI) average Mw 750 KDa from Alamanda company, polyethylene glycol diglycidyl ether (PEGDE), polyethylene glycol 400, Phosphate buffered saline (PBS), strontium nitrate ($Sr(NO_3)_2$), potassium chloride (KCl), sodium acetate, and potassium hexacyanoferrate(III) ($K_3Fe(CN)_6$, 99+%) were purchased from Sigma-Aldrich. SPCEs (DRP-110) purchased from Dropsense with a diameter of 4 mm. Synthetic HPLC-grade oligonucleotides DNA probes were purchased from Biomers.net (Ulm, Germany):

Capture probe: NH_2-5'-ttt ttt ttt ttt ttt

Complementary probe (P): HRP-5'-aaa aaa aaa aaa aaa

Non-specific probe (NSC): NH_2-5'-aaa aaa aaa aaa aaa

All the electrochemical measurements were performed on a PC controlled PGSTAT12 Autolab potentiostat (EcoChemie, The Netherlands) using screen printed carbon (DRP-110) with configuration: working electrode: carbon disk (ϕ=4 mm), reference electrode: silver, counter electrode: carbon.

ELONA functionalization:

3 µL of each 0.05 mM PLL solution (4 KDa, 50 KDa, 120 KDa) or PEI, 0.1 mM NH2-poly 15T, 0.25 mM PEGDE were mixed and vortex together and drop-casted on the ELONA well. The plate was incubated for overnight (or till complete dryness) under vacuum. After dryness, the plate was washed 3 times with distilled water and incubated with the 20 nM complementary (poly A-HRP) for 30 min, then TMB for 2min and the reaction stopped by the addition of 0.0 5M H_2SO_4. The absorbance was read at 450 nm using a spectrophotometer.

SPCEs surface functionalization:

8.4 µL of each 0.05 mM PLL solution, 0.1 mM NH2-poly 15T, 0.25 mM PEGDE were mixed and vortexed together and drop-casted on the SPCE surface. The electrodes were incubated for overnight (or till complete dryness) under vacuum. After dryness, the SPCEs were washed for 2 min with distilled water and incubated with 1x Denhardt´s solution for 1 h at 40^{O}C.

Chrono-amperometric detection:

The electrodes were washed with distilled water and incubated with 20 nM poly A-HRP for 30 min at 40^{O}C. For CA measurements, the electrode immersed in the 0.05 M PBS, and a potential of -0.2 V has been applied for 250 sec. At t= 100 s, 100 µL of TMB were added to the PBS solution while the measurement was being recorded. At the end of the 250 seconds, the difference between the readings before and after TMB addition has been recorded for each electrode.

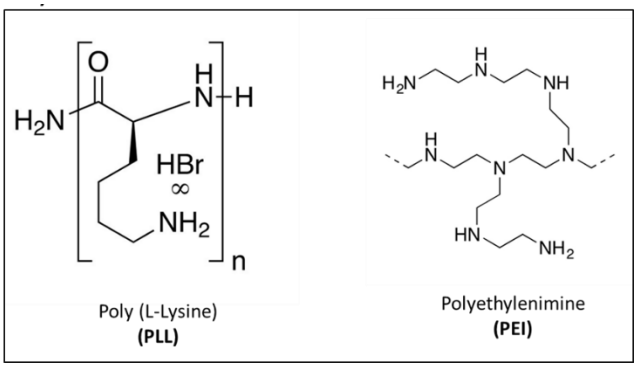

Figure (2.9): *Chemical structure of PLL and PEI*

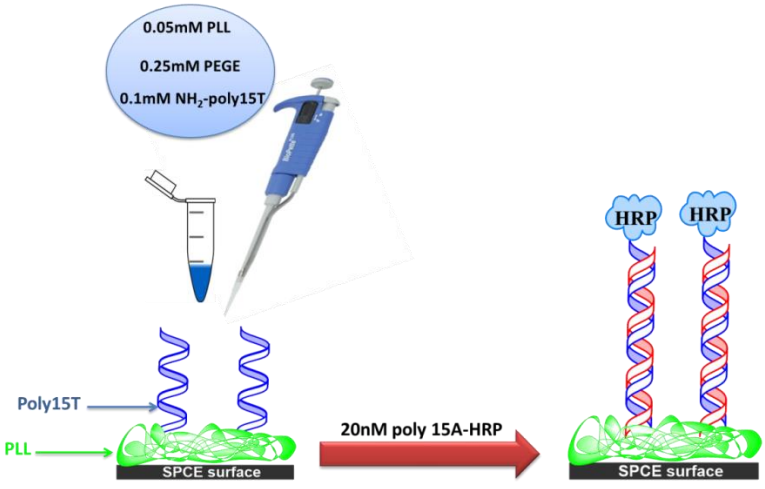

Figure (2.10): *Schematic representation for surface functionalization with PLL and NH_2-polyT*

2.2.4. Results and discussion:

Different molecular weights of PLL has been tested and compared with the PEI which contains 4 primary amines, 3 secondary and 4 tertiary amines. The approach has been tested with ELONA first and the MW that showed the best response has been transferred to the SPCEs.

ELONA system:

The performances of the polymers on ELONA plate, different MWs with and without the cross-linker, i.e. PEGDE were tested. The results show that the lowest MW resulted to higher specific to non-specific ratio in the response; besides, there is no need for the PEGDE, which indicates the interaction between the polymer and the DNA is an electrostatic interaction (table (2.2)).

With PEGDE

Polymer	Non-specific control	Specific probe	Ratio
PEI	0.477	1.3	2.73
PLL 120KDa	0.082	0.287	3.50
PLL 50KDa	0.54	2.28	4.22
PLL 4KDa	0.12	1.96	16.33

No PEGDE

Polymer	Non-specific control	Specific probe	Ratio
PEI	0.3	1.12	3.73
PLL 120KDa	0.065	0.182	2.80
PLL 50KDa	0.1	0.52	5.20
PLL 4KDa	0.08	1.81	22.63

Table (2.2): *Spectrophotometric absorbance at 450 nm for ELONA plates functionalized by different polymers with the non-specific probe (poly 15A) and specific probe (poly 15T), the reporter is poly A-HRP. The measurements are with and without the use of the cross-linker (PEGDE), in the case of no PEGDE distilled water was used instead*

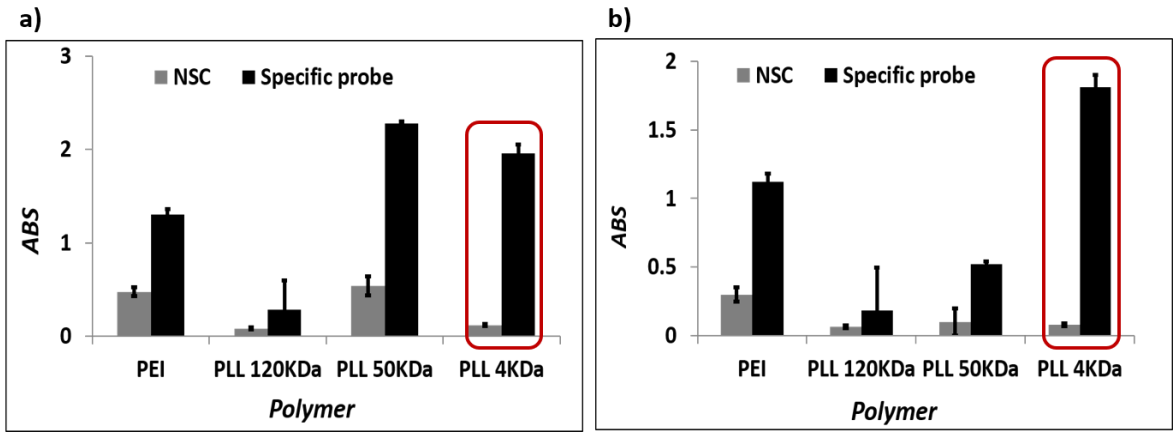

Figure (2.11): *Spectrophotometric absorbance at 450 nm for ELONA plates functionalized by different polymers with the non-specific probe (poly 15A) and specific probe (poly 15T), the reporter is poly A-HRP. The measurements are **a)** without and **b)** with the use of the cross-linker (PEGDE), in the case of no PEGDE distilled water was used instead*

PLL functionalization with poly 15T on SPCEs:

Parameters optimization:

1. *Surface blocking:*

Due to the use of HRP as an electrochemical indicator there is a very high risk for HRP non-specific adsorption. The surface of the SPCEs is very rough and irregular; this would make the HRP adsorbed strongly on the surface and cannot be removed by washing. To prevent this, a blocking agent should be used to reduce this non-specific adsorption.

2. *PEGDE:*

After the system has been tested with ELONA it has been transferred to the SPCEs surface. By using the same approach and testing the use of the PEGDE in order to determine the type of the interaction between the polymer and the DNA on the SPCEs surface.

Surface characterization:

Cyclic voltammetry characterization of the functionalized SPCE with PLL and NH_2-polyT using the PEGDE compared with the bare SPCE using different scan rates is shown in figure (2.12). The PLL is positively charged so it will attract the negatively charged $[Fe(CN)_6]^{-3/-2}$ and enhances the linearity of the peak currents (IP) VS $(scan\ rate)^{1/2}$.

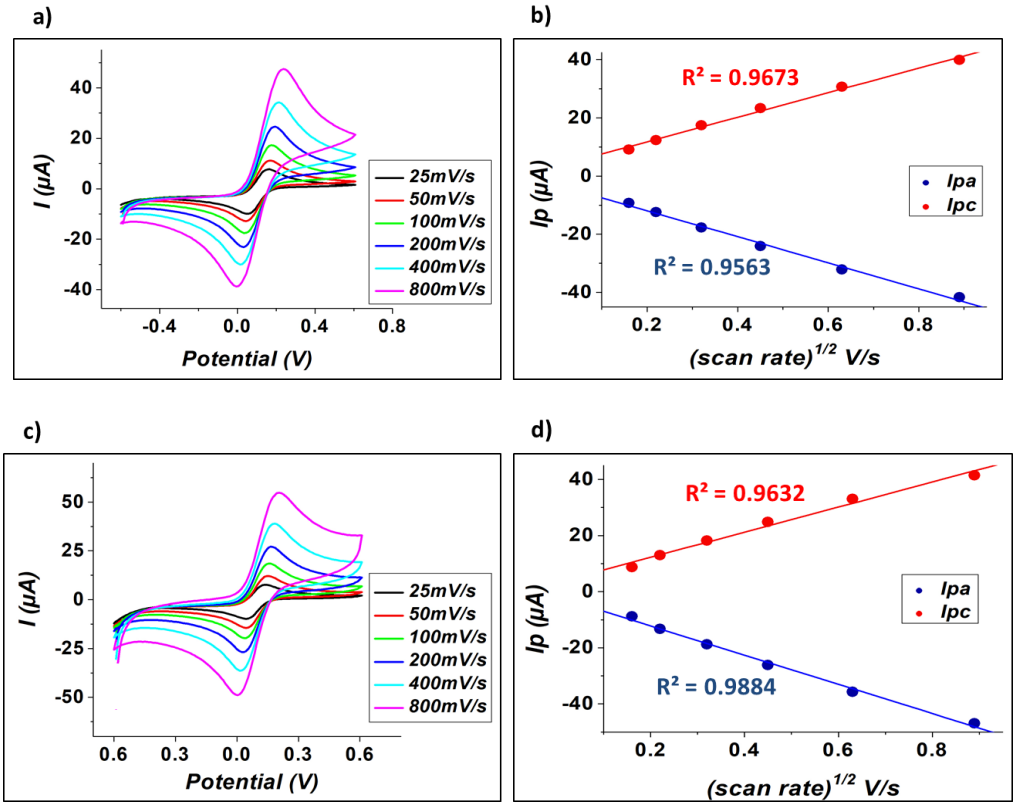

Figure (2.12): *Cyclic voltammetry characterization using 1 mM $[Fe(CN)_6]^{-3/-2}$ containing 50 mM Sr (NO_3) electrolyte for:* ***a)*** *and* ***b)*** *bare SPCEs,* ***c)*** *and* ***d)*** *modified SPCE with 0.0 5 mM PLL + 0.1 mM NH_2-poly T + 0.25 mM PEGDE*

Cyclic voltammetry and impedance characterization of the functionalized SPCE with PLL and NH_2-polyT using the PEGDE compared with the bare SPCE is shown in figure (2.13) and table (2.3). The surface is still conductive for electron transfer same as for bare SPCE; this may be because of the positive charge of the PLL. The oxidation peak is slightly shifted besides the increase in the apparent electron diffusion after poly T linking. The EIS shows the difference between each step, where the Rct is slightly bigger after modification with the PLL and NH_2-polyT. The DNA linked to the PLL may act as a molecular wire for electron transfer, increasing the apparent diffusion rate. All of these are indicating the successful surface modification of the SPCEs with PLL and poly T using the PEGDE as a cross-linker.

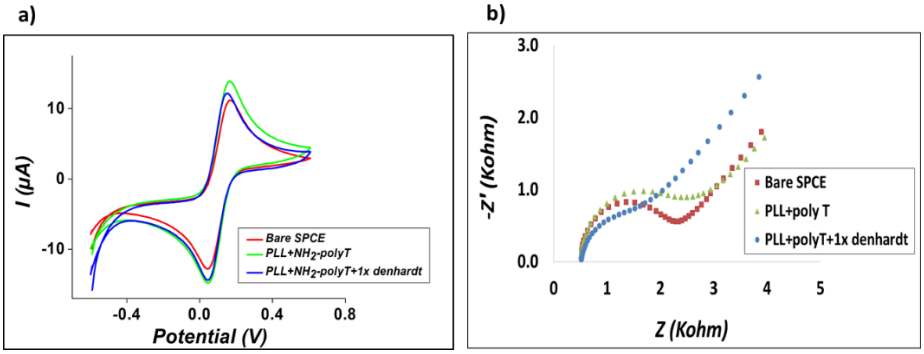

Figure (2.13): a) *Electrochemical impedance spectroscopy at 0.1 V, frequency range from 1000 to 0.01 HZ, and 10 mV points per decade and* ***b)*** *Cyclic Voltammetry characterization using 1 mM $[Fe(CN)_6]^{-3/-2}$ containing 50 mM $Sr(NO_3)$ electrolyte for bare SPCE modified SPCE with 0.05 mM PL L+ 0.1 mM NH_2-poly T + 0.25 mM PEGDE*

Electrode	*Rs (Ω)*	*Rct (Ω)*	*-Z'' (Ω)*
Bare SPCE	520	2160	932
After PLL+NH_2-polyT	519	2500	971
After PLL+NH_2-polyT+1xdenhardt	519	1717	543

Table (2.3): *EIS characterization parameters obtained at 0.1 V, frequency range from 1000 to 0.01 HZ, and 10 mV points per decade and using 1 mM $[Fe(CN)_6]^{-3/-2}$ containing 50 mM Sr(NO3) electrolyte for bare SPCE modified SPCE with diazonium electro-grafting, after FwP linking to the –COOH groups on the grated diazonium and after RPA on the surface of SPCE. Where the Rs is the solution resistance, Rct is the resistance at the solid-liquid interface, -Z'' is the component of impedance*

CA detection:

CA measurements show one order of magnitude difference between the specific signals to non-specific control on SPCEs surface is shown in figure (2.14). The calibration curve using different concentrations of poly A-HRP ranging from 0 nM to 500 nM shows a logarithmic response with a linear range from 2.5 nM to 50 nM with a LOD of 1.2 nM.

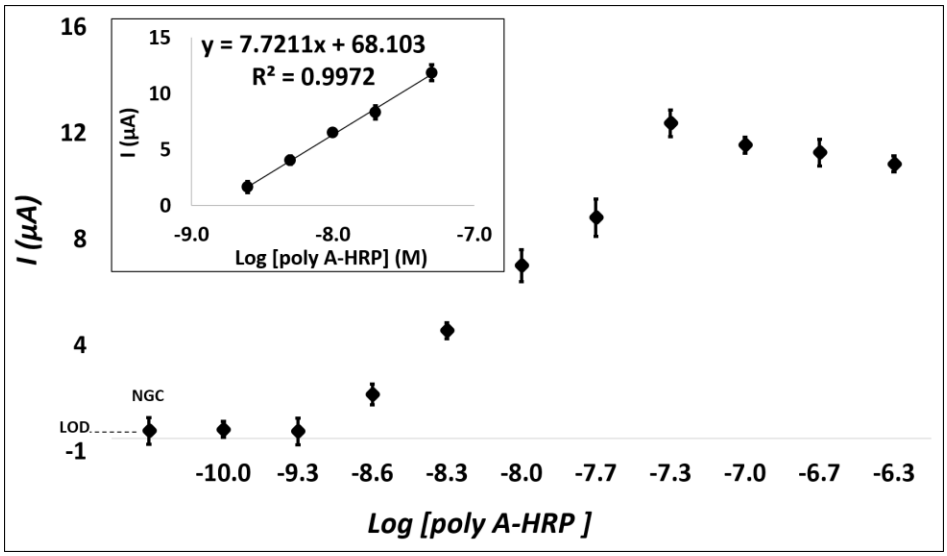

Figure (2.14): *Poly A-HRP concentration calibration curve for PLL drop-casting on SPCEs surface, concentration range from 0 nM to 500 nM, the linear range from 2.5 nM to 50 nM, the LOD was found to be 1.2 nM for 30 min hybridization. measurements were performed at -0.2V potential for 250 s using 100 µL PBS 0.5 M for the first 100 s and 100 µL TMB substrate was added after 100 s.*

2.2.5. Conclusion:

Poly (L-Lysine) polymer (PLL) has been successfully drop-casted and linked with DNA aminated general probes (poly T). High molecular weight of PLL shows less responses for hybridization and detection. This could be due to the high positive charge of the polymer could attract the negative backbone of the poly A-HRP to be immobilized on the polymer rather than hybridized with the capture probe. The interaction between the PLL and poly T is a mixture between an electrostatic interaction due to the positive charge on the PLL and the negative charge of the DNA backbone, and covalent interaction due to the use of the PEGDE where it links the amine in the PLL to the amine in poly T. PEGDE is participating in blocking the HRP non-specific adsorption, so we may consider it beside its role as a cross-linker a antifouling agent. The LOD was found to be 1.2 nM and the linear range is from 2.5 nM to 50 nM.

III. Other approaches did not work on screen printed electrodes

Some approaches have been tested and did not work for DNA immobilization and detection on SPCEs surface, such as:

a) Direct adsorption of the DNA probes on the SPCEs surface. The drop-casting of the DNA on the surface did not show any significant difference between the specific and non-specific control. This is due to the roughness and very high surface area, and irregular surface of the SPCEs surface.

a) Hydrogenation/chlorination of the SPCEs surface[140]: This method has been proved to be working for GCEs and the process as shown in figure (2.15). Polished GCEs was immersed in 2 M HCl and a potential of -5 V for 10 min was applied. Then the electrode was immersed in a mixture of 3:1 HCl: HNO_3 and a potential of +2.5 V for 5 min applied. The acidic concentrations and the positive voltage for chlorination were too high for the printed carbon ink and eventually the surface was damaged.

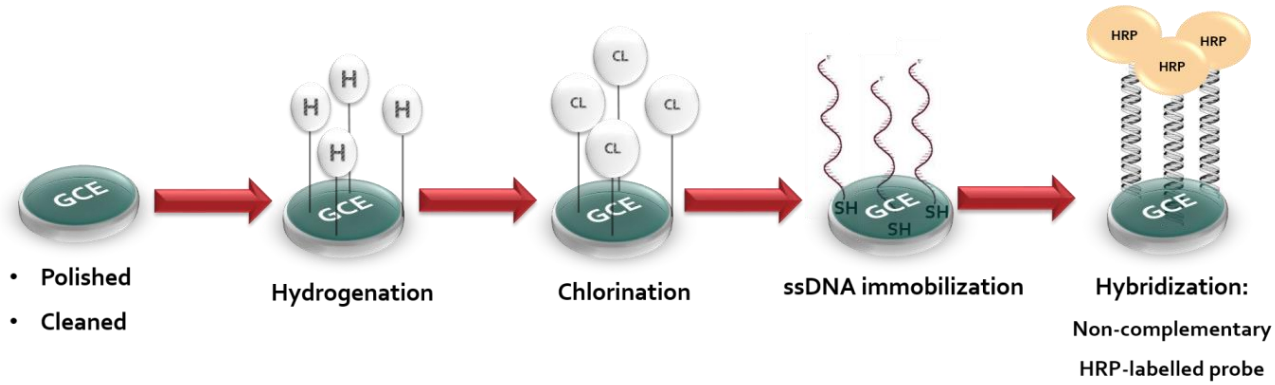

Figure (2.15): *GCEs surface modification by hydrogenation and chlorination by applying -5 V for 10 min followed by chlorination by applying +2.5 V for 5 min*

CHAPTER III

APPLICATIONS

1. SOLID-PHASE RPA

Introduction

After successful functionalization of the SPCEs surface for DNA immobilization and detection, the model system should be applied for real systems. The model system has been optimized for two direct and simple steps, immobilization and hybridization. Also, the use of the general DNA sequences makes the model system very simple. So, to use the model system as a real system for target detection, DNA amplification should be introduced. We have chosen RPA as our amplification method because it is an isothermal amplification method could be performed at room temperature. And because our final aim is to construct an integrated microfluidic system based on our developed system of SPCEs, RPA is the excellent candidate for target amplification.

We have tested two RPA amplification methods with our developed systems. RPA mixture contains a lot of matrix components such as enzymes, proteins, crowding agents like PEG …etc. And due to the addition of more steps and more reagents we have added complexity to the system. Hence, another surface optimization should be performed to control the HRP non-specific adsorption. Here in this and the next chapters we are discussing the new optimized systems as real systems for K. armiger amplification and detection using two RPA approaches.

In this chapter we are introducing the RPA into the system as solid-phase RPA on the surface. This has been achieved by immobilization of the aminated forward primer on the surface of SPCEs. The amplification was achieved by incubating with the RPA mixture for a specific time. And even better with one of the developed systems has the ability for amplification and hybridization at the same time in just 20 min by using a reverse primer labelled with HRP. This is an important step towards developing the integrated MD device for point-of-need application, since it obviates one additional hybridization step.

I. Diazonium electro-grafting on screen printed electrodes

3.1.1. Problem:

To use the successful strategy used before to modify the surface of SPCEs with diazonium salt electro-grafting to perform solid phase RPA on SPCEs surface. The DNA probe is the NH_2-FwP, one of the RPA primers.

3.1.2. Solution:

We are demonstrating a new electrochemical system for DNA detection for applications in molecular diagnostics based on screen printing technology. The system should be achieved at low cost and should complete the analysis in less than 45 min (sample in-result out). We are prooving it is possible to develop a generic electrochemical system which could be functionalized and modified depending on its objective-application. As a demonstration *karlodinium spp*., a toxic micro-algae species will be used as target for the proof of principle of environmental monitoring and protection of the marine environment. We are using a poly 15 T tailed forward primer (FwP), and a reverse primer contains a tail that is complementary to a reporter HRP. Our developed system achieves a LOD of 2.8 pM and a linear range from 5-500 pM for synthetic ssDNA and a LOD of 0.1 fM for synthetic dsDNA and a linear range from 0.5 fM to 5 pM.

3.1.3. Materials and methods:

All reagents were used as received. N-cyclohexyl-N-(2-morpholinoethyl)-carbodiimide methyl-p-toluene-sulfonate (CDMI), Phosphate buffered saline (PBS), strontium nitrate, sodium acetate, potassium hexacyanoferrate (III), ruthenium hexamine (III) chloride, and ethanolamine hydrochloride were purchased from Sigma-Aldrich. N-cyclohexyl-N-(2-morpholinoethyl)-carbodiimide methyl-p-toluene-Sulfonate (DCOOH) and 4-chlorophenyl benzene diazonium hexafluorophosphate (DCl) were prepared as hexafluorophosphate salts as previously reported[141]. SPCEs (DRP-110) were purchased from DropSens® with a working electrode diameter of 4 mm. Synthetic HPLC-grade DNA probes were purchased from Biomers.net (Ulm, Germany) having the following sequences:

Karlodenium armgier tailed forward primer (KA. FwP): 5'-NH2-ttt ttt ttt ttt ttt ata gct tca cag cag agg tta caa c-3'

Karlodenium armgier tailed reverse primer (KA. RevP primer): 5'-ttt ttt ttt ttt ttt tgt aaa acg acg gcc agt - 5 - aca cac atc caa cca tyt cac tg-3'

Karlodenium armgier reporter (complementary/KA.HRP reporter): 5'-HRP- act ggc cgt cgt ttt aca-3'

Karlodenium armgier DNA (template): ata gct tca cag cag agg tta caa cac caa tgc tgc tcc gct acc cgc gat ctc atg cac cag gga gcg gca aga agc cag agc ttc aag aca ccc cta ccc ccg tgc agg agc tca caa aga aag ttc aca gtg aga tgg ttg gat gtg tgt

All the electrochemical measurements were performed with a PC controlled PGSTAT12 Autolab potentiostat (EcoChemie, The Netherlands). The electrochemical configuration had a carbon disk working electrode (ϕ=4 mm), a silver reference electrode, and a carbon counter electrode.

Diazonium grafting:

Mixed layers of DCOOH and DCl were electro-grafted as follows: 5 mM of DCOOH in distilled water was grafted electrochemically by applying 1 potential cycle from +0.1 to -1 V using 50 mV/s scan rate. Then, 5 mM of DCl was grafted electrochemically by applying 3 cycles in the same potential range using 50 mV/s scan rate. The grafted electrodes were washed with acetate buffer pH 5.0 for 30 min, dried with argon. Electro-grafting characterization was performed by recording the CV using Fe^{+3}/Fe^{+2} solution (*1 mM* $[Fe(CN)_6]^{-3/-2}$ *containing 50 mM* $Sr(NO)_3$. The electrodes were stored until used.

Aminated k. armiger FwP immobilization:

The surface was activated by 200 mM CDMI, incubated for 30 min at 40^{O}C and washed with distilled water. 30 µL of 5 µM KA. FwP in 0.05 M PBS buffer pH 7.4 was drop-casted on the surface for 2 h; then was washed with distilled water. 30 µL of 5 mM ethanolamine in distilled water at pH 8.0 was drop-casted and incubated for 30 min at 40^{O}C to block all non-linked diazonium carboxylic groups on the surface, washed with distilled water dried with argon. The electrodes were stored until used.

Solid-phase RPA on SPCE surface:

RPA cocktail: The final volume was adjusted to be 50 µL as described by the manufacturer as in table (3.1). Distilled water, rehydration buffer, and reverse primer HRP were added and vortexed in a 500 µL Eppendorf. Then the pellet was dropped inside the mixture and left for 1 min till it dissolves completely. Then the target was added in case for positive samples or distilled water for the negative control. Finally, the magnesium acetate was added to the mixture to initiate the amplification reaction. To drop-cast the mixture on the SPCEs surface, formation of any air bubbles should be avoided.

	Volume per reaction (µL)
Milliq	10.6
Rehrydation buffer	29.5
RvP tailed 10 µM	2.4
Pellet	0.5
MgAcet 280mM	2.5
Target 10nM/milliq	5
Total	***50***

Table (3.1): *Solid-phase RPA mixture drop-casted on the modified SPCEs surface with mixed layer diazonium electro-grafting and* NH_2*-capture probe*

25 µL of the prepared RPA mixture was drop-casted on the modified SPCEs surface with FwP and was incubated for a specific time at 40^{O}C (40 min for all measurements except for RPA time optimization), and then were washed with a stirred distilled water. The different *k. armiger* dilutions have been

prepared as describe in table (3.2), the concentrations represented in the calibration curves are the final concentrations of the *k. armiger* in the 50 µL RPA mixture.

K. armiger	Stock	1st dilution	2nd dilution
ssDNA	100 µM	1 µM	10 nM
dsDNA	50 nM	1 nM	-

Used [ssDNA] (M)	Final [ssDNA] (M)	Used [dsDNA] (M)	Final [dsDNA] (M)
0	0	0	0
5.E-13	5.E-14	5.E-15	5E-16
5.E-12	5.E-13	5.E-14	5E-15
5.E-11	5.E-12	5.E-13	5E-14
5.E-10	5.E-11	5.E-12	5E-13
1.E-09	1.E-10	5.E-11	5E-12

Table (3.2): *Dilutions for k. armiger target used for solid-phase RPA reactions and calibration curves for ssDNA and ds DNA*

dsDNA target generation:

The dsDNA target has been produced by running a PCR reaction using the same primers used for RPA for 15 cycles. The product was purified and verified by running a gel electrophoresis. The concentration was determined as follows: the product was quantified using the nanodrop. And by using a free online software to find the complementary for the ssDNA target, the total molecular weight for the product was calculated then the final concentration was easily calculated.

Detection:

For detection, the hybridized electrodes were incubated with 20 nM complementary probe (which it is complementary to the tail in the reverse primer) (*KA.HRP reporter*) in 10 mM tris buffer in 1 M NaCl for 30 min at 40^{O}C, and were washed for 2 min by a stirred distilled water before CA measurement. For CA measurements, 100 µL of 0.05 M PBS pH 7.4 was placed on the functionalized SPCE surface and the signal was being recorded, then 200 µL of TMB was added. The PBS measurements corresponds to the noise, and with the addition of the TMB a reduction current jump was recorded. The difference between the PBS reading and the TMB reading will represent the final measurements excluding the noise.

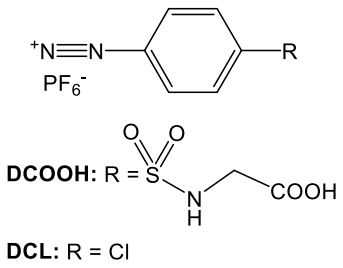

Figure (3.1): *Structures of DCOOH and DCL diazonium salts*

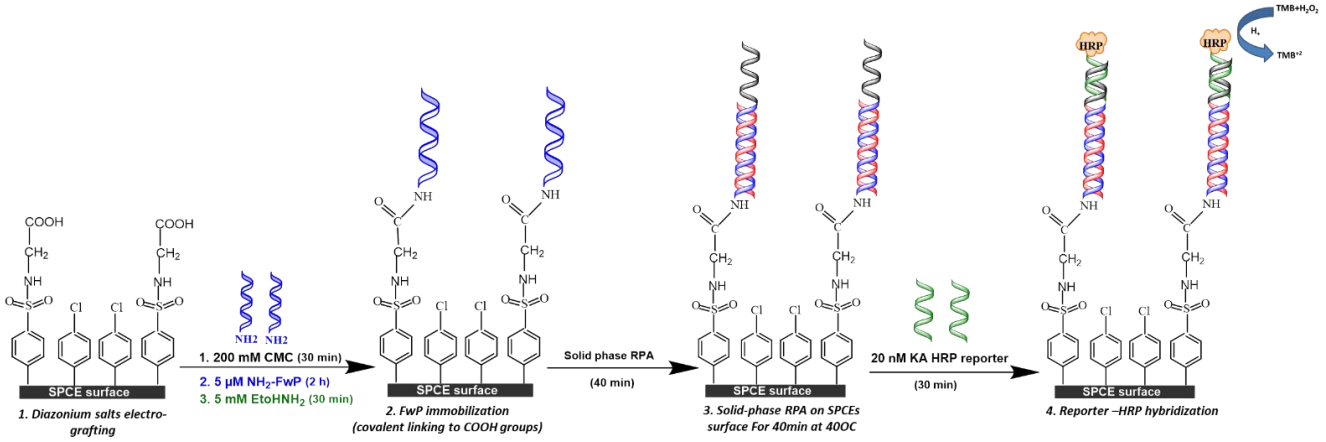

Figure (3.2): *Schematic representation for surface functionalization with NH_2-capture probe after mixed diazonium salts electro-grafting, RPA mixture components and reaction, and RPA hybridization on the functionalized surface for 40min at 40^{O}C.*

3.1.4. Results and discussion:

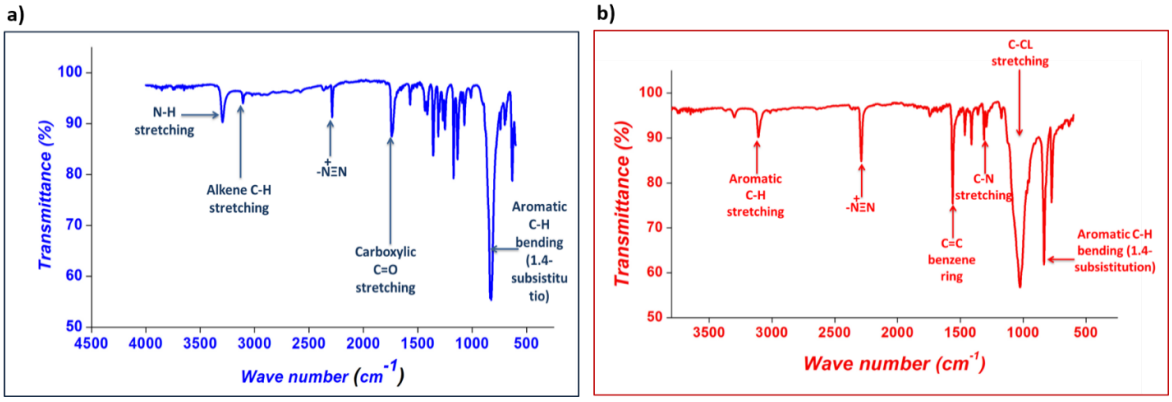

Figure (3.3): *IR characterization spectrum for: a) DCOOH and b) DCl*

FTIR analysis for the purified products is shown in fig (3.3). The DCOOH shows the characteristic bands for N-H stretching at 3400 cm^{-1}, and 1750 cm^{-1} for C=O stretching. While the DCl shows the characteristic band for the diazonium functional group stretching at 1000 cm^{-1} instead of 800 cm^{-1}. This shift could be due to the direct linking between the Cl and the aromatic ring.

<u>Parameters optimization:</u>

To quickly verify the system on SPCE surface ssDNA K. armiger target has been used in order to have a known starting concentration which is not as easy with dsDNA target. That means the system has been optimized with the ssDNA target and then compared with the response of the dsDNA target. As seen in figure (3.4), neither the developed system nor a mixture of two diazonium salts DCOOH and DCl did not show difference between the positive and

negative samples. Then instead of mixing the diazonium salts we opt to electro-graft them one by one in a so-called layer-by-layer electro-grafting (figure (3.5)).

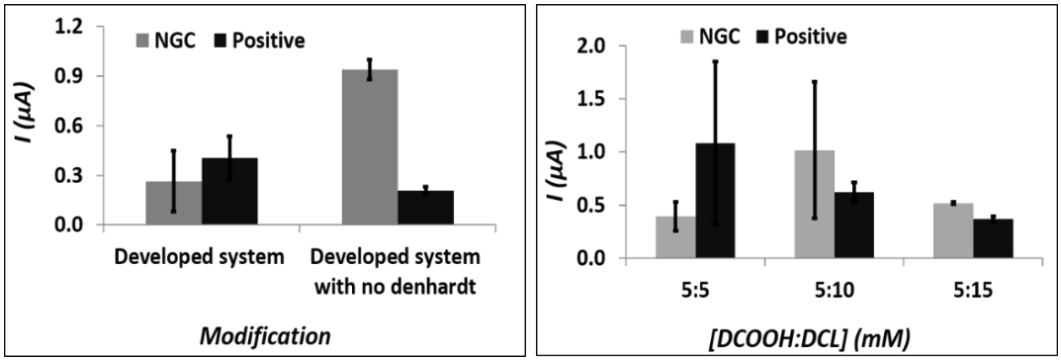

Figure (3.4): *CA measurements for:* ***a)*** *the developed system in chapter (2) using 2 cycles of DCOOH for electro-grafting and 1x Denhardt´s reagent as a blocking agent,* ***b)*** *Different concentration mixtures of DCOOH and DCL using DCL as a blocking agent or a back-filler*

The electro-grafting has been performed and monitored by CV; as well as grafted layer characterization after electro-grafting (figure 3.5b). The surface area is decreasing with more DCl cycles, which indicates surface coverage with the back filler. This has been confirmed by CV characterization where the surface after electro-grafting shows less acceibility. The FwP has been linked covalently to the –COOH groups in the grafted diazonium on the surface using the CDMI. Then the RPA mixture containing the reverse primer and the target was drop-casted on the surface and incubated for 40 min at 40^{O}C. The RevP contains a tail that is complementary to a reporter HRP. By hybridization for 30 min with this reporter we can detect if the amplification has taken place. Figure (3.5c) shows the system optimization using as criterion the ratio between the positive sample containing the target and the negative control (which contains no target, i.e. blank). The results obtained when applying 2 cycles and 1 cycle for each diazonium salts are comparable but higher HRP non-specific adsorption on the surface observed for 1 cycle application. This confirms the blocking behavior of the DCL by applying more cycles. This has been confirmed by using the 1 cycle of the DCOOH and adding more cycles of DCL. The maximum response obtained by applying 1 cycle of the DCOOH and 3 cycles of DCL; more cycles of DCL will block the surface and hinder the RPA reaction on the SPCE surface.

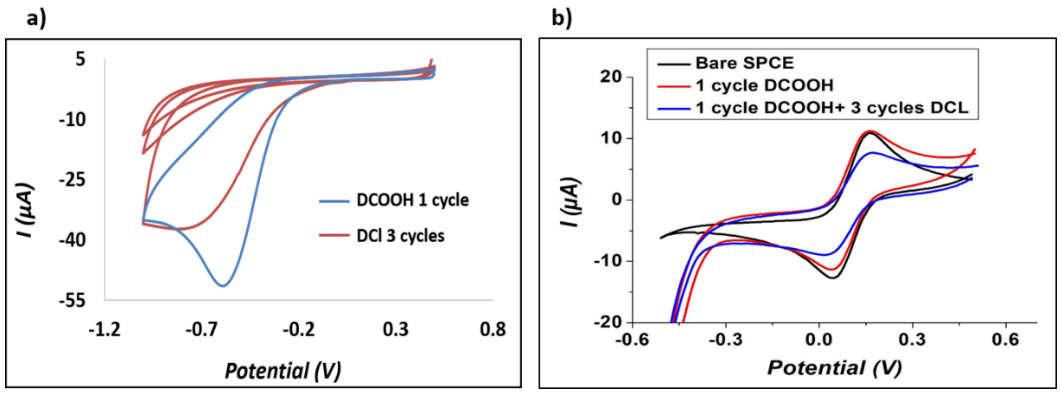

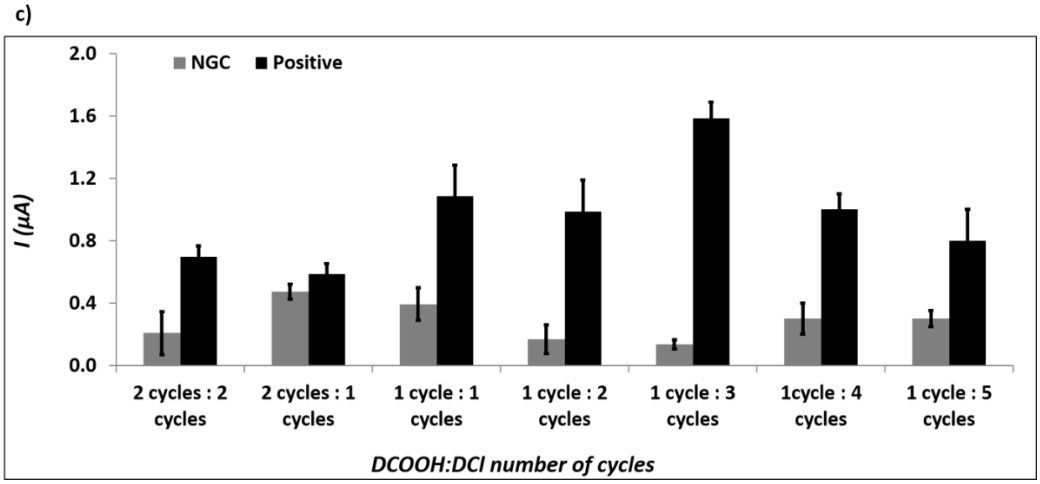

Figure (3.5): a) *Electro-grafting of DCOOH for 1 cycle and DCL for 3 cycles from 0.5 to -1 V at 50mV/s,* ***b)*** *cyclic voltammetry characterization after DCOOH and DCL electro-grafting for different DCOOH: DCl number of cycles ratio using 1mM $[Fe(CN)_6]^{-3/-2}$ containing 50mM Sr $(NO_3)_2$ electrolyte,* ***c)*** *CA measurements for optimization for DCOOH: DCl number of cycles needed to obtain a maximum CA response for hybridization of covalently linked FwP to COOH terminated electro-grafted diazonium after solid-phase RPA for ss K. armiger target on SPCEs surface*

Also, by using ssDNA *K. armiger* target it has been found that 30 min of RPA reaction on SPCE surface is enough to reach saturation of amplification (figure 3.6a). The hybridization should be for 30 min to produce the maximum response for the system (figure 3.6b). although at just 5 minutes more than 60% of the response is achieved.

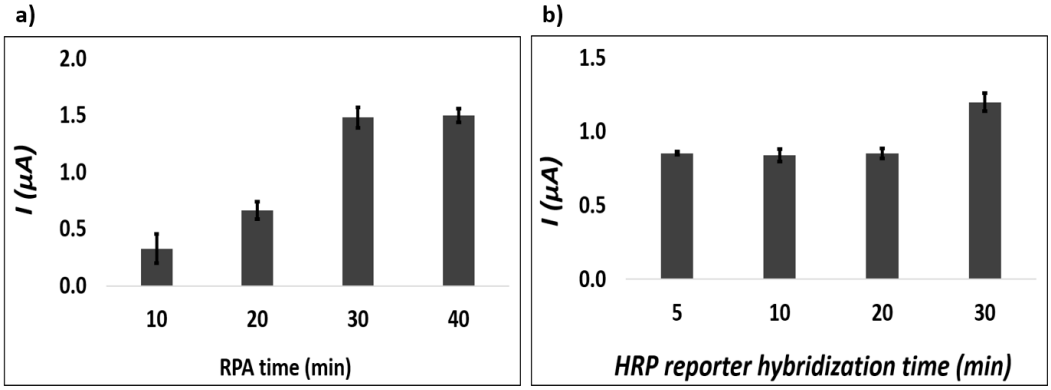

Figure (3.6): *CA measurements for the described system:* ***a)*** *RPA time optimization,* ***b)*** *HRP-reporter hybridization time optimization*

<u>Electro-grafted mix-layer characterization:</u>

CV characterization for the diazonium modified SPCE compared with the bare SPCE (figure 3.7) shows that electron transfer is inhibited with modification. This confirms the surface blocking by the mixed layers of diazonium salts. Besides, the reaction of the oxidation reduction for the Fe^{+3}/Fe^{+2} redox couple exhibits quasi-reversible behavior and an increase of capacitive current. It is believed that the terminated -COOH groups are directly affecting the electron

transfer process for the Fe^{+3}/Fe^{+2}. The protonation of these –COOH groups leads to instability of $[Fe(CN)_6]^{-3/-2}$ solution[142]

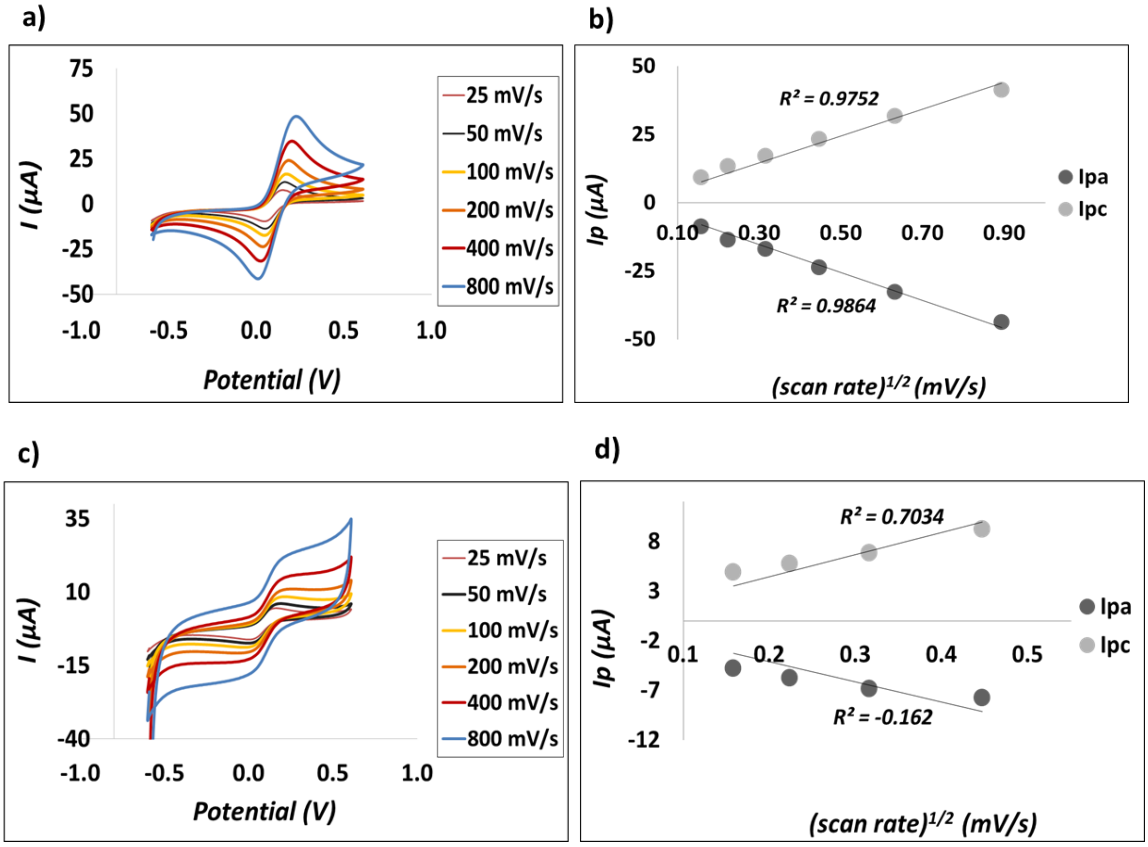

Figure (3.7): *Cyclic Voltammetry characterization using 1 mM $[Fe(CN)_6]^{-3/-2}$ containing 50 mM Sr $(NO_3)_2$ electrolyte:* ***a)*** *and* ***b)*** *Bare SPCE,* ***c)*** *and* ***d)*** *modified SPCE surface with diazonium mixed layers (DCOOH: DCL 1 cycle:3 cycles), c) and d) After capture probe immobilization*

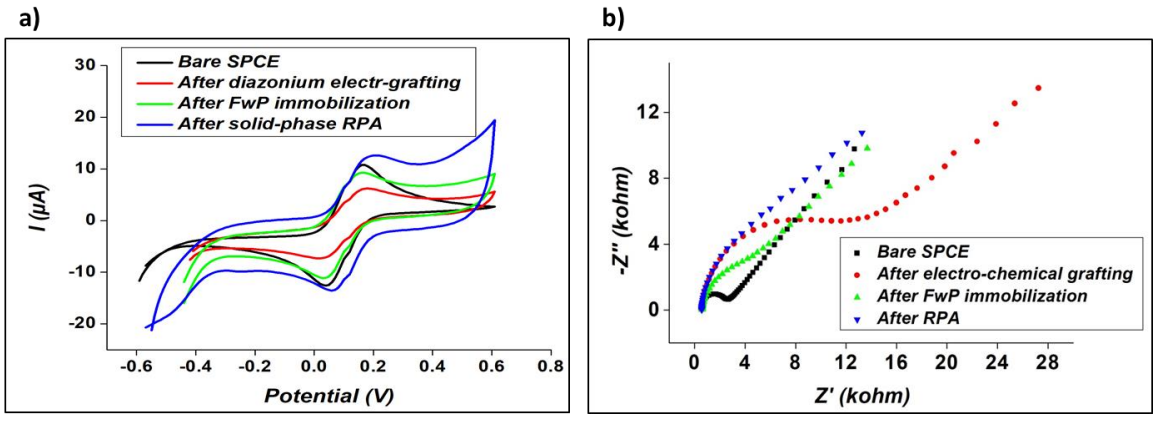

Figure (3.8): ***a)*** *Cyclic Voltammetry characterization using 1 mM $[Fe(CN)_6]^{-3/-2}$ containing 50 mM $Sr(NO_3)_2$ electrolyte for bare SPCE modified SPCE with diazonium electro-grafting, after FwP linking to the –COOH groups on the grated diazonium and after RPA for ssDNA target on the surface of SPCE using 100 mV/s scan rate; and* ***b)*** *Electrochemical impedance spectroscopy at 0.1 V, frequency range from 1000 to 0.01 HZ, and 10 mV points per decade*

CV characterization for SPCEs surfaces throughout the surface modifications is shown in fig (3.8a). The electro-grafting of diazonium results in CVs with lower peak currents which can be interpreted as blocking of the surface. After FwP linking the capacitive current appears to increase. Electro-grafting formed a layer on the surface of the SPCE that hinders electron transfer possibly by blocking the surface. These results are in agreements with the EIS results.

Electrode	Rs (Ω)	Rct (Ω)	-Z'' (Ω)
Bare SPCE	580	2600	1000
After electro-grafting	510	5300	11000
After FwP immobilization	554	3800	3000
After RPA	552	4000	4000

Table (3.3): *EIS characterization parameters obtained at 0.1 V, frequency range from 1000 to 0.01 HZ, and 10 mV points per decade and using 1 mM $[Fe(CN)_6]^{-3/-2}$ containing 50 mM $Sr(NO_3)_2$ electrolyte for bare SPCE modified SPCE with diazonium electro-grafting, after FwP linking to the –COOH groups on the grated diazonium and after RPA of ssDNA target on the surface of SPCE. Where the Rs is the solution resistance, Rct is the resistance at the solid-liquid interface, -Z'' is the imaginary component of impedance, C (Z) is the capacitance at the real impedance, and C (-Z'') is the capacitance at the imaginary component of impedance*

Figure (3.8b) shows the electrochemical impedance spectroscopy (EIS) characterization for the bare and modified SPCEs. The bare SPCE shows an equivalent electrical circuit containing of the solution resistance, a capacitance, and a constant phase element (CPE). The electro-grafting is increasing the capacitance and the interface resistance; this is because of the presence of the multi-layers on the surface. This grafted layer on the surface increases the amount of charging needed (capacitance) for the electron transfer. This value is well reduced when the -COOH terminal groups were linked to the FwP; this could be due to the electron diffusion facility by the ssDNA backbone, Table (3.3) summarizes the parameters. This is well shown even after RPA; the diffusion is very dominant with some small capacitor behavior, i.e. very small capacitance (solid-liquid interface phase charging value). It seems the FwP works as a molecular wire for ion transportation and this is even enhanced by hybridization. It is believed that the hybridization makes some conformational changes that enhance the electro-activity of the multi-layers-DNA film affects the solid-liquid interface.[143]

Figure (3.9) shows the XPS analysis for bare, grafted, and functionalized SPCEs surface. Carbon XPS analysis summarized in tables (3.4) shows that surface modification with the diazonium salts has led to a decrease in the intensity of the C-C due to the surface coverage and it decreased more after FwP immobilization. After electro-grafting the peak corresponds to C-O-C disappeared and it appeared back after FwP immobilization. Nitrogen XPS shows the NH characteristic peak after grafting and after functionalization with FwP. Besides, the presence of the amide peak at 403 after FwP functionalization, which confirms the successful functionalization. Oxygen XPS shows the characteristic peak for the organic CO for all three electrodes surfaces, which is expected.

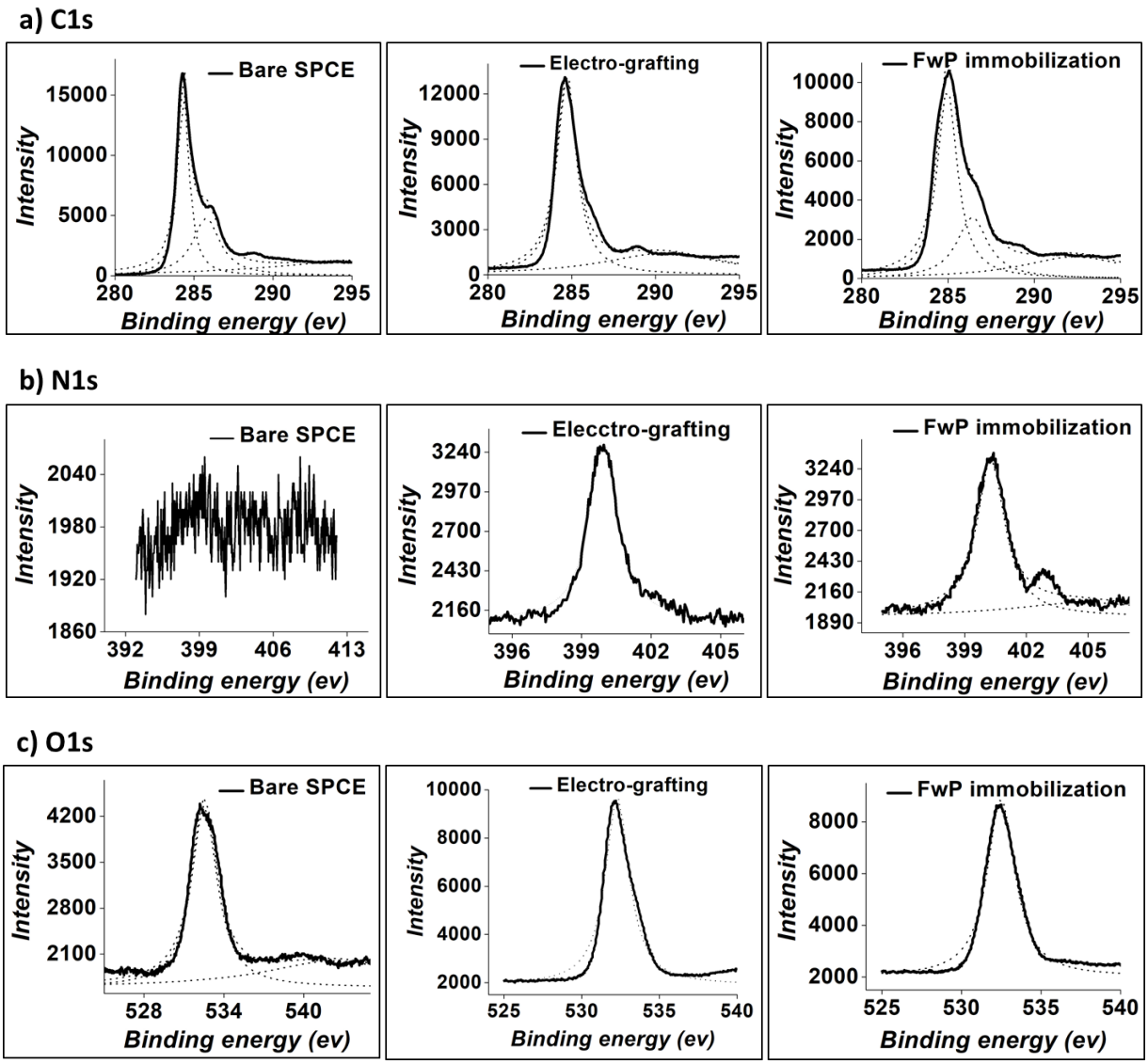

Figure (3.9): *X-Ray photoelectron spectroscopy (XPS) analysis (SPECS PHOIBOS 150 hemispherical energy analyzer) for bare, electro-grafted and modified SPCEs; the elements are:* ***a)*** *Carbon,* ***b)*** *Nitrogen,* ***c)*** *Oxygen*

1			2			3		
Bare SPCE			Diazonium electro-grafting			FwP immobilization		
Functional group	Binding energy (ev)	Intensity	Functional group	Binding energy (ev)	Intensity	Functional group	Binding energy (ev)	Intensity
C-C	284.3	16794	C-C	285	1282	C-C	285.2	1019
C-O-C	286	5271	C-O-C	-	-	C-O-C	286.8	4430
O-C=O	289	1623	O-C=O	289	1680	O-C=O	289.7	1510

Table (3.4): *C1s XPS characterization for:* ***1)*** *Bare SPCEs,* ***2)*** *After diazonium electro-grafting, and* ***3)*** *After FwP immobilization*

CA Detection:

Selectivity:

To demonstrate the selectivity of the developed system for ssDNA target and dsDNA target of *K. armiger*, a test against *K veneficum* was performed as in figure (3.10a and b). The selectivity for the ssDNA and dsDNA target is comparable with 3-4 times difference between the positive sample and the non-specific control (NSC) and the negative control (NGC). The dsDNA target was generated from the ssDNA target with PCR using the same primers used for the RPA for 15 cycles. The concentration was determined as follows: the product was quantified using the nanodrop. And by using a free online software to find the complementary for the ssDNA target, the total molecular weight for the product was calculated then the final concentration.

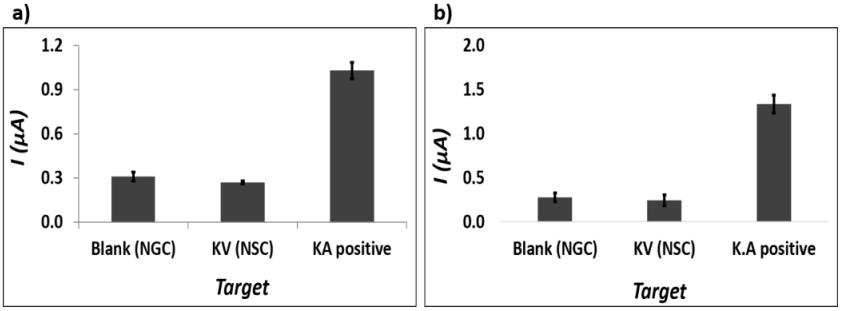

Figure (3.10): *System selectivity for the described system against karlodinium veneficum species (KV), 40 min RPA and 30 min hybridization:* ***a)*** *ssDNA target using 5 nM target final concentration and* ***b)*** *dsDNA target using 5 pM target final concentration; the NGC is the blank with no target, the KV is the non-specific control (NSC)*

Calibration curves:

The calibration curve for concentrations ranging from 0 to 10 nM concentrations for the ssDNA and from 0 to 50 pM for dsDNA KA target shows a logarithmic response (figure 3.11). The LOD for ssDNA target was found to be 2.8 pM with a linear range from 5 to 500 pM and 0.1 fM with a linear range from 0.5 fM to 5 pM respectively. The response of the NGC for the LOD graph for dsDNA is higher than the one obtained for the selectivity measurements. This is well noticeable for dsDNA target measurements and all the other measurements are shifted with the same shift in the NGC. Then the ratio between the NGC and all other measurements is stable. This could be due to the difference in mixing the RPA reaction before the drop-casting, were it could be left for 1 min and sometimes less for complete pellet dissolves.

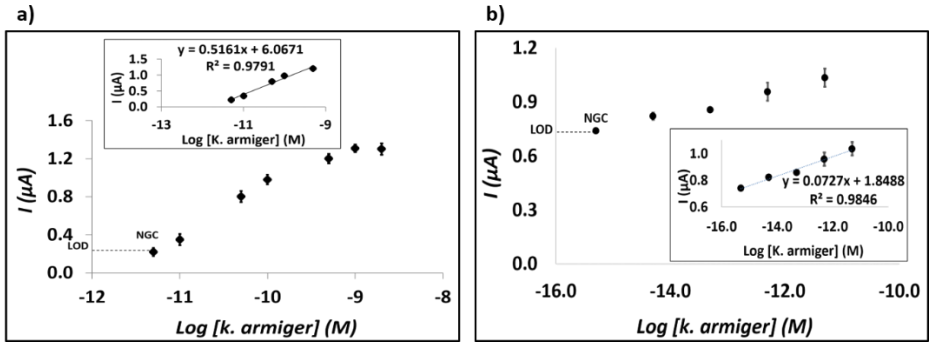

Figure (3.11): *Attempts to calculate the KA target LOD for the described solid-phase RPA system based on diazonium electro-grafting for 40 min RPA and 30 min hybridization on SPCEs surface:* ***a)*** *ssDNA target with a LOD of 2.8 pM with a linear range from 5 to 500 pM, and* ***b)*** *dsDNA target with a LOD of 0.1 fM with a linear range from 0.5 fM to 5 pM, NGC is the non-template control, measurements were performed at -0.2V potential for 250 s using 100 µL PBS 0.5 M for the first 100 s and 100 µL TMB substrate was added after 100 s.*

Parameter	**Target**	
	ssDNA	***dsDNA***
Selectivity against k. veneficum	√	√
LOD	2.8 pM	0.1 fM
Linear range	5 to 500 pM	0.5 fM to 5 pM

Table (3.5): *CA detection parameters*

<u>Real samples analysis:</u>

Genomic samples were analyzed using the developed system and the developed calibration curve for dsDNA solid phase amplification. The results obtained are listed in table (3.6) and compared with the values obtained by other amplification techniques. The system was able to estimate the genomic sample which are above the blank measurements and could detect a mixture of two different karlodinium species.

Sample	**Diazonium (fM)**	**qPCR (fM)**	**FC-labelled dATP (fM)**	**Recovery (%)**
S_1	-	0.5	0.7	-
S_2	-	1.3	1.3	-
S_3	13.5	11	6.7	118

Table (3.6): *Genomic real samples measurements compared with other methods*[144]*, S_1 is K. veneficum, S_2 and S_3 are a mixture of K. armiger and veneficum.*

3.1.5. Conclusion:

A system based mixed-layer electro-grafting on SPCEs surface for DNA detection has been developed. The system was successful, and the selectivity has been proved for ssDNA target and dsDNA target for proof-of-concept target *K. armiger* amplification and detection on the surface. The LOD for ssDNA target was found to be 2.8 pM with a linear range from 5 pM to 500pM for and 0.1 fM with a linear range from 0.5 fM to 5 pM. Real genomic samples have been tested and the system was able to estimate the genomic samples which are above the blank measurements.

II. Poly (L-Lysine) polymer drop-casting on screen printed electrodes

3.2.1. Problem:

To use the successful strategy used before to modify the surface of SPCEs using poly (L-Lysine) polymer (PLL) and aminated forward primer and polyethylene glycol diglycidyl ether (PEGDE) to perform solid phase RPA on SPCEs surface. The DNA probe is the NH_2-FwP, one of the RPA primers.

3.2.2 Solution:

In this study we are reporting a novel, fast, easy and efficient method for DNA amplification and detection. The system is based on SPCE modified with PLL, where the interaction between the DNA and PLL is a mixture between an electrostatic interaction and covalent interaction. The positive charge on the PLL interacts electrostatically with the negatively charge on the DNA backbone. And the amine could be covalently linked to aminated DNA probe using a cross-linker. The PLL was linked with the aminated forward primer (FwP) and the amplification takes place by adding the target and a reverse primer labeled with HRP (revP-HRP). Our approach of using revP-HRP has proven to decrease the amplification time and the assay time by eliminating an extra step for hybridization with a reporter. The LOD achieved by this method using synthetic DNA is 16.8 pM and a linear range from 50 pM to 50 nM for ssDNA and 0.1 fM and the liner range is from 0.75 fM to 7 fM for dsDNA for *k. armiger* target.

3.2.3 Materials and methods:

All reagents were used as received, Poly (L-lysine hydrobromide) PLK B20 average MW 4200 from Alamanda company. N-cyclohexyl-N-(2-morpholinoethyl)-carbodiimide methyl-p-toluene-Sulfonate (CMC), polyethylene glycol diglycidyl ether (PEGDE),), polyethylene glycol 400, polyethylene glycol 2000, phosphate buffered saline (PBS), strontium nitrate (Sr $(NO_3)_2$), potassium chloride (KCl), Sodium acetate, potassium hexacyanoferrate(III) ($K_3Fe(CN)_6$, 99+%), ruthenium hexamine chloride (III), and ethanolamine hydrochloride were purchased from Sigma-Aldrich. SPCEs (DRP-110) purchased from Dropsense with a diameter of 4 mm. Synthetic HPLC-grade oligonucleotides DNA probes were purchased from Biomers.net (Ulm, Germany):

Karlodinium armiger tailed forward primer (KA. FWP): 5'-NH2-ttt ttt ttt ttt ttt ata gct tca cag cag agg tta caa c-3'
Karlodinium armiger tailed reverse primer (KA. RevP primer): 5'-ttt ttt ttt ttt ttt tgt aaa acg acg gcc agt - 5 - aca cac atc caa cca tyt cac tg-3'
Karlodinium armiger reporter (complementary/KA.HRP reporter): 5'-HRP- act ggc cgt cgt ttt aca-3'
Karlodinium armiger DNA (template): ata gct tca cag cag agg tta caa cac caa tgc tgc tcc gct acc cgc gat ctc atg cac cag gga gcg gca aga agc cag agc ttc aag aca ccc cta ccc ccg tgc agg agc tca caa aga aag ttc aca gtg aga tgg ttg gat gtg tgt
Karlodinium veneficum DNA (non-specific control): ata gct tcg cag aca aag gtg aat ccc aat gct gct cca cta ccc gcg aac tgc taa cgc cag ggt gcg gaa gag aac tac ccc aac ccc cgc gca aga gct cac aaa gaa gtt cac agt gaa atg gtt gga tgt

All the electrochemical measurements were performed with a PC controlled PGSTAT12 Autolab potentiostat (EcoChemie, The Netherlands) using screen printed carbon (DRP-110). The electrochemical setup for SPCEs: working electrode: carbon disk (ϕ=4 mm), reference electrode: Ag/AgCl, counter electrode: carbon.

SPCEs surface modification:

A 25 µL of a mixture of 25% v/v of 0.5 mM PLL solution, 0.25 mM PEGDE solution, 5 mM PEG 400, and 0.1 mM NH_2-FwP was drop-casted on the SPCE surface. The electrodes were incubated overnight (or until complete dryness) under vacuum. After dryness, the SPCEs were, and incubated with 5 mM PEG400 for 1 h at 40^{O}C then washed for 2 min with a stirred distilled water. Reagent concentrations for optimization experiments were as follows:

Reagent	Concentrations used (mM)	constant reagent	Concentrations used (mM)
PLL	0, 0.05, 0.5	PEGDE, NH_2-FwP	0.25, 0.1
PEGDE	0, 0.25, 2.5	PLL, NH_2-FwP	0.5, 0.1
NH_2-FwP	0,0.005, 0.01, 0.02, 0.05, 0.1	PLL, PEGDE	0.5, 0.25

Table (3.7): *PLL, PEGDE, and NH2-FwP concentrations optimization experimental design*

dsDNA target generation:

The dsDNA target has been produced by running a PCR reaction using the same primers used for RPA for 15 cycles. The product was purified and verified by running a gel electrophoresis. The concentration was determined as follows: the product was quantified using the nanodrop. And by using a free online software to find the complementary for the ssDNA target, the total molecular weight for the product was calculated then the final concentration was easily calculated.

Solid-phase RPA on SPCE surface:

RPA cocktail, k. armiger dilutions, and CA detection were as described previously in the first section except for the hybridization we have followed two strategies: **(i)** if the RPA mixture includes the tailed reverse primer then the functionalized electrodes would be incubated with 20 nM complementary probe (which it is complementary to the tail in the reverse primer) (*KA.HRP reporter*) in 10 mM tris buffer in 1 M NaCl for 30 min at 40^{O}C, **(ii)** if the RPA mixture includes the reverse primer labelled with HRP, then the detection could be performed directly after the amplification. 25 µL of the prepared RPA mixture was drop-casted on the modified SPCEs surface with aminated FwP and incubated for 20 min at 40^{o}C inside atmosphere-controlled chamber for SPCEs; formation of any air bubbles while drop-casting should be avoided. Then the electrodes were washed by immersing in a magnetic stirred distilled water for 2 min, and they were ready for CA measurements. To perform the CA measurements using -0.2 V potential, 100 µL of 0.5 M PBS buffer was drop-casted on the functionalized surface and the CA response was recorded for 200 sec, then another 100 µL for 100 sec of TMB for ELISA was added to follow the change in signal due to the reduction and color change from colorless to blue could be observed as well.

3.2.4. Results and discussion:

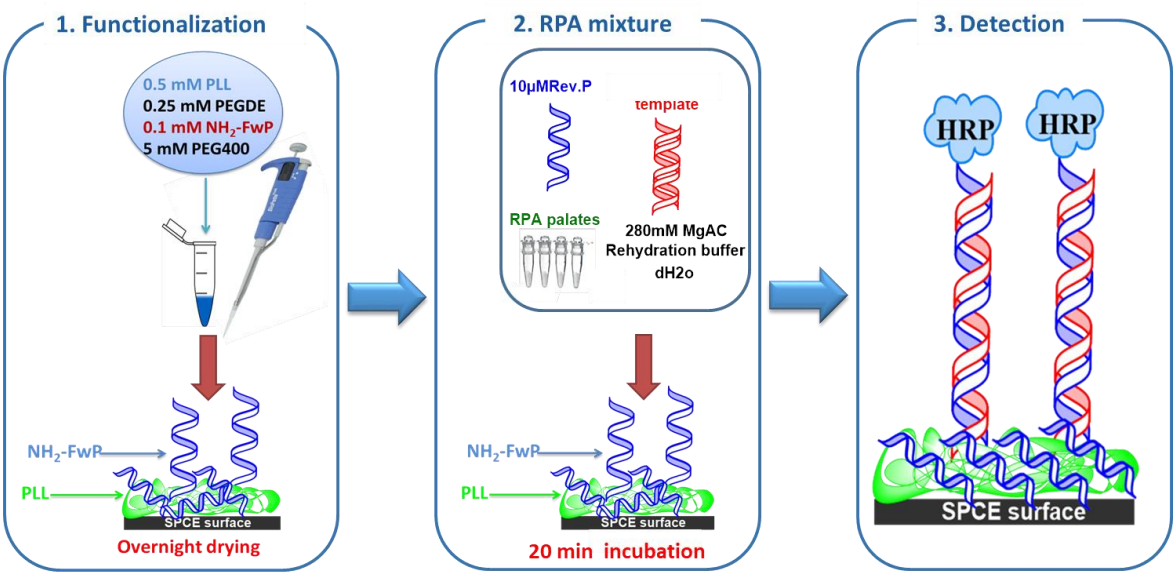

Figure (3.12): *Schematic representation for surface functionalization with PLL and NH_2-Fw primer, and RPA mixture components and reaction on the functionalized surface for 20 min at 40^oC.*

Parameters optimization:

As previously described in section (1) ssDNA K. armiger target has been used to optimize the system. The use of HRP as an electrochemical redox indicator has the drawback that it will be non-specifically adsorbed on the SPCEs surface. Considering the rough, irregular, and non-homogenous surface, a suitable blocking agent should be used in order to minimize the HRP non-specific adsorption. Different tests using different concentrations of PEG 400 has been performed in order to block the surface of the SPCEs against HRP non-specific adsorption. Also, the use of the reverse primer labeled with HRP versus the reporter HRP for the CA detection has been studied as in table (3.8). For solid phase the amplification must take place on the surface, where the forward primer is immobilized on the surface and the reverse primer and the target would be added with the RPA cocktail. The use of the labelled reverse primer with HRP showing the best difference between the negative control and the positive k. armiger sample. This leads to ability for the detection right after the amplification and eliminating one extra step for reporter hybridization. Then by using this HRP-labelled primer the number of reagents and steps were decreased, and the assay was faster.

PLL (mM)	PEG400 con-immobilized (mM)	PEG400/1h (mM)	NGC (µA)	KA positive (µA)	Ratio*	Reporting probe
0.5	5	25	1.18	2.35	1.99	KA reporter-HRP
0.5	-	7.5	1.48	3.69	2.49	Rev.P-HRP
0.5	5	5	1.69	9.75	5.77	Rev.P-HRP
0.5	10	-	3.11	9.02	2.90	Rev.P-HRP

Table (3.8): *Testing two different concentrations of PEG400 for surface blocking or to reduce HRP non-specific adsorption, the detection has been tested either by using a k. armiger reporter complementary to a tail in the reverse primer or by a labelled reverse primer with HRP, the Ratio* is the ratio between the response of the k. armiger positive sample and that of the negative control (NGC)*

A study has been performed to evaluate the effect of concentration of PLL, FwP and PEGDE to determine the optimum concentration (Figure 3.13). The results show that the optimum concentration for PLL and PEGDE to obtain the maximum and reproducible signal for solid phase RPA is 0.5 mM and 0.25 mM respectively (table 3.9). The PEGDE contains two very reactive epoxy groups can cross-kink two amines, the PLL contains one primary amine that means each one molecule of PEGDE will link two molecules of PLL. Then we can say this is a confirmation that there is a mixed interaction on the surface, one is an electrostatic interaction where the FwP probes will be oriented randomly. Also, a covalent cross-linking interaction where the FwP probes will be chemically cross-linked by the PEGDE to the amine in the PLL, this interaction provides the probes orientation for amplification and hybridization.

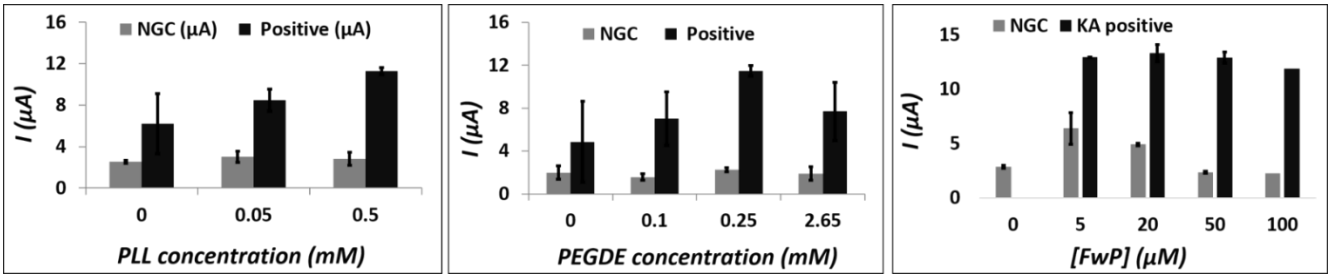

Figure (3.13): *Concentration optimization for ss K. armiger target for the described system:* ***a)*** *PLL using 0.25 mM PEGDE and 0.1 mM NH_2-FwP,* ***b)*** *PEGDE using 0.5 mM PLL and 0.1 mM NH_2-FwP, and* ***c)*** *NH_2-FwP using 0.5 mM PLL and 0.25 mM PEGDE*

a)

[PLL] (mM)	Ratio*
0	2.5
0.05	2.8
0.5	4.0

b)

[PEGDE] (mM)	Ratio*
0	2.5
0.1	4.5
0.25	5.1
2.65	4.1

c)

[FwP] (mM)	Ratio*
0	-
0.005	2.03
0.02	2.71
0.05	5.51
0.1	5.32

Table (3.9): *Ratio* is the ratio between the negative and the ss k. armiger positive for:* ***a)*** *PLL using 0.25 mM PEGDE and 0.1 mM NH_2-FwP,* ***b)*** *PEGDE using 0.5 mM PLL and 0.1 mM NH_2-FwP, and* ***c)*** *NH_2-FwP using 0.5 mM PLL and 0.25 mM PEGDE*

To optimize the RPA time on the SPCEs surface, another systematic study was performed for different RPA times. It was found that 20 min for RPA on the surface is showing the maximum response, i.e. the amplification reaches saturation after 20 min (table 3.10 summarizes the values for the negative controls, *k. armiger* positive samples, and the ratio between the negative control and the positive). The signal has been evaluated by taking the ratio between the positive and the negative control (blank, i.e. no target). To confirm the 20 min RPA time on the surface, different target concentrations have been compared for 20 min and 40 min RPA on the surface. Figure (3.14) and confirms the amplification saturation after 20 min. Then we can say we have developed a 20 min assay for RPA and detection.

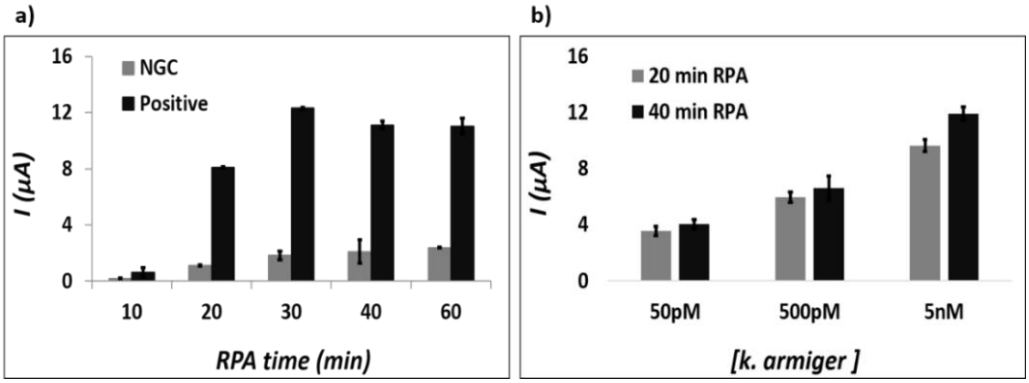

Figure (3.14): *CA measurements for the described system using 0.5 mM PLL, 0.25 mM PEGDE, and 0.1 mM NH_2-FwP SPCEs:* ***a)*** *RPA time optimization,* ***b)*** *Different k. armiger target concentrations responses comparison at 20 min and 40 min RPA reaction time for modified SPCEs surface with*

RPA time (min)	Ratio*
10	3.65
20	7.30
30	6.75
40	5.30
60	4.62

Table (3.10): *Ratio between the negative and the ss k. armiger positive for different RPA times on SPCEs surface*

PLL film characterization:

Figure (3.15) shows the electrochemical CV characterization; the linearity observed after modification with the PLL and the NH_2-FwP compared with the bare electrode indicates that the electron diffusion process has not been blocked due to the modification.

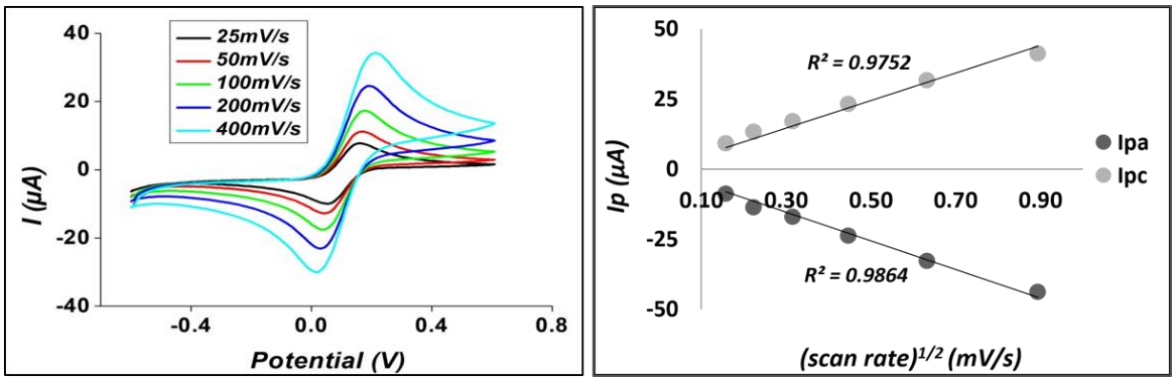

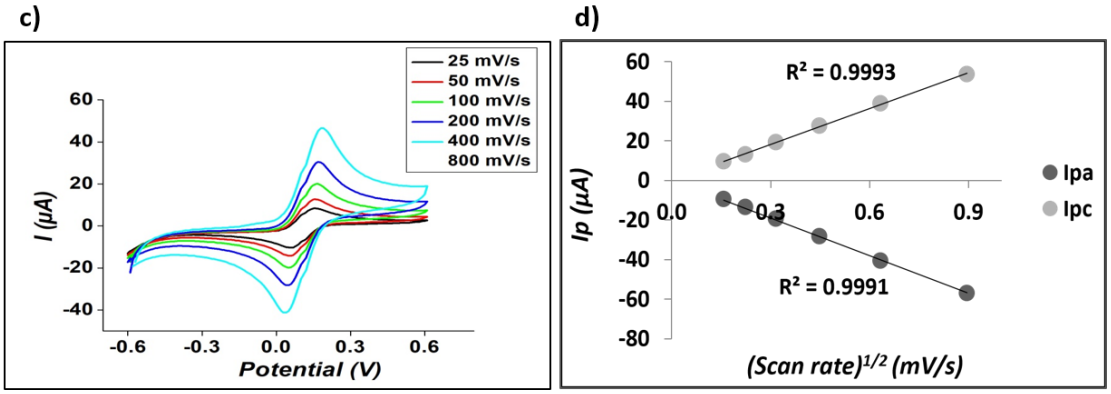

Figure (3.15): *Cyclic Voltammetry characterization using 1 mM $[Fe(CN)_6]^{-3/-2}$ containing 50 mM Sr (NO_3) electrolyte:* ***a)*** *Peak current VS (scan rate)$^{1/2}$ for bare electrode,* ***b)*** *Maximum of peak current VS (scan rate)$^{1/2}$ for the bare SPCE,* ***c)*** *) Peak current VS (scan rate)$^{1/2}$ for modified SPCE surface with PLL, and* ***d)*** *Maximum of peak current VS (scan rate)$^{1/2}$ for the modified SPCE surface with PLL, the modification performed by using 0.5 mM PLL, 0.25 mM PEGDE, and 0.1 mM NH_2-FwP*

As in Figure (3.16a), the CV surface characterization shows that there is an increase in capacitance with every modification step. with every modification step. The difference in the CV shape for bare and modified electrode is not significant and not showing any evidence for any surface modification with the PLL, but after RPA on the surface the shape changes. The shape is more like a polymeric surface coating which indicates the presence of a dense layer on the surface yet permeable to the diffusing species. This could be due to the amplification on the surface as well as the presence of all residues of the RPA reaction on the surface even after washing.

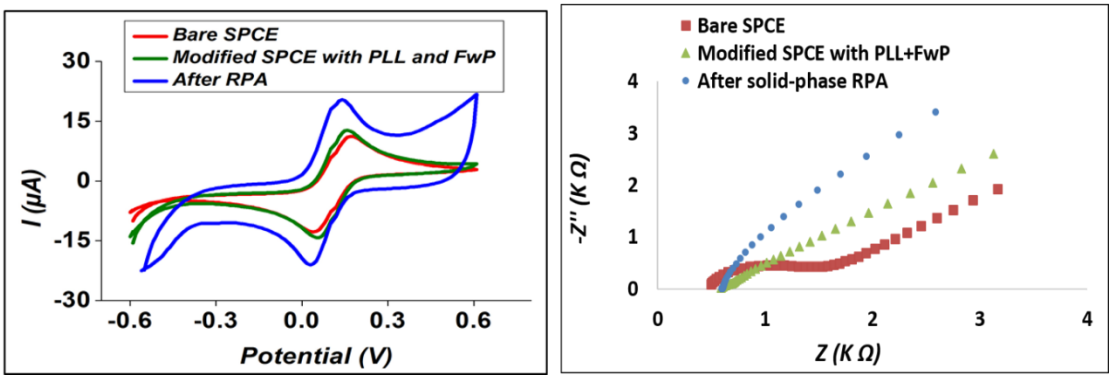

Figure (3.16): ***a)*** *Cyclic Voltammetry characterization using 1 mM $[Fe(CN)_6]^{-3/-2}$ containing 50 mM Sr (NO_3) electrolyte for bare SPCE and modified SPCE (using 0.5mM PLL, 0.25 mM PEGDE, and 0.1 mM NH_2-FwP), and after RPA on the surface of SPCE at 100 mV/s scan rate.* ***b)*** *Electrochemical impedance spectroscopy at 0.1 V, frequency range from 1000 to 0.01 HZ, and 10 mV points per decade for bare SPCE, modified with PLL and FwP, and after RPA for ssDNA target*

EIS measurements for each modification step compared with the bare SPCEs (Figure 3.16b, and table (3.11) show a significant change between the bare and modified SPCE. the system electronic circuit has changed from having a charging capacitance behavior to fully permeable membrane for modified SPCEs with PLL and FwP.

Electrode	Z' (KΩ)	-Z'' (KΩ)
Bare SPCE	495.6	91.9
modified with PLL and FwP	590.4	24.6
After RPA	594.8	6.1

Table (3.11): *EIS real and imaginary components of resistance obtained at 0.1 V, frequency range from 1000 to 0.01 HZ, and 10 mV points per decade and using 1 mM $[Fe(CN)_6]^{-3/-2}$ containing 50 mM Sr (NO_3) electrolyte for bare SPCE, modified SPCE with PLL and FwP, and after RPA on the surface of SPCE*

CA detection:

Selectivity:

To demonstrate the selectivity of the developed system for ssDNA target and dsDNA target of karlodinium armiger, a test against karlodinium veneficum was performed as in figure (3.17). The ssDNA target used for the selectivity measurements is half the concentration used for optimization. This explains the 3-4 times difference between the negative control (NGC) or the non-specific control (NSC) compared with the 7 times difference on the optimization. The dsDNA target was generated from the ssDNA target with PCR using the same primers used for the RPA for 15 cycles. The concentration was determined as follows: the product was quantified using the nanodrop. And by using a free online software to find the complementary for the ssDNA target, the total molecular weight for the product was calculated then the final concentration.

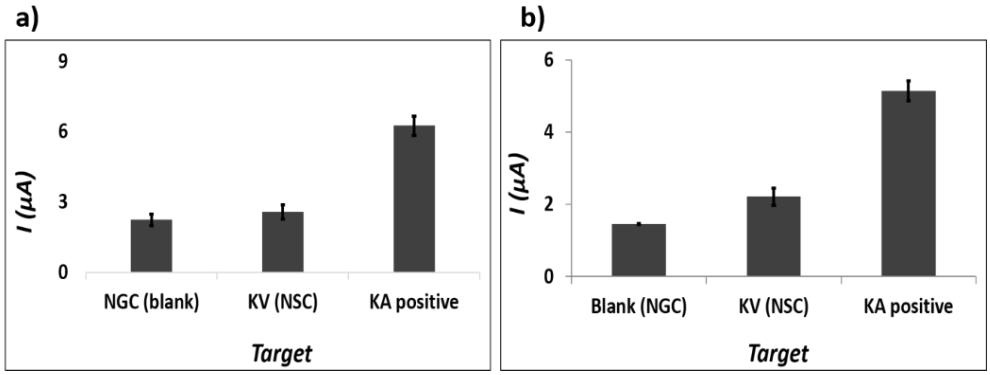

Figure (3.17): *System selectivity for the described system against karlodinium veneficum species (KV), 20 min RPA:* ***a)*** *ssDNA target using 5 nM target final concentration and* ***b)*** *dsDNA target using 5 pM target final concentration; the NGC is the blank with no target, the KV is the non-specific control (NSC)*

Calibration curves:

To determine the LOD a series of concentrations have been tested for ssDNA and dsDNA taregt, shown in Figure (3.18). The LOD for ssDNA target is found to be 16.8 pM and a linear range from 50 pM to 50 nM for the 20 min RPA. The LOD for dsDNA target was found to be 0.13 fM, and the liner range is from 0.75 fM to 7 fM. All the parameters obtained for the CA detection are summarized in table (3.12).

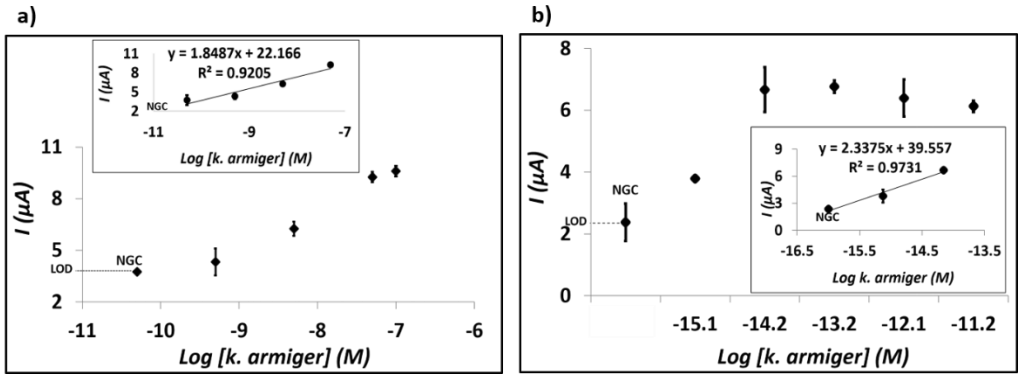

Figure (3.18): *Attempts to calculate the KA target LOD for the described solid-phase RPA system based on PLL drop-casting for 20 min RPA on SPCEs surface for:* ***a)*** *ssDNA target with a LOD of 16.8 pM and a linear range from 50 pM to 50 nM,* ***b)*** *dsDNA target, the LOD is 0.13 fM , and the linear range is from 0.75 fM to 7 fM. NGC is the non-template control; measurements were performed at -0.2V potential for 250 s using 100 µL PBS 0.5 M for the first 100 s and 100 µL TMB substrate was added after 100 s*

Parameter	**Target**	
	ssDNA	***dsDNA***
Selectivity against *K. veneficum*	√	√
LOD	16.8 pM	0.13 fM
Linear range	50 pM – 50 nM	0.75 – 7 fM

Table (3.12): *CA detection parameters*

Real sample analysis:

Genomic samples were analyzed using the developed system and the developed calibration curve for dsDNA solid phase amplification. The results obtained are listed in table (3.13) and compared with the values obtained by other amplification techniques. The system was able to estimate the genomic sample which are above the blank measurements and could detect a mixture of two different karlodinium species.

Sample	**PLL (fM)**	**qPCR (fM)**	**FC-labelled dATP (fM)**	**Recovery (%)**
S_1	-	0.5	0.7	-
S_2	0.67	1.3	1.3	51.5
S_3	1	11	6.7	10

Table (3.13): *Genomic real samples measurements compared with other methods*[144]*, S_1 is K. veneficum, S_2 and S_3 are a mixture of K. armiger and veneficum.*

3.2.5. Conclusion:

A novel, fast, simple, easy, and direct method has been developed for DNA amplification and detection on SPCEs surface using poly (L-Lysine) polymer. The interaction between the PLL and DNA is a mixture between an electrostatic interaction and covalent interaction by using PEGDE as a cross-linker. The method has been tested for ssDNA target amplification as well as for dsDNA target, and it was shown to work for both targets with more favorable for dsDNA target. This confirms the suitability of our approach for real sample analysis. The LOD for ssDNA target is found to be 16.8 pM and a linear range from 50 pM to 50 nM and for dsDNA target was found to be 0.13 fM, and the liner range is from 0.75 fM to 7 fM.

CHAPTER IV

APPLICATIONS

2. LIQUID-PHASE RPA

Introduction

In this chapter we are performing RPA in liquid-phase. The RPA was performed by using the forward and reverse primers with the RPA reagents. The incubation was performed for the specific time at 40^{O}C. The surface of SPCEs has been optimized and tested for functionalization with the capture probe. After amplification the hybridization on the SPCEs surface was achieved. The reverse primer labelled with HRP has been used as well, to reduce the number of assay steps. The analysis time for the two developed systems is 35 min, which is good and well below the design requirements we had set for the developed POC system.

The results in this chapter indicates that the systems are more stable and reliable for the solid phase RPA compared with the liquid phase RPA. Solid phase RPA is easier, simpler, and faster; besides the results are more reproducible. Also, solid phase RPA provides lower LODs for especially for the system developed for large scale production, i.e. polymer-based system.

I. Liquid-phase RPA

4.1.1. Problem:

Liquid-phase RPA parameters optimization

4.1.2. Solution:

Recombinase polymerase amplification (RPA) is a fast and simple approach for DNA amplification. It is a rapid process because there is no need for cycling, and it can be performed for a wide range of temperature (20 to 45^{O}C). It is simple because you just need two sets of primers, forward primer and reverse primer, binding proteins, amplification enzyme, and some crowding reagents. The detection can be done by gel electrophoresis as well as electrochemistry or fluorescence. The gel electrophoresis allows better insight of the amplification process because it separates products according to their size. Especially with the use of the labelled reverse primer with the HRP the amplicon size can be altered and detected on the gel. In this section there is a full description for the amplification in solution and gel characterization afterwards. Also, we are studying the influence of using labelled reverse primer with HRP compared to using an un-labelled one.

4.1.3. Materials and methods:

Agarose gel, 1x TBE buffer, Synthetic HPLC-grade DNA probes were purchased from Biomers.net (Ulm, Germany) having the following sequences:

Karlodinium armiger tailed capture probe (KA. Capture probe): 5'-NH2- ttc att gag ttc gtc gta at ttt ttt ttt ttt ttt-3'

Karlodinium armiger tailed reverse primer (KA. RevP primer): 5'-ttt ttt ttt ttt ttt tgt aaa acg acg gcc agt - 5 - aca cac atc caa cca tyt cac tg-3'

Karlodinium armiger tailed forward primer (KA. FwP primer): 5'- att acg acg aac tca atg aa - 5 - ata gct tca cag cag agg tta caa c-3'

Karlodinium armiger reporter (complementary/KA.HRP reporter): 5'-HRP- act ggc cgt cgt ttt aca-3'

Karlodinium armiger DNA (template): ata gct tca cag cag agg tta caa cac caa tgc tgc tcc gct acc cgc gat ctc atg cac cag gga gcg gca aga agc cag agc ttc aag aca ccc cta ccc ccg tgc agg agc tca caa aga aag ttc aca gtg aga tgg ttg gat gtg tgt

Liquid-phase RPA:

RPA cocktail: The final volume was adjusted to be 50 µL as described by the manufacturer, RPA reaction was incubated for 40 min at 40^{O}C and the product was purified before running the gel electrophoresis. The mixture was as follows: 10.6 µL distilled water, 29.5 µL rehydration buffer, 2.4 µL RevP (10 µM), 2.4 µL FwP (10 µM), 1 pellet, 2.5 µL MgAcet (280 mM), 5 µL of 20 nM target. For the negative control, 5 µL of distilled water was used. Proteinase K was added to digest all the proteins involved in the RPA amplification process. The product was purified and verified with gel electrophoresis.

PCR for ssDNA target to generate dsDNA target:

The dsDNA target has been produced by running a PCR reaction using the same primers used for RPA for 15 cycles. The concentration was determined as follows: the product was quantified using the nanodrop. And by using a free online software to find the complementary for the ssDNA target, the total molecular weight for the product was calculated then the final concentration. The product after purification seen as in Figure (4.1.).

4.1.4. Results and discussion:

Parameters optimization:

In order to optimize the time needed for the amplification to reach saturation, the RPA reaction was run for different times as in figure (4.1a). From the figure, 30 min is enough to reach amplification saturation. The dsDNA target has been produced by running a PCR reaction for 15 cycles, the product after purification seen in Figure (4.1b).

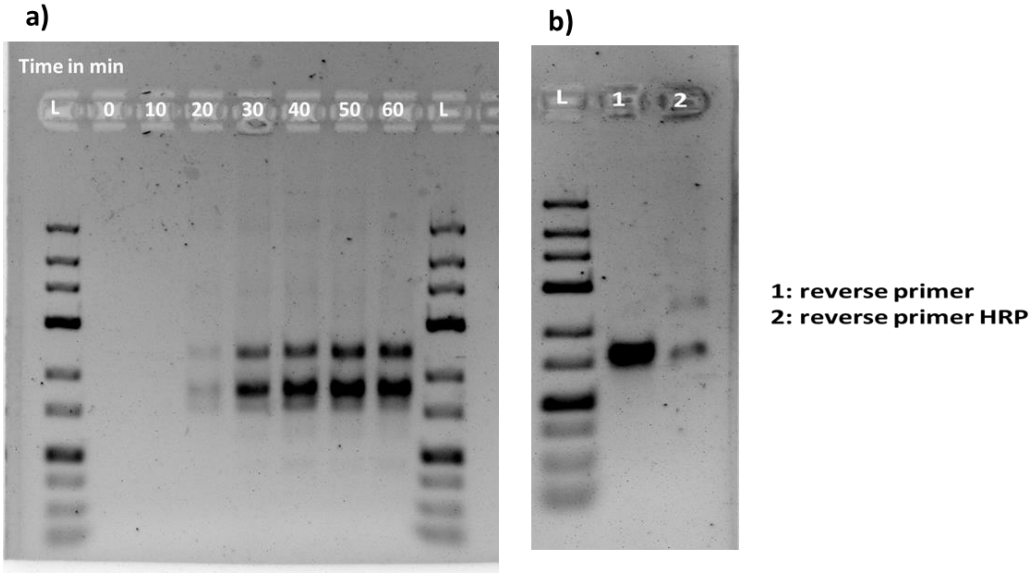

Figure (4.1): a) *RPA time optimization,* ***b)*** *PCR purified product for ssDNA target amplification*

As seen from figure (4.1a), there is an extra band with higher molecular weight than the amplified target. To compare between the use of ssDNA and dsDNA target, a calibration curve for different concentrations for ssDNA target and dsDNA target has been performed and the extra band appears for the ssDNA target but not for dsDNA target. To verify this extra band an extra study was performed using un-labelled reverse primer vs labelled reverse primer as shown in figure (4.2).

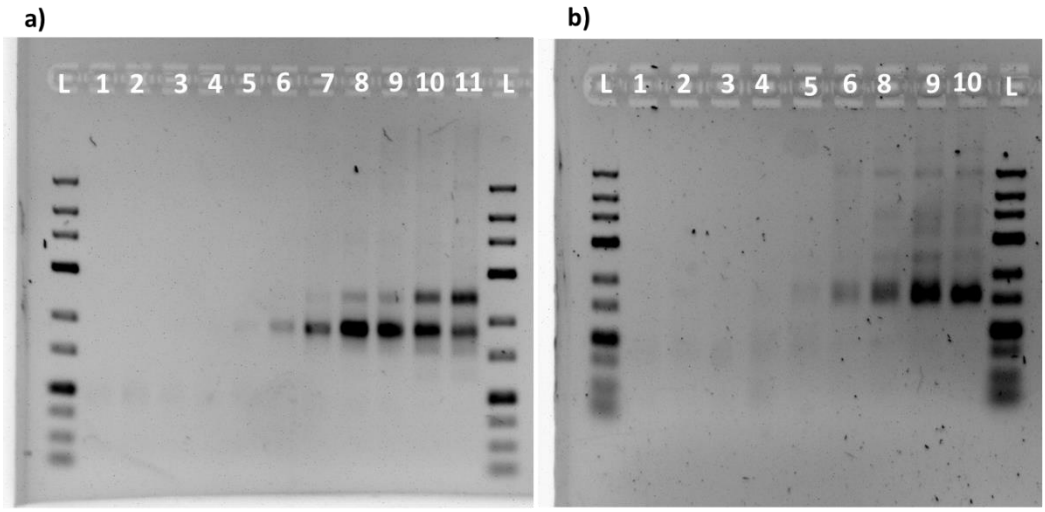

No	1	2	3	4	5	6	7	8	9	10	11
[target]	0	5pM	10pM	50pM	100pM	500pM	1nM	5nM	10nM	50nM	100nM

Figure (4.2): *Liquid phase RPA for different target concentrations:* ***a)*** *ssDNA target,* ***b)*** *dsDNA target*

In order to evaluate the nature of this second product, different RPA reactions have been performed for ssDNA and dsDNA target with and without the pellet. As seen from figure (4.3), without the pellet there is no amplification take place. The dry pellet contains the required enzymes, chelating agents, and proteins for amplification. It´s noted that there is no primer dimer or template dimer when the reagents mixed in the absence of the pellet, and there is no by product amplification with the use of the non-labelled reverse primer with HRP. Then we can conclude that the extra band for ssDNA amplification is because of the use of the reverse primer labelled with HRP, and one more evidence is well shown in figure (4.1) where the PCR for the ssDNA performed to obtain the dsDNA *k. armiger* target. Despite the dissolution and no-stability of the labelled reverse primer with the HRP, the extra band could be seen and identified in the gel even after purification.

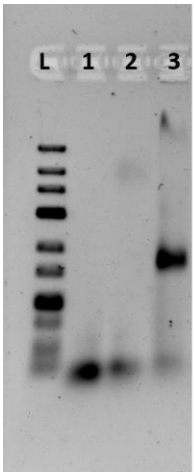

L = Ladder

1 = RPA reaction mixture without the pellet and ssDNA *k. armiger* target using tailed reverse primer

2 = RPA reaction mixture without the pellet and ssDNA *k. armiger* target using reverse primer labelled with HRP

3 = RPA reaction mixture included the pellet and ssDNA *k. armiger* target

Figure (4.3): *Liquid phase RPA for ssDNA and dsDNA target for k. armiger with and without the pellet*

4.1.5. Conclusion:

Using the reverse primer labelled with HRP for liquid phase RPA has been proven working for ssDNA and dsDNA target. The ssDNA target amplification shows an extra amplified band, this may affect the LOD when performing the electrochemical detection because the two amplified products will compete for hybridization with the surface probe.

II. Diazonium electro-grafting on screen printed electrodes

4.1.1. Problem:

K. armiger amplification using liquid-phase RPA and electrochemical detection of the amplificon on SPCEs surface using diazonium electro-grafting and covalently linking the NH_2-capture probe.

4.1.2. Solution:

The electrochemical detection could be performed on SPCEs surface using *k. armiger* capture probe. A response could not be obtained for ssDNA due to the formation of unlabelled dsDNA before any label could be incorporated. The developed system was un-successful for electrochemical detection for ssDNA. And in order to be able to calculate the true LOD for dsDNA, a smaller concentration range should be performed.

4.1.3. Materials and methods:

All reagents are as described in chapter (3) section (1).

Diazonium grafting:

Same as described in chapter (3) section (1).

Aminated KA. capture probe immobilization:

The surface was activated by 200 mM CDMI, was incubated for 30 min at 40^{O}C and was washed with distilled water. 30 µL of 5 µM KA. Capture probe in 0.05 M PBS buffer pH 7.4 was drop-casted on the surface for 2 h; then was washed with distilled water. 30 µL of 5 mM ethanolamine in distilled water at pH 8.0 was drop-casted and was incubated for 30 min at 40^{O}C to block all non-linked diazonium carboxylic groups on the surface, then was washed with distilled water dried with argon. The electrodes were stored until used.

Liquid-phase RPA:

RPA cocktail: The final volume was adjusted to be 50 µL as described by the manufacturer as in table (3.2.1). k. armiger dilutions, and CA detection were as described previously in chapter (3) section (2), where the RPA mixture includes the reverse primer labelled with HRP then the detection could be performed directly after the amplification.

Volume per reaction (µL)	
milliQ	12.2
Rehrydation buffer	29.5
RvP tailed 10uM	2.4
FwP tailed 10uM	2.4
Pellet	0.5
MgAcet 280mM	2.5
target 1nM/milliQ	1
TOTAL	***46.5***

Table (4.1): *Liquid-phase RPA mixture incubated for 40 min at 40^{O}C then drop-casted on the modified SPCEs surface with mixed layer diazonium electro-grafting and NH2-capture probe*

Hybridization on SPCEs:

Same as described in chapter (3) section (1).

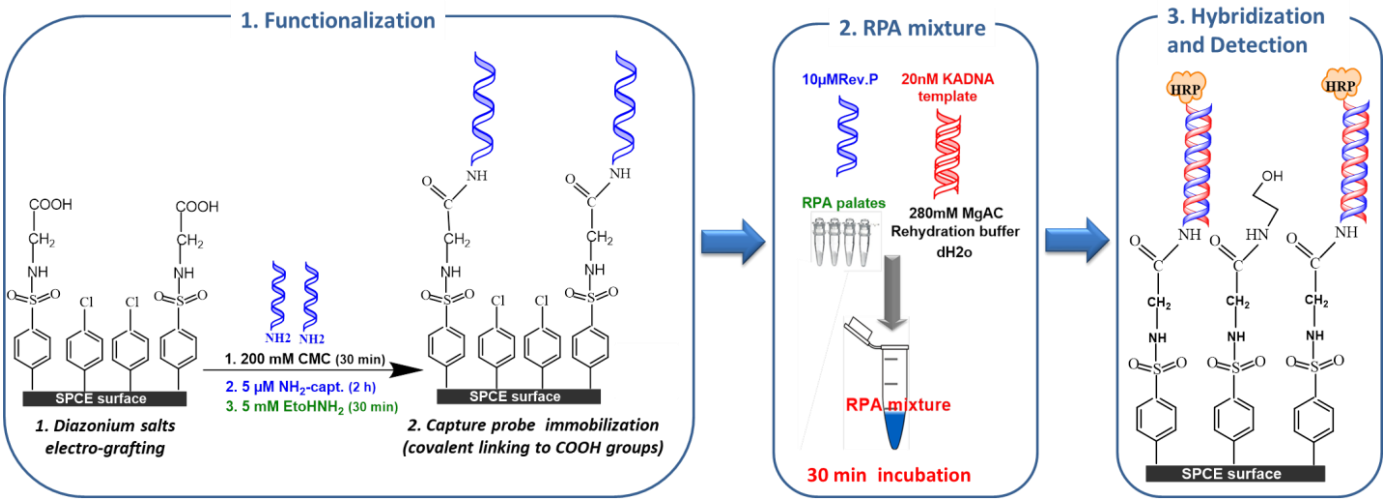

Figure (4.4): *Schematic representation for surface functionalization with PLL and NH_2-capture probe, RPA mixture components and reaction, and hybridization and detection on the functionalized surface*

4.1.4. Results and discussion:

Electro-grafted mix-layer characterization:

As explained before in chapter (3) section (1) for the solid-phase RPA, the electron transfer seems to be inhibited. This confirms the surface blocking by the mixed layers of diazonium salts.

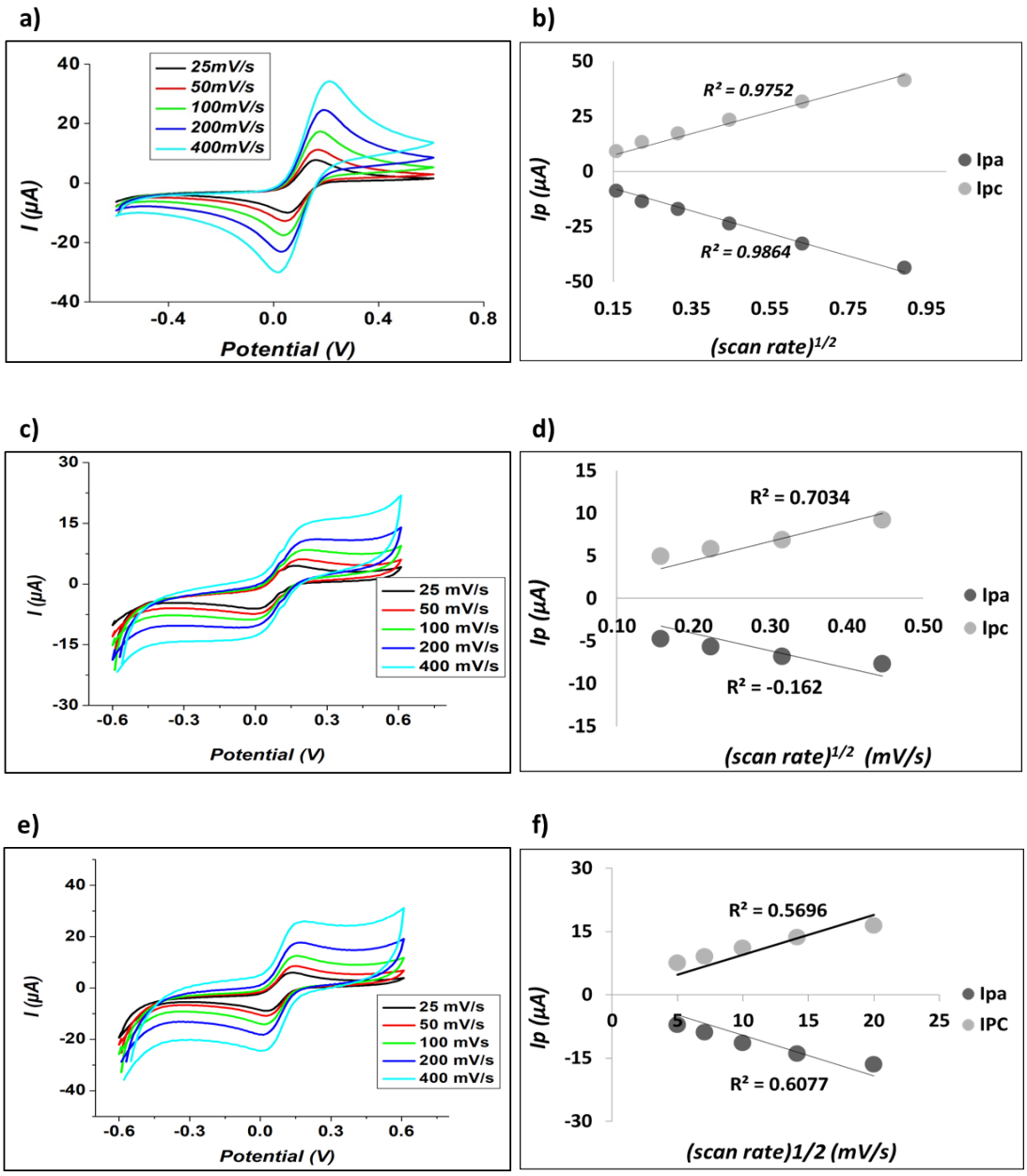

Figure (4.5): *Cyclic Voltammetry characterization using 1 mM $[Fe(CN)_6]^{-3/-2}$ containing 50 mM Sr (NO_3) electrolyte:* ***a)*** *and* ***b)*** *Bare SPCE,* ***c)*** *and* ***d)*** *modified SPCE surface with diazonium mixed layers (DCOOH: DCL 1 cycle:3 cycles),* ***e)*** *and* ***f)*** *After capture probe immobilization*

Table (4.2) summarizes the cathodic and anodic peak currents and potentials for CV characterization for bare SPCE modified SPCE with diazonium electro-grafting, after capture probe immobilization.

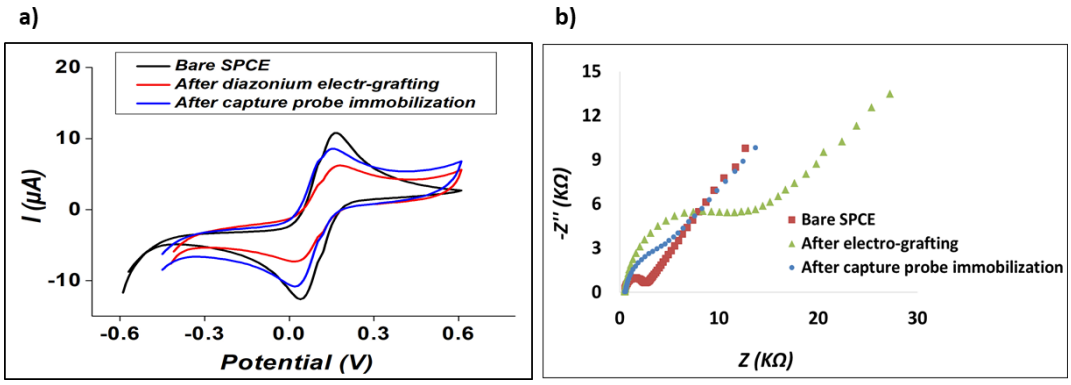

Figure (4.6): a) *Cyclic Voltammetry characterization using 1 mM $[Fe(CN)_6]^{-3/-2}$ containing 50 mM $Sr(NO_3)$ electrolyte for bare SPCE modified SPCE with diazonium electro-grafting, after capture probe linking to the –COOH groups on the grated diazonium and after RPA on the surface of SPCE using 100 mV/s scan rate; and* ***b)*** *Electrochemical impedance spectroscopy at 0.1 V, frequency range from 1000 to 0.01 HZ, and 10 mV points per decade*

Electro-grafting success appears to be detected with CV since the electrochemical behaviour of the Fe^{+2}/Fe^{+3} redox couple is obviously affected. The covalent linking of the capture probe produces (as before) yet another change evidenced with an increased apparent capacitance. These results are in agreements with the EIS results (figure 4.6b)).

Electrode	Rs (Ω)	Rct (Ω)	-Z'' (Ω)
Bare SPCE	320.5	1427	840
After electro-grafting	365.9	7334.5	3160.6
After capture probe immobilization	365.9	997.4	1397.6

Table (4.2): *EIS characterization parameters obtained at 0.1 V, frequency range from 1000 to 0.01 HZ, and 10 mV points per decade and using 1 mM $[Fe(CN)_6]^{-3/-2}$ containing 50 mM $Sr(NO_3)_2$ electrolyte for bare SPCE modified SPCE with diazonium electro-grafting, after FwP linking to the –COOH groups on the grated diazonium and after RPA on the surface of SPCE. Where the Rs is the solution resistance, Rct is the resistance at the solid-liquid interface, -Z'' is the imaginary component impedance,*

Parameters optimization:

As in chapter (1) ssDNA *K. armiger* target has been used to optimize the system. Figure (4.7) shows the CA measurement for different RPA reaction times and hybridization time after RPA. The experiment was performed using 1 nM target and 5 min hybridization time on SPCEs. 20 min is enough for RPA reaction and 7 min hybridization gives reproducible responses and acceptable difference between the negative control and positive samples.

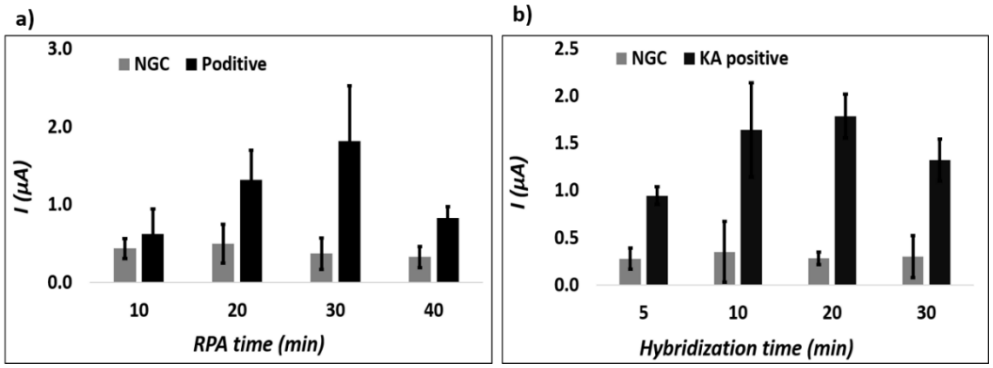

Figure (4.7): *CA measurements for the described system using reverse primer HRP for:* ***a)*** *different RPA reaction times, and* ***b)*** *Different hybridization times after RPA reaction, using 1 nM target and 5 min hybridization time on SPCEs*

a)

Time	Ratio*
5	3.40
10	4.69
20	6.35
30	4.40

b)

Time	Ratio*
5	4.60
10	2.59
20	3.11

Table (4.3): *Ratio between the negative and the k. armiger positive for:* ***a)*** *different RPA reaction times, and* ***b)*** *Different hybridization times after RPA reaction, using 1 nM target and 7 min hybridization time on SPCEs*

Detection:

Selectivity:

To demonstrate the selectivity of the developed system for ssDNA target and dsDNA target of karlodinium armiger, a test against karlodinium veneficum was performed as in figure (4.8). The ratio between the positive and the non-specific control (NSC) or the negative control (NGC) is less than that shown for optimization for the same reason explained before, i.e. testing the selectivity at low target concentration. The dsDNA target was generated same as described before in section (1).

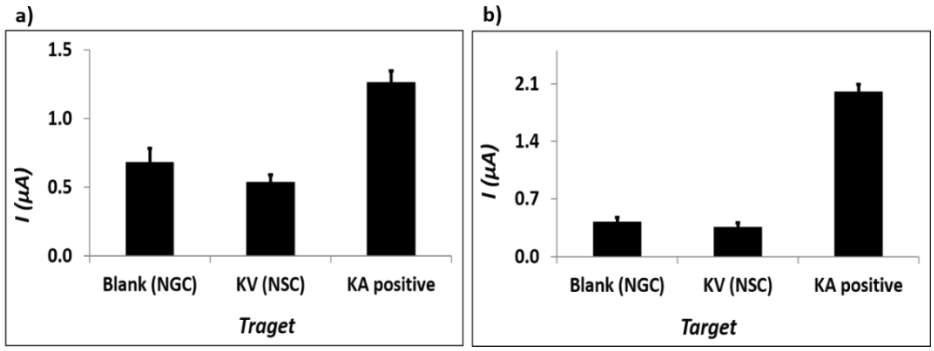

Figure (4.8): *System selectivity for the described system against karlodinium veneficum species (KV) using reverse primer HRP, 40 min RPA and 5 min hybridization:* ***a)*** *ssDNA target using 50 pM target final concentration and* ***b)*** *dsDNA target using 5 pM target final concentration; the NGC is the blank with no target, the KV is the non-specific control (NSC)*

Calibration curves:

The constructed calibration curves were not very informative, because the concentration range used was very high compared with the response range. The calibration curve for concentrations ranging from 0 to 500 pM concentrations for the ssDNA and from figure (4.9) this system seems not working. And the attempt to calculate the LOD for dsDNA target 0.33 fM with a linear range from 0.5 fM to 5 pM. A smaller concentration range for dsDNA target should be performed in order to obtain the true LODs.

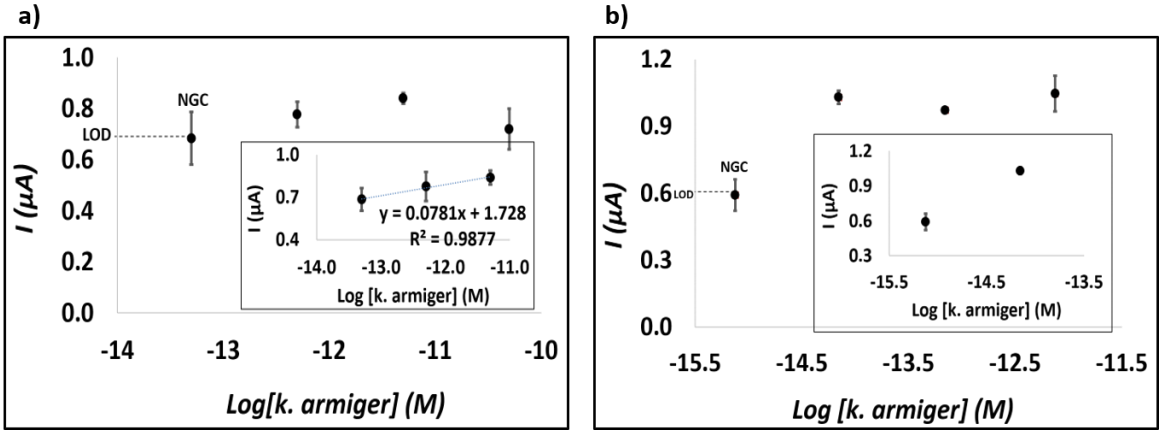

Figure (4.9):): *Attempts to calculate the KA target LOD for described liquid-phase RPA system based on diazonium electro-grafting on SPCEs surface, 40 min RPA and 5 min hybridization:* ***a)*** *ssDNA target with a LOD of 39.8 pM with a linear range from 50 fM to 5 pM, and* ***b)*** *dsDNA target with a LOD of 0.33 fM with a linear range from 0.5 to 5 fM, NGC is the non-template control; measurements were performed at -0.2V potential for 250 s using 100 µL PBS 0.5 M for the first 100 s and 100 µL TMB substrate was added after 100 s.*

Parameter	**Target**	
	ssDNA	***dsDNA***
Selectivity	√	√
LOD	39.8 fM	0.33 fM
Linear range	50 fM to 5 pM	0.5 – 5 fM

Table (4.4): *CA detection parameters*

3.1.5. Conclusion:

The developed system was un-successful for electrochemical detection for ssDNA. And in order to be able to calculate the true LOD for dsDNA, a smaller concentration range for ssDNA target and dsDNA target should be performed in order to obtain the true LODs.

III. Poly (L-Lysine) polymer drop-casting on screen printed electrodes

4.3.1. Problem:

K. armiger amplification using liquid-phase RPA and electrochemical detection of the amplification on SPCEs surface using poly (L-Lysine) polymer (PLL) and aminated forward primer and polyethylene glycol diglycidyl ether (PEGDE) as a cross-linker.

4.3.2. Solution:

After verifying the solution phase RPA amplification by gel electrophoresis, the electrochemical detection could be performed on SPCEs surface using *k. armiger* capture probe. The developed system was un-successful for electrochemical detection for dsDNA. But in order to be able to calculate the true LOD, a smaller concentration range target and dsDNA target should be performed in order to obtain the true LODs.

4.3.2. Materials and methods:

All reagents are as described in chapter (3) section (2).

SPCEs surface functionalization:

Same as described in chapter (3) section (2).

Liquid-phase RPA:

RPA cocktail, k. armiger dilutions, and CA detection were as described previously in chapter (3) section (2)

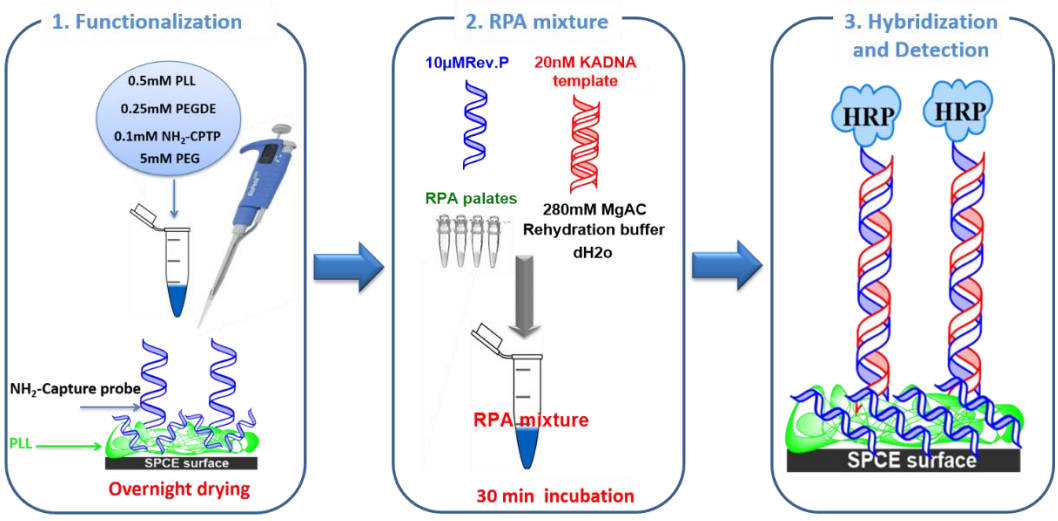

Figure (4.10): *Schematic representation for surface functionalization with PLL and NH_2-capture probe, RPA mixture components and reaction, and hybridization and detection on the functionalized surface.*

4.3.3. Results and discussion:

Parameters optimization:

As in chapter (1) and chapter (2) section (2), ssDNA K. armiger target has been used to optimize the system. Same optimization study has been performed as in chapter (3) section (2), with the same conclusions.

PLL (mM)	PEG400 co-immobilized (mM)	PEG400/1h (mM)	NGC (µA)	KA positive (µA)	Ratio	Reporting probe
0.5	5	25	-1.31	-6.63	**5.06**	KA reporter-HRP
0.5	-	2.5	-2.52	-5.41	**2.15**	KA reporter-HRP
0.5	5	5	-2.53	-4.06	**1.60**	KA reporter-HRP
0.5	5	5	-0.68	-4.39	**6.46**	Rev.P-HRP
0.5	-	7.5	-0.74	-2.6	**3.51**	Rev.P-HRP
0.5	5	-	-2.49	-5.14	**2.06**	Rev.P-HRP

Table (4.5): *Blocking agent co-immobilized, used after surface functionalization, and co-immobilized plus blocking after surface functionalization*

Figure (4.11) shows the optimization for concentrations for PLL, PEGDE, and capture probe; as well as the time for hybridization after RPA. Low concentrations of PLL shows irreproducible results compared with the 0.5 mM. 0.25 mM of PEGDE shows the reproducibility as well as the best difference between the specific signal and negative control. No significant difference obtained for different concentrations of the capture probe, except for the slight blocking behaviour for the 50 and 100 µM, which indicates some blocking behaviour, but it is not dominant as in the solid-phase RPA, all the data were summarized in table (4.6). For solid-phase RPA, the amplification takes place at the SPCEs surface while for the liquid-phase the RPA mixture hybridizes on the surface. For this reason, the steric hindrance when the density of DNA probes increases is more important in the solid-phase compared with the liquid-phase.

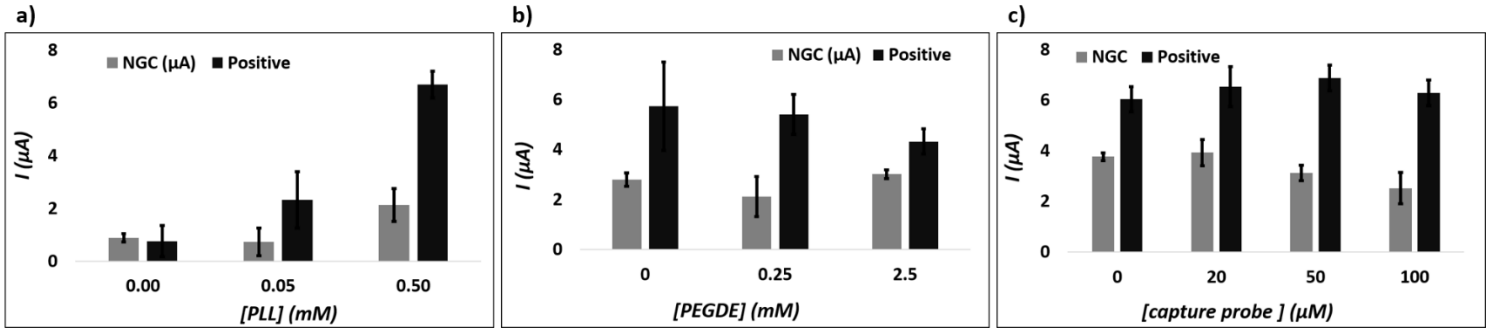

Figure (4.11): *CA responses for the described system using 100 pM target final concentration after 40 min RPA and 5 min hybridization on SPCEs using reverse primer HRP:* ***a)*** *Different concentrations of PLL using 0.1 mM capture probe and 0.25 mM PEGDE,* ***b)*** *Different concentrations of PEGDE, using 0.1 mM capture probe and 0.5 mM PLL,* ***c)*** *Different concentrations of capture probe using 0.5 mM PLL and 0.25 mM PEGDE*

a)

PLL (mM)	Ratio*
0	0.86
0.05	3.17
0.5	3.14

b)

PEGDE (mM)	Ratio*
0	2.05
0.25	2.56
2.5	1.44

c)

Capture probe (µM)	Ratio*
0	1.60
20	1.66
50	2.21
100	2.50

Table (4.6): *Ratio is the ratio between the negative and the k. armiger positive for:* ***a)*** *PLL using 0.25 mM PEGDE and 0.1 mM NH_2-FwP,* ***b)*** *PEGDE using 0.5 mM PLL and 0.1 mM NH_2-FwP, and* ***c)*** *NH_2-FwP using 0.5 mM PLL and 0.25 mM PEGDE*

Figure (4.12) and table (4.7) show the CA measurement for different RPA reaction times. The experiment was performed using 100 pM target final concentration and 7 min hybridization time on SPCEs.

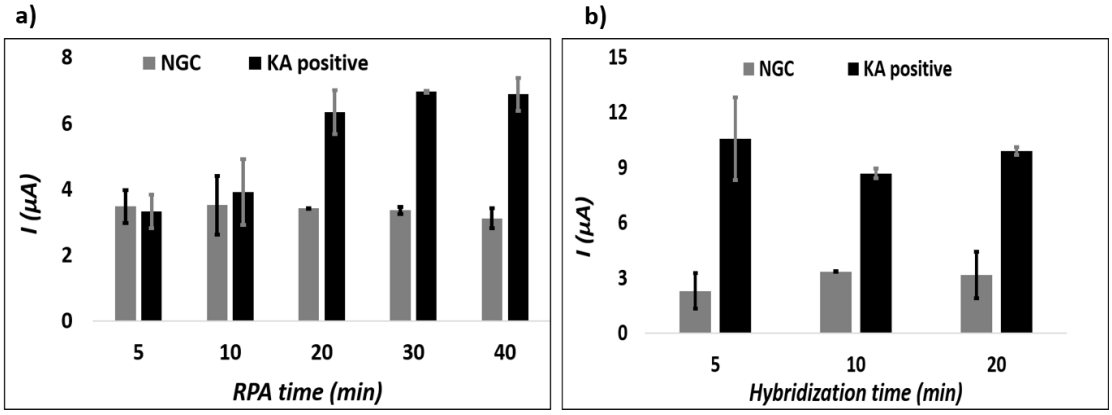

Figure (4.12): *CA measurements for the described system using 100 pM target final concentration on SPCEs using reverse primer HRP:* ***a)*** *Different RPA reaction times using 5 min hybridization, and* ***b)*** *Different hybridization times after 40 min RPA reaction*

a)

RPA time (min)	Ratio
5	0.95
10	1.11
20	1.85
30	2.07
40	2.21

b)

Hybridization time (min)	Ratio
5	4.60
10	2.59
20	3.11

Table (4.7): *Ratio between the negative and the k. armiger positive for:* ***a)*** *different RPA reaction times, and* ***b)*** *Different hybridization times after RPA reaction, using 100 pM target final concentration and 7 min hybridization time on SPCEs*

PLL film characterization:

Same results obtained for FwP in chapter (3) section (2).

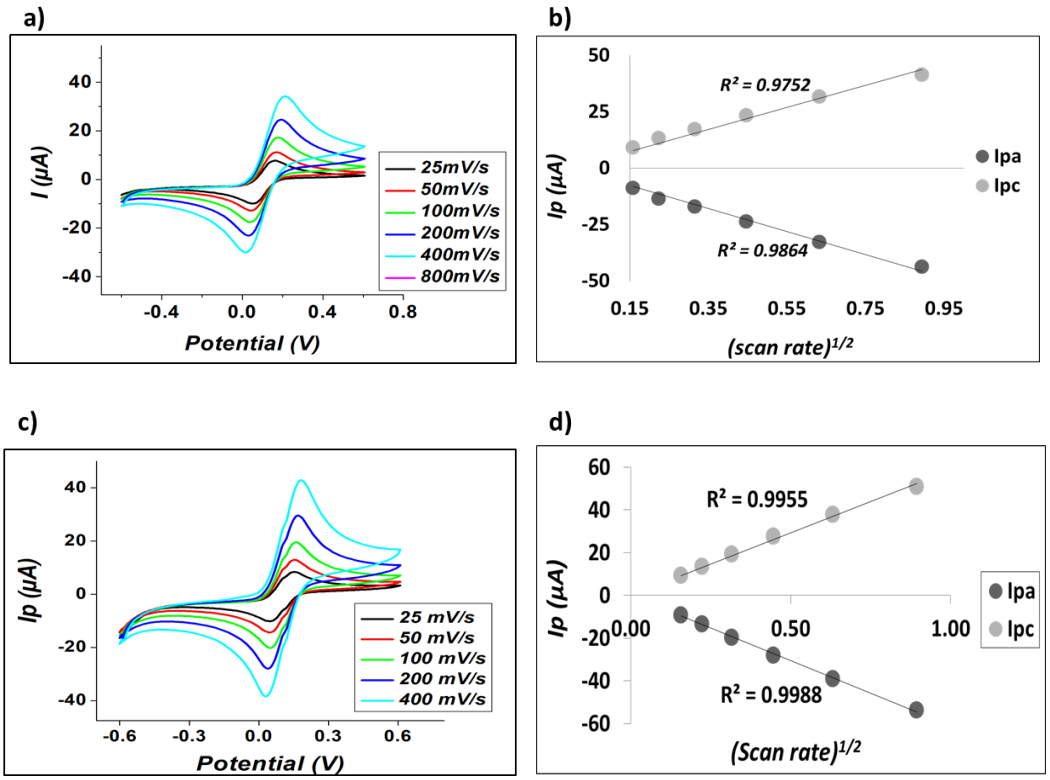

Figure (4.13): *Cyclic Voltammetry characterization using 1 mM $[Fe(CN)_6]^{-3/-2}$ containing 50 mM Sr (NO_3) electrolyte:* ***a)*** *and* ***b)*** *Bare SPCE,* ***c)*** *and* ***d)*** *modified SPCE surface with PLL and NH_2-FwP using PEG400*

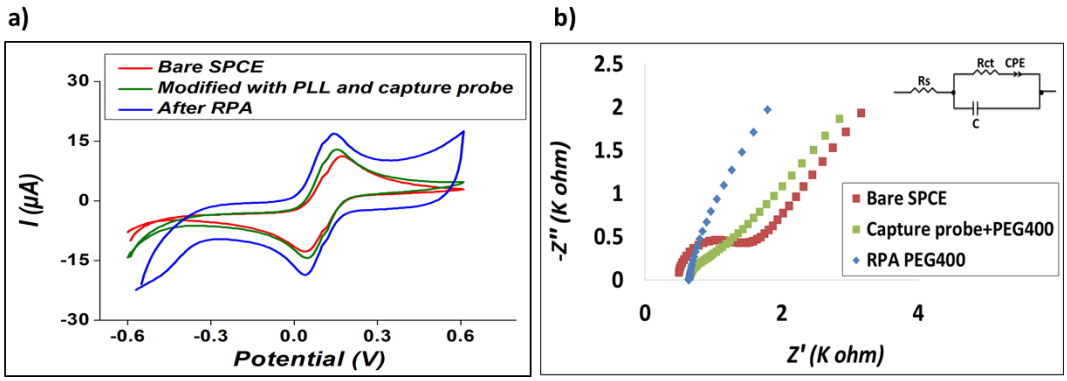

Figure (4.14): ***a)*** *Cyclic Voltammetry characterization using 1 mM $[Fe(CN)_6]^{-3/-2}$ containing 50 mM Sr (NO_3) electrolyte for bare SPCE and modified SPCE PLL and FwP and after RPA on the surface of SPCE using 100 mV/s scan rate.* ***b)*** *Electrochemical impedance spectroscopy at 0.1 V, frequency range from 1000 to 0.01 HZ, and 10 mV points per decade for bare SPCE, modified with PLL and FwP, and after RPA*

Electrode	*Z' (Ω)*	*-Z'' (Ω)*
Bare SPCE	495.6	91.9
modified with PLL and capture probe	650.2	44.2
After RPA and hybridization	642.1	4.8

Table (4.8): *Electrochemical impedance spectroscopy (EIS) parameters for bare, modified SPCEs surface with PLL, PEGDE, PEG400 and capture probe, and after RPA*

Detection:

Selectivity:

To demonstrate the selectivity of the developed system for ssDNA target and dsDNA target of karlodinium armiger, a test against karlodinium veneficum was performed as in figure (4.15). The dsDNA target was generated same as described before in section (1).

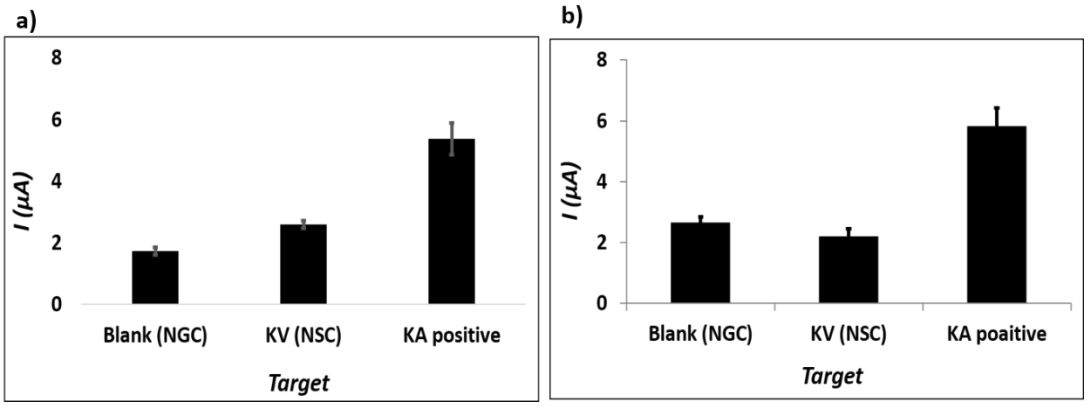

Figure (4.15): *System selectivity for the described system against karlodinium veneficum species (KV), 40 min RPA and 5 min hybridization:* ***a)*** *ssDNA target using 5 nM target final concentration and* ***b)*** *dsDNA target using 5 pM target final concentration; the NGC is the blank with no target, the KV is the non-specific control (NSC)*

Calibration curves:

The calibration curve for the ssDNA, figure (4.16) shows a LOD of 1.3 pM and a linear range from 5 to 50 pM. The attempt to calculate the LOD for dsDNA was un-successful and in order to be able to calculate the true LOD, a smaller concentration range should be performed.

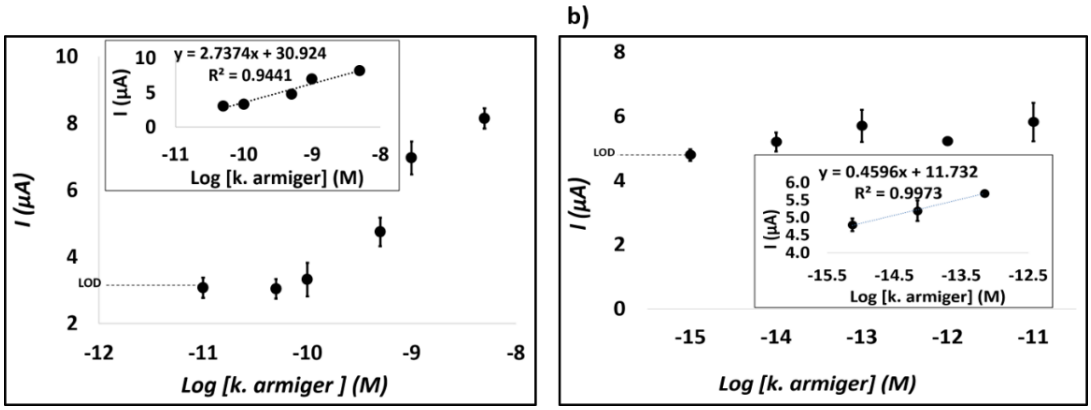

Figure (4.16): *Attempts to calculate the KA target LOD for described liquid-phase RPA system based on PLL drop-casting on SPCEs surface, RPA 40 min and 5 min hybridization:* ***a)*** *ssDNA target with a LOD of 1.3 pM with a linear range from 5 to 50 pM, and* ***b)*** *dsDNA target with a LOD of 1.4 fM with a linear range from 5 fM to 5 pM, NGC is the non-template control; measurements were performed at -0.2V potential for 250 s using 100 µL PBS 0.5 M for the first 100 s and 100 µL TMB substrate was added after 100 s*

Parameter	Target	
	ssDNA	***dsDNA***
Selectivity	√	√
LOD	1.3 pM	1.4 fM
Linear range	5 to 50 pM	5 fM to 5 pM

Table (4.9): *CA detection parameters*

3.1.5. Conclusion:

The developed system was un-successful for electrochemical detection for dsDNA. And in order to be able to calculate the true LOD, a smaller concentration range target and dsDNA target should be performed in order to obtain the true LODs.

CHAPTER V

GENERAL CONCLUSIONS AND FUTURE WORK

I. General conclusions

The original general objective of the thesis was to develop an integrated microfluidic device based on screen printed carbon electrodes (SPCEs) for molecular diagnostics. This general objective has been divided into specific objectives:

I. Screen printed electrodes surface modification

II. Recombinase Polymerase Amplification (RPA) introduction

III. Microfluidic device construction

Due to the roughness and highly irregular nature of the SPCEs surface the results were irreproducible and not reliable. So, it was convenient to focus on finding the best strategies for surface modification in order to increase the signal ratio between the specific sample and non-specific control and to produce reproducible and robust results. Among many strategies tested, we were able to investigate and compare two different strategies for SPCEs surface modification as well as introducing the RPA in the two systems. We are introducing a novel general platform that could be functionalized depends on the needs. The response has been tested using a general platform then the RPA has been introduced after the successful surface modification. The two different strategies for SPCEs surface modification are as follows:

1. ***Different systems based on carboxylated diazonium electro-grafting on SPCEs for DNA hybridization and detection has been developed:***

a) A generic proof-of-concept system has been developed using aminated poly T capture probes as the recognition layer. 1x Denhardt's solution was used to reduce the HRP non-specific adsorption achieving a difference of one order of magnitude between the positive and the non-specific control. The assay time is 30 min, and the hybridization was achieved by using the complementary poly A-HRP reaching a LOD of 9.6 nM and a linear range from 20 - 200 nM.

b) A system for DNA amplification and detection has been developed using *karlodinium armiger* as a proof-of-concept for real systems. The recognition layer is the aminated DNA probes linked to the electro-grafted diazonium salt via covalently. Two different amplification approaches have been tested:

i. ***Solid phase RPA:*** The recognition layer is the aminated forward primer linked to the electro-grafted diazonium salt. The amplification is solid phase RPA and was achieved on the surface of the SPCEs by incubation with the RPA reagents. The detection was achieved by using a primer in the RPA mixture

contains a tail that is complementary to a reporter labelled with HRP. Electro-grafting of mixed layers of DCOOH and DCl were used to reduce the HRP non-specific adsorption achieving a difference of almost one order of magnitude between the positive and the negative control (NGC) or the non-template control. The assay time, i.e. time from sample introduction to results is **60 min**. The LOD was found to be 0.1 fM with a linear range of 0.5 fM - 5 pM.

ii. ***Liquid phase RPA:*** The recognition layer is the aminated capture probe linked to the electro-grafted diazonium salt. The amplification is liquid phase RPA and was achieved by performing the RPA and confirm it by the gel electrophoresis. The hybridization was achieved by incubation with the mixture after gel electrophoresis amplification confirmation. The reverse primer is labelled with HRP then the detection could be achieved immediately after hybridization. Electro-grafting of mixed layers of DCOOH and DCl were used to reduce the HRP non-specific adsorption. The time from sample introduction to results is **40 min**, and the developed system was un-successful for electrochemical detection for ssDNA. And in order to be able to calculate the true LOD, a smaller concentration range target and dsDNA target should be performed in order to obtain the true LODs. The attempt to calculate the LOD was as follows: 0.33 fM LOD with a linear range of 0.5 fM – 5 pM.

2. ***Different systems based on poly (L-Lysine) polymer (PLL) drop-casting on SPCEs for DNA hybridization and detection has been developed:***

a) A generic proof-of-concept system has been developed using aminated poly T capture probes as the recognition layer. 1x Denhardt's solution was used to reduce the HRP non-specific adsorption achieving a difference of one order of magnitude between the positive and the non-specific control. The assay time is 30 min, and the hybridization was achieved by using the complementary poly A-HRP reaching a LOD of 1.2 nM and a linear range from 2.5 - 50 nM;

b) A system for DNA amplification and detection has been developed using *karlodinium armiger* as a proof-of-concept for real systems. The recognition layer is the aminated DNA probes linked to PLL using PEGDE as a cross-linker and PEG400 was used to reduce the HRP non-specific adsorption. Two different amplification approaches have been tested:

i. ***Solid phase RPA:*** The recognition layer is the aminated forward primer linked to the PLL. The amplification is solid phase RPA and was achieved on the surface of the SPCEs by incubation with the

RPA reagents. The detection was achieved immediately after the solid phase RPA by using a primer labelled with HRP in the RPA mixture. PEG400 was used to reduce the HRP non-specific adsorption achieving a difference of around 7 times between the positive and the negative control (NGC) or the non-template control. The time from sample introduction to results is **20 min**. The LOD was found to be 0.13 fM with a linear range of 0.75 fM - 7 fM.

ii. ***Liquid phase RPA:*** The recognition layer is the aminated capture probe linked to PLL. The amplification is liquid phase RPA and was achieved by performing the RPA and confirm it by the gel electrophoresis. The hybridization was achieved by incubation with the mixture after gel electrophoresis amplification confirmation. The reverse primer is labelled with HRP then the detection could be achieved immediately after hybridization. PEG400 was used to reduce the HRP non-specific adsorption. The time from sample introduction to results is **40 min**. The developed system was un-successful for electrochemical detection for dsDNA. But in order to be able to calculate the true LOD, a smaller concentration range target and dsDNA target should be performed in order to obtain the true LODs.

The developed system for solid-phase RPA is easy, fast, direct and cost-efficient to meet the requirements for the design requirements for molecular diagnostic systems developed for resources-limited environments.

II. Future work

The developed system would be integrated in a fully printed microfluidic device based on screen printed electrodes for molecular diagnostics. And in order to achieve this final goal, small objectives should be achieved:

1) To overcome the problems of the dried reagents system, the HRP reporter will be changed to AuNPs because they are efficient for drying and reconstitution.

2) Develop a system using reverse primer labelled with AuNPs and ferrocene like the system developed for DNA amplification and detection using reverse primer labelled with HRP. The AuNPs could be produced and characterized easily in house, as well as the functionalization of the AuNPs with ferrocene and the reverse primer. This will reduce the cost and then makes the device more suitable for mass production.

3) Print the integrated device and test the performance using the developed assay and real samples.

CHAPTER VI

BIBLIOGRAPHY

Bibliography

[1] S. E. Levy and R. M. Myers, "Advancements in Next-Generation Sequencing," *Annu. Rev. Genom. Hum. Genet*, vol. 17, p. :95–115, 2016.

[2] R. C. M. 2521, "Molecular Diagnostics Market," *Pune*, 2018.

[3] C. Dincer, R. Bruch, A. Kling, S. Dittrich, and G. A. Urban, "Multiplexed Point-of-Care Testing – xPOCT," *Trends Biotechnol.*, vol. 35, no. 8, 2017.

[4] M. Tsaloglou *et al.*, "Handheld isothermal ampli fi cation and electrochemical detection of DNA in resource-limited settings," *Anal. Biochem.*, vol. 543, no. December 2017, pp. 116–121, 2018.

[5] L. M. Santiago, D. Bejarano-nosas, P. Lozano-sanchez, and I. Katakis, "Screen-printed microsystems for the ultrasensitive electrochemical detection of alkaline phosphatase," *Analyst*, vol. 135, pp. 1276–1281, 2010.

[6] D. Bejarano, P. Lozano, D. Mata, S. Cito, and M. Constant, "Screen printing as a holistic manufacturing method for multifunctional microsystems and microreactors," *J. Micromech. Microeng*, vol. 19, no. 1, p. 15007, 2009.

[7] A. P. Washe, P. Lozano, D. Bejarano, and I. Katakis, "Eletrochemically Actuated Stop – Go Valves for Capillary Force-Operated Diagnostic Microsystems," *ChemPhysChem*, vol. 14, pp. 2164–2173, 2013.

[8] M. Wade, Y.-C. Li, and G. M. Wahl, "Sensitive electrochemical detection of horseradish peroxidase at disposable screen-printed carbon electrode," *Nat. Rev. Cancer*, vol. 13, no. 2, pp. 83–96, 2013.

[9] F. Ricci and K. W. Plaxco, "E-DNA sensors for convenient, label-free electrochemical detection of hybridization," *Microchim. Acta*, vol. 163, no. 3–4, pp. 149–155, 2008.

[10] F. Lucarelli, G. Marrazza, A. P. F. Turner, and M. Mascini, "Carbon and gold electrodes as electrochemical transducers for DNA hybridisation sensors," *Biosens. Bioelectron.*, vol. 19, no. 6, pp. 515–530, 2004.

[11] Y. Lin, F. Lu, and J. Wang, "Disposable Carbon Nanotube Modified Screen-Printed Biosensor for Amperometric Detection of Organophosphorus Pesticides and Nerve Agents," *Electroanalysis*, vol. 16, no. 12, pp. 145–149, 2004.

[12] S. Bouden *et al.*, "Trace lead analysis based on carbon-screen-printed-electrodes modified via 4-carboxy-phenyl diazonium salt electroreduction," *Talanta*, vol. 106, pp. 414–421, 2013.

[13] J. Jasmin *et al.*, "XPS and NRA investigations during the fabrication of gold nanostructured functionalized screen-printed sensors for the detection of metallic pollutants," *Appl. Surf. Sci.*, vol. 397, pp. 159–166, 2017.

[14] S. A. Lim and M. U. Ahmed, "A label free electrochemical immunosensor for sensitive detection of porcine serum albumin as a marker for pork adulteration in raw meat," *Food Chem.*, vol. 206, pp. 197–203, 2016.

[15] G. Martínez-García, L. Agüí, P. Yáñez-Sedeño, and J. M. Pingarrón, "Multiplexed electrochemical

immunosensing of obesity-related hormones at grafted graphene-modified electrodes," *Electrochim. Acta*, vol. 202, pp. 209–215, 2016.

[16] R. K. Mishra, A. Hayat, G. Catanante, C. Ocaña, and J. L. Marty, "A label free aptasensor for Ochratoxin A detection in cocoa beans: An application to chocolate industries," *Anal. Chim. Acta*, vol. 889, pp. 106–112, 2015.

[17] K. Y. Goud, G. Catanante, A. Hayat, M. Satyanarayana, K. V. Gobi, and J. Louis, "Disposable and portable electrochemical aptasensor for label free detection of aflatoxin B1 in alcoholic beverages," *Sensors Actuators B. Chem.*, vol. 235, pp. 466–473, 2016.

[18] G. Istamboulié, N. Paniel, L. Zara, L. R. Granados, L. Barthelmebs, and T. Noguer, "Development of an impedimetric aptasensor for the determination of aflatoxin M1 in milk," *Talanta*, vol. 146, pp. 464–469, 2016.

[19] S. Liu *et al.*, "Detection of Abrin by Electrochemiluminescence Biosensor Based on Screen Printed Electrode," *Sensors*, vol. 18, no. 2, p. 357, 2018.

[20] E. B. Setterington and E. C. Alocilja, "Electrochemical biosensor for rapid and sensitive detection of magnetically extracted bacterial pathogens," *Biosensors*, vol. 2, no. 1, pp. 15–31, 2012.

[21] S. Z. Mousavisani, J. B. Raoof, R. Ojani, and Z. Bagheryan, "Bioelectrochemistry An impedimetric biosensor for DNA damage detection and study of the protective effect of deferoxamine against DNA damage," *Bioelectrochemistry*, vol. 122, pp. 142–148, 2018.

[22] Y. Pei, L. Yook, and H. Yee, "A quantification strategy for DNA hybridization via measurement of adsorbed anthraquinone monosulphonic acid on silica nanospheres," *Measurement*, vol. 135, pp. 640–650, 2019.

[23] W. Sheryn, M. A. Shamsuddin, L. Y. Heng, J. Latip, S. A. Hasbullah, and N. I. Hassan, "An Electrochemical DNA Biosensor for Carcinogenicity of Anticancer Compounds Based on Competition between Methylene Blue," *Sensors*, vol. 19, p. 5111, 2019.

[24] N. Diyana, L. Yook, R. Swathe, and P. Malon, "Electrochemical DNA biosensor for potential carcinogen detection in food sample," *Food Chem.*, vol. 269, no. September 2017, pp. 503–510, 2018.

[25] V. Mazzaracchio *et al.*, "A label-free impedimetric aptasensor for the detection of Bacillus anthracis spore simulant," *Biosens. Bioelectron.*, vol. 126, no. November 2018, pp. 640–646, 2019.

[26] A. Alawad, G. Istamboulié, C. Calas-blanchard, and T. Noguer, "A reagentless aptasensor based on intrinsic aptamer redox activity for the detection of tetracycline in water," *Sensors Actuators B Chem.*, vol. 288, no. October 2018, pp. 141–146, 2019.

[27] H. Ilkhani and S. Farhad, "A novel electrochemical DNA biosensor for Ebola virus detection," *Anal. Biochem.*, vol. 557, no. May, pp. 151–155, 2018.

[28] D. Quesada-gonz and A. Merkoçi, "Analytica Chimica Acta Electrochemical detection of plant virus using gold nanoparticle-modi fi ed electrodes," *Anal. Chim. Acta*, vol. 1046, pp. 123–131, 2019.

[29] B. Nagar, M. Balsells, A. De Escosura-muñiz, and P. Gomez-romero, "Fully printed one-step

biosensing device using graphene / AuNPs composite," *Biosens. Bioelectron.*, vol. 129, no. July 2018, pp. 238–244, 2019.

[30] K. Toth, R. A. Durst, D. R. The, G. S. Wilson, and P. X. De Marne, "ELECTROCHEMICAL BIOSENSORS : RECOMMENDED DEFINITIONS AND CLASSIFICATION *," *Anal. Lett.*, vol. 34, no. 5, pp. 635–659, 2001.

[31] D. R. The, K. Toth, R. A. Durst, and G. S. Wilson, "Technical report Electrochemical biosensors : recommended definitions and classification," *Biosens. Bioelectron.*, vol. 16, pp. 121–131, 2001.

[32] P. Mehrotra, "Biosensors and their applications – A review," *J. oral Biol. craniofacial Res.*, no. 2015, pp. 1–7, 2016.

[33] D. Grieshaber, R. MacKenzie, J. V. Os, and E. Reimhult, "Electrochemical Biosensors - Sensor Principles and Architectures," *Sensors*, no. March, pp. 1400–1458, 2008.

[34] N. J. Ronkainen, H. Brian, and W. R. Heineman, "Electrochemical biosensors," *Chem.Soc.Rev*, vol. 39, pp. 1747–1763, 2010.

[35] B. R. Eggins, *Chemical Sensors and Biosensors*. West Sussex: John Wiley & Sons, 2002.

[36] Y. Yeh, B. Creran, and V. M. Rotello, "Gold nanoparticles : preparation , properties , and applications in," *Nanoscale*, vol. 4, pp. 1871–1880, 2012.

[37] M. Sengani, A. Mihai, and V. D. Rajeswari, "Recent trends and methodologies in gold nanoparticle synthesis – A prospective review on drug delivery aspect," *Open nano*, vol. 2, no. July, pp. 37–46, 2017.

[38] N. Elahi, M. Kamali, M. Hadi, M. Kamali, and M. Hadi, "Recent biomedical applications of gold nanoparticles: A review," *Talanta*, vol. 184, pp. 537–556, 2018.

[39] N. C. Veitch, "Horseradish peroxidase : a modern view of a classic enzyme," *Phytochemistry*, vol. 65, pp. 249–259, 2004.

[40] F. W. Krainer and A. Glieder, "An updated view on horseradish peroxidases : recombinant production and biotechnological applications," *Appl Microbiol Biotechnol*, vol. 99, pp. 1611–1625, 2015.

[41] T. Berthelot *et al.*, "'Versatile toolset' for DNA or protein immobilization: Toward a single-step chemistry," *Appl. Surf. Sci.*, vol. 257, no. 8, pp. 3538–3546, 2011.

[42] C. Fan, K. W. Plaxco, and A. J. Heeger, "Electrochemical interrogation of conformational changes as a reagentless method for the sequence-specific detection of DNA," *PNAS*, vol. 100, no. 16, pp. 9134–9137, 2003.

[43] C. E. Immoos, S. J. Lee, and M. W. Grinstaff, "DNA-PEG-DNA Triblock Macromolecules for Reagentless DNA Detection," *J. Am. Chem. Soc.*, vol. 82, pp. 10814–10815, 2004.

[44] H. H. Thorp, "Reagentless detection of DNA sequences on chemically modified electrodes," *Trends Biotechnol.*, vol. 21, no. 12, pp. 522–524, 2003.

[45] Y. Fu, R. Yuan, Y. Chai, L. Zhou, and Y. Zhang, "Coupling of a Reagentless Electrochemical DNA

Biosensor with Conducting Polymer Film and Nanocomposite as Matrices for the Detection of the HIV DNA Sequences," *Anal. Lett.*, vol. 39, pp. 467–482, 2006.

[46] Y. Xiang, X. Qian, Y. Chen, Y. Zhang, Y. Chai, and R. Yuan, "A reagentless and disposable electronic genosensor : from multiplexed analysis to molecular logic gates w," *Chem. Commun*, vol. 47, pp. 2080–2082, 2011.

[47] A. A. Rowe, R. J. White, A. J. Bonham, and K. W. Plaxco, "Fabrication of Electrochemical-DNA Biosensors for the Reagentless Detection of Nucleic Acids , Proteins and Small Molecules Fabrication of Electrochemical-DNA Biosensors for the Reagentless Detection of Nucleic Acids , Proteins and Small Molecules," *J. Vis. Exp.*, vol. 52, pp. 1–6, 2011.

[48] M. Green, N. S. Gilhooly, S. Abedeen, D. J. Scott, M. S. Dillingham, and P. Soultanas, "Biosensors and Bioelectronics Engineering a reagentless biosensor for single-stranded DNA to measure real-time helicase activity in Bacillus," *Biosens. Bioelectron.*, vol. 61, pp. 579–586, 2014.

[49] W. R. De Araujo, C. M. R. Frasson, W. A. Ameku, J. Ø. R. Silva, L. Angnes, and T. R. L. C. Paix, "Single-Step Reagentless Laser Scribing Fabrication of Electrochemical Paper-Based Analytical Devices Angewandte," *Angew. Chem. Int*, vol. 56, pp. 15113–15117, 2017.

[50] S. Cinti, "Preparation of paper-based devices for reagentless electrochemical (bio) sensor strips," *Nat. Protoc.*, vol. 14, no. August, pp. 2437–245, 2019.

[51] G. Xu, M. Lai, R. Wilson, A. Glidle, J. Reboud, and J. M. Cooper, "Branched hybridization chain reaction — using highly dimensional DNA nanostructures for label-free , reagent-less , multiplexed molecular diagnostics," *Microsystems Nanoeng.*, vol. 37, pp. 1–7, 2019.

[52] W. Schuhmann, "From Reagentless Biosensors to Biofuel Cells and Self-Powered Bioelectrochemical Devices," *Proceedings*, vol. 1, p. 829, 2017.

[53] K. B. Mullis, "The Unusual Origin of the Polymerase Chain Reaction," *Sci. Am.*, no. April, pp. 56–65, 1990.

[54] L. Garibyan and N. Avashia, "Research Techniques Made Simple: Polymerase Chain Reaction (PCR)," *J Invest Dermatol*, vol. 133, no. 3, pp. 1–8, 2014.

[55] J. Can, "The polymerase chain reaction: An overview and development of diagnostic PCR protocols at the LCDC," *Infect Dis.*, vol. 2, no. 2, pp. 89–91, 1991.

[56] M. Agne, A. Valones, R. L. Guimarães, L. André, and C. Brandão, "PRINCIPLES AND APPLICATIONS OF POLYMERASE CHAIN REACTION IN MEDICAL DIAGNOSTIC FIELDS : A REVIEW," *Brazilian J. Microbiol.*, vol. 40, pp. 1–11, 2009.

[57] M. J. Espy *et al.*, "Real-Time PCR in Clinical Microbiology : Applications for Routine Laboratory Testing," *Clin. Microbiol. Rev.*, vol. 19, no. 1, pp. 165–256, 2006.

[58] N. T. Salihah, M. M. Hossain, and H. Lubis, "Trends and advances in food analysis by real-time polymerase chain reaction," *J Food Sci Technol*, vol. 53, no. May, pp. 2196–2209, 2016.

[59] S. A. Wood *et al.*, "Molecular genetic tools for environmental monitoring of New Zealand ' s aquatic habitats , past , present and the future," *New Zeal. J. Mar. Freshw. Res.*, vol. 8330, pp. 90–119,

2013.

[60] K. M. Ruppert, R. J. Kline, and S. Rahman, "Past , present , and future perspectives of environmental DNA (eDNA) metabarcoding : A systematic review in methods , monitoring , and applications of global eDNA," *Glob. Ecol. Conserv.*, vol. 17, pp. 1–29, 2019.

[61] O. Piepenburg, C. H. Williams, D. L. Stemple, and N. A. Armes, "DNA Detection Using Recombination Proteins," *PLoS Biol.*, vol. 4, no. 7, pp. 2–9, 2006.

[62] O. Mayboroda *et al.*, "Isothermal solid-phase amplification system for detection of Yersinia pestis," *Anal Bioanal Chem*, vol. 408, pp. 671–676, 2016.

[63] E. S. Yamanaka, L. A. Tortajada-genaro, and Á. Maquieira, "Low-cost genotyping method based on allele-specific recombinase polymerase amplification and colorimetric microarray detection," *Microchim Acta*, vol. 184, pp. 1453–1462, 2017.

[64] I. Magrina and C. K. O'Sullivan, "Recombinase polymerase ampli fi cation : Basics , applications and recent advances ~ a," *Trends Anal. Chem.*, vol. 98, pp. 19–35, 2018.

[65] S. Kersting, V. Rausch, F. F. Bier, and M. Von Nickisch-rosenegk, "Rapid detection of Plasmodium falciparum with isothermal recombinase polymerase amplification and lateral flow analysis," *Malar. J.*, pp. 1–9, 2014.

[66] Z. A. Crannell, B. Rohrman, and R. Richards-kortum, "Equipment-Free Incubation of Recombinase Polymerase Amplification Reactions Using Body Heat," *PLoS One*, vol. 9, no. 11, pp. 1–8, 2014.

[67] J. Singleton *et al.*, "Electricity-Free Amplification and Detection for Molecular Point-of-Care Diagnosis of HIV-1," *PLoS One*, pp. 1–20, 2014.

[68] X. Xia, Y. Yu, M. Weidmann, Y. Pan, S. Yan, and Y. Wang, "Rapid Detection of Shrimp White Spot Syndrome Virus by Real Time , Isothermal Recombinase Polymerase Amplification Assay," *PLoS One*, vol. 9, no. 8, pp. 1–8, 2014.

[69] D. Elsa *et al.*, "Modular development of an inline monitoring system for waterborne pathogens in raw and drinking water," *Env. Earth Sci*, vol. 75, p. 1481, 2016.

[70] Y. D. Wu *et al.*, "Recombinase polymerase amplification (RPA) combined with lateral flow (LF) strip for detection of Toxoplasma gondii in the environment," *Vet. Parasitol.*, vol. 243, no. June, pp. 199–203, 2017.

[71] X. Du and Y. Zang, "Recombinase Polymerase Amplification Combined with Lateral Flow Strip for Listeria monocytogenes Detection in Food," *J. Food Sci.*, vol. 83, pp. 1041–1047, 2018.

[72] P. Zhu *et al.*, "Rapid Detection of Vibrio parahaemolyticus in Shellfish by Real-Time Recombinase Polymerase Amplification," *Food Anal. Methods*, vol. 11, pp. 2076–2084, 2018.

[73] H. Yang *et al.*, "A sample-in-digital-answer-out system for rapid detection and quantitation of infectious pathogens in bodily fluids," *Anal. Bioanal. Chem.*, vol. 410, pp. 7019–7030, 2018.

[74] J. Chen *et al.*, "Sensitive and rapid detection of pathogenic bacteria from urine samples using multiplex recombinase polymerase amplification," *Lab Chip*, vol. 18, pp. 2441–2452, 2018.

[75] L. A. Tortajada-Genaro, S. Santiago-Felipe, M. Amasia, A. Russom, and Á. Maquieira, "Isothermal solid-phase recombinase polymerase amplification on microfluidic digital versatile discs (DVDs)," *RSC Adv.*, vol. 5, no. 38, pp. 29987–29995, 2015.

[76] J. Sabaté, I. M. Lobato, O. Mayboroda, I. Katakis, and C. K. O. Sullivan, "Enhanced solid-phase recombinase polymerase amplification and electrochemical detection," *Anal Bioanal Chem*, vol. 409, pp. 3261–3269, 2017.

[77] G-WHITESIDES *et al.*, "Handheld isothermal amplification and electrochemical detection of DNA in resource-limited settings," *Anal. Biochem.*, vol. 543, no. December 2017, pp. 116–121, 2018.

[78] S. Kersting, V. Rausch, F. F. Bier, and M. Von Nickisch-rosenegk, "Multiplex isothermal solid-phase recombinase polymerase amplification for the specific and fast DNA-based detection of three bacterial pathogens," *Microchim Acta*, vol. 181, pp. 1715–1723, 2014.

[79] O. Mayboroda, I. Katakis, and C. K. O. Sullivan, "Multiplexed isothermal nucleic acid amplification," *Anal. Biochem.*, vol. 545, no. November 2017, pp. 20–30, 2018.

[80] Z. Crannell, A. Castellanos-gonzalez, and R. Richards-kortum, "Multiplexed Recombinase Polymerase Amplification Assay To Detect Intestinal Protozoa," *Anal. Chem.*, vol. 88, pp. 1610–1616, 2016.

[81] Z. Li, Y. Liu, Q. Wei, Y. Liu, W. Liu, and X. Zhang, "Picoliter Well Array Chip-Based Digital Recombinase Polymerase Amplification for Absolute Quantification of Nucleic Acids," *PLoS One*, vol. 10, pp. 1–15, 2016.

[82] S. Santiago-felipe, L. A. Tortajada-genaro, and R. Puchades, "Parallel solid-phase isothermal amplification and detection of multiple DNA targets in microliter-sized wells of a digital versatile disc," *Microchim Acta*, vol. 183, pp. 1195–1202, 2016.

[83] H. Y. Lau, Y. Wang, E. J. H. Wee, J. R. Botella, and M. Trau, "Field Demonstration of a Multiplexed Point-of-Care Diagnostic Platform for Plant Pathogens," *Anal. Chem*, vol. 88, pp. 8074–8081, 2016.

[84] K. M. Koo, E. J. H. Wee, P. N. Mainwaring, Y. Wang, and M. Trau, "Toward Precision Medicine : A Cancer Molecular Subtyping Nano-Strategy for RNA Biomarkers in Tumor and Urine," *small*, vol. 12, no. 45, pp. 6233–6242, 2016.

[85] E. J. H. Wee and M. Trau, "Simple Isothermal Strategy for Multiplexed, Rapid, Sensitive, and Accurate miRNA Detection," *Sensors*, vol. 1, pp. 670–675, 2016.

[86] M. Valiadi, S. Kalsi, I. G. F. Jones, C. Turner, J. M. Sutton, and H. Morgan, "Simple and rapid sample preparation system for the molecular detection of antibiotic resistant pathogens in human urine," *biomed microdevices*, vol. 18, pp. 1–10, 2016.

[87] A. Virol, J. Wang, J. Wang, L. Liu, and W. Yuan, "Development of a real-time recombinase polymerase amplification assay for rapid and sensitive detection of porcine circovirus 2," *Arch. Virol.*, vol. 2, pp. 10–13, 2017.

[88] C. Eid and J. G. Santiago, "blood using isotachophoresis and recombinase," *Analyst*, vol. 142, pp. 48–54, 2017.

[89] Y. Yang, X. Qin, Y. Sun, G. Cong, Y. Li, and Z. Zhang, "Development of Isothermal Recombinase Polymerase Amplification Assay for Rapid Detection of Porcine Circovirus Type 2," *Hindawi*, vol. 2017, pp. 1–9, 2017.

[90] K. M. Koo, E. J. H. Wee, and M. Trau, "High-speed biosensing strategy for non-invasive profiling of multiple cancer fusion genes in urine," *Biosens. Bioelectron.*, vol. 89, no. September 2016, pp. 715–720, 2017.

[91] B. Koo *et al.*, "An isothermal, label-free, and rapid one-step RNA amplification/detection assay for diagnosis of respiratory viral infections," *Biosens. Bioelectron.*, vol. 90, no. September 2016, pp. 187–194, 2017.

[92] H. Joda *et al.*, "Biosensors and Bioelectronics Modi fi ed primers for rapid and direct electrochemical analysis of coeliac disease associated HLA alleles," *Biosens. Bioelectron.*, vol. 73, pp. 64–70, 2015.

[93] F. Mo, G. Dong, Y. Zhang, and J. Wang, "Recent applications of arene diazonium salts in organic synthesis," *Biomol. Chem.*, pp. 1582–1593, 2013.

[94] W. Reusch, "Reactions of aryl diazonium salts," in *Virtual Textbook of Organic Chemistry*, vol. 4, pp. 10–11.

[95] S. Betelu *et al.*, "Raman Characterization of Phenyl-Derivatives : From Primary Amine to Diazonium Salts Abstract," *iMedPub Journals*, pp. 1–10, 2017.

[96] N. Marshall, A. Rodriguez, and S. Crittenden, "Diazonium-functionalized thin films from the spontaneous reaction of p- phenylenebis(diazonium) salts," *RSC Adv.*, vol. 8, pp. 6690–6698, 2018.

[97] A. Mattiuzzi *et al.*, "Electrografting of calix[4]arenediazonium salts to form versatile robust platforms for spatially controlled surface functionalization," *Nat. Commun.*, 2012.

[98] D. A. Links, "Electrografting : a powerful method for surface modification," *Chem Soc Rev*, vol. 40, pp. 3995–4048, 2011.

[99] T. Menanteau, E. Levillain, A. J. Downard, and T. Breton, "Electrografting via Diazonium Chemistry: The Key Role of the Aryl Substituent in the Layer Growth Mechanism," *J. Phys. Chem. C*, vol. 120, pp. 4423–4429, 2016.

[100] A. J. Hilmer *et al.*, "Role of Adsorbed Surfactant in the Reaction of Aryl Diazonium Salts with Single-Walled Carbon Nanotubes," *Langmuir*, vol. 28, pp. 13.09-1321, 2012.

[101] A. Berisha, C. Combellas, F. Kanoufi, J. Pinson, and F. I. Podvorica, "Physisorption vs grafting of aryldiazonium salts onto iron : A corrosion study," *Electrochim. Acta*, vol. 56, pp. 10762–10766, 2011.

[102] S. Bouden, N. Bellakhal, A. Chaussé, M. Dachraoui, and C. Vautrin-Ul, "Correlations between the grafting conditions and the copper detection by diazonium functionalized carbon screen-printed electrodes," *Electrochim. Acta*, vol. 125, pp. 149–155, 2014.

[103] C. Ocaña, A. Hayat, R. K. Mishra, A. Vasilescu, and J. Marty, "Label free aptasensor for Lysozyme detection : A comparison of the analytical performance of two aptamers," *Bioelectrochemistry*, vol.

105, pp. 72–77, 2015.

[104] A. Mesnage, X. Lefèvre, P. Jégou, G. Deniau, and S. Palacin, “Spontaneous grafting of diazonium salts: Chemical mechanism on metallic surfaces,” *Langmuir*, vol. 28, no. 32, pp. 11767–11778, 2012.

[105] M. Torréns, M. Ortiz, A. P. F. Turner, V. Beni, and C. K. O’Sullivan, “Amperometric detection of Francisella tularensis genomic sequence on Zn-mediated diazonium modified substrates,” *Electrochem. commun.*, vol. 53, pp. 6–10, 2015.

[106] M. Revenga-Parra *et al.*, “Simple diazonium chemistry to develop specific gene sensing platforms,” *Anal. Chim. Acta*, vol. 813, no. September 2016, pp. 41–47, 2014.

[107] F. Le Floch, J. P. Simonato, and G. Bidan, “Electrochemical signature of the grafting of diazonium salts: A probing parameter for monitoring the electro-addressed functionalization of devices,” *Electrochim. Acta*, vol. 54, no. 11, pp. 3078–3085, 2009.

[108] J. Jasmin, K. Ouhenia-ouadahi, F. Miserque, E. Dumas, C. Cannizzo, and A. Chaussé, “Straightforward grafting approach for cyclam-functionalized screen-printed electrodes for selective Cu (II) determination,” *Electrochim. Acta*, vol. 200, pp. 115–122, 2016.

[109] G. Catanante, R. K. Mishra, A. Hayat, and J. Marty, “Sensitive analytical performance of folding based biosensor using methylene blue tagged aptamers,” *Talanta*, vol. 153, pp. 138–144, 2016.

[110] J. Puy-llovera, C. Pérez-ràfols, N. Serrano, J. M. Díaz-cruz, C. Ariño, and M. Esteban, “Selenocystine modi fi ed screen-printed electrode as an alternative sensor for the voltammetric determination of metal ions,” *Talanta*, vol. 175, no. July, pp. 501–506, 2017.

[111] O. Hosu, M. Terti, G. Melinte, B. Feier, S. Robert, and C. Cristea, “Mucin 4 detection with a label-free electrochemical immunosensor,” *Electrochem. commun.*, vol. 80, no. May, pp. 39–43, 2017.

[112] W. Wang, L. Tetley, and I. F. Uchegbu, “The Level of Hydrophobic Substitution and the Molecular Weight of Amphiphilic Poly- L -lysine-Based Polymers Strongly Affects Their Assembly into Polymeric Bilayer Vesicles,” *J. Colloid Interface Sci.*, vol. 237, pp. 200–207, 2001.

[113] J. Park and M. J. Mcshane, “Dual-Function Nanofilm Coatings with Diffusion Control and Protein Resistance,” *Appl. Mater. interfaces*, vol. 2, no. 4, pp. 991–997, 2010.

[114] C. H. O. N. Ho, E. Odermatt, I. Berndt, and J. C. Tiller, “Ways of Selective Polycondensation of L -Lysine Towards Linear a - and e -Poly- L -Lysine,” *J. Polym. Sci. Part A Polym. Chem.*, vol. 46, pp. 5053–5063, 2008.

[115] Alamanda compay, *“Poly-L-Lysine and Poly-D-Lysine | Alamanda Polymers - Polyamino Acids, Superior by Design.”* 2019, pp. 1–3.

[116] J. C. M. and A. E. D. Arnold G. Fogg, Ramin Pirzad, “Improving the Performance of Screen-printed Carbon and Polished Platinum and Glassy Carbon Voltammetric Electrodes by Modification with Poly-L-lysine,” *Anal. Proc. Incl. Anal. Commun.*, vol. 32, no. June, pp. 0–3, 1995.

[117] X. Zhou, L. Wu, and J. Zhou, “Fabrication of DNA Microarrays on Nanoengineered Polymeric Ultrathin Film Prepared by Self-Assembly of Polyelectrolyte Multilayers,” *Langmuir*, no. 13, pp.

8877–8885, 2004.

[118] L. Berti, T. Woldeyesus, Y. Li, and K. S. Lam, “Maximization of Loading and Stability of ssDNA : Iron Oxide Nanoparticle Complexes Formed through Electrostatic Interaction,” *Langmuir*, vol. 26, no. 11, pp. 18293–18299, 2010.

[119] M. F. Bergamini, D. P. Santos, and M. V. B. Zanoni, “Screen-Printed Carbon Electrode Modified with Poly-,” *J. Braz. Chem. Soc.*, vol. 20, no. 1, pp. 100–106, 2009.

[120] C. Jiang, T. Yang, K. Jiao, and H. Gao, “A DNA electrochemical sensor with poly- l -lysine / single-walled carbon nanotubes films and its application for the highly sensitive EIS detection of PAT gene fragment and PCR amplification of NOS gene,” *Electrochim. Acta*, vol. 53, pp. 2917–2924, 2008.

[121] A. E. Vasdekis, C. P. O. Neil, J. A. Hubbell, and D. Psaltis, “Microfluidic Assays for DNA Manipulation Based on a Block Copolymer Immobilization Strategy,” *Biomacromolecules*, vol. 11, pp. 827–831, 2010.

[122] Y. Murakami, Y. Zhang, T. Takeuchi, T. Noda, K. Noda, and A. Kuroda, “Sensors and Actuators B : Chemical Application of an enteric coat increases the resistance to gastric juices for swallowable biosensors,” *Sensors Actuators B*, vol. 160, pp. 379–383, 2011.

[123] G. A. M. Mersal, M. Khodari, and U. Bilitewski, “Optimisation of the composition of a screen-printed acrylate polymer enzyme layer with respect to an improved selectivity and stability of enzyme electrodes,” *Biosens. Bioelectron.*, vol. 20, pp. 305–314, 2004.

[124] X. Zhou and J. Zhou, “Protein microarrays on hybrid polymeric thin films prepared by self-assembly of polyelectrolytes for multiple-protein immunoassays,” *Proteomics*, vol. 6, pp. 1415–1426, 2006.

[125] G. A. Nascimento *et al.*, “Electrochemical DNA biosensor for bovine papillomavirus detection using polymeric film on screen-printed electrode,” *Biosens. Bioelectron.*, vol. 38, pp. 61–66, 2012.

[126] M. Soon, S. Hiang, K. Peng, C. Toh, and V. T. Chow, “Impedimetric cell-based biosensor for real-time monitoring of cyto- pathic effects induced by dengue viruses,” *Biosens. Bioelectron.*, vol. 70, pp. 74–80, 2015.

[127] X. Feng, N. Gan, H. Zhang, T. Li, Y. Cao, and F. Hu, “Biosensors and Bioelectronics Ratiometric biosensor array for multiplexed detection of microRNAs based on electrochemiluminescence coupled with cyclic voltammetry,” *Biosens. Bioelectron.*, vol. 75, pp. 308–314, 2016.

[128] A. Peng *et al.*, “Electrochemical Determination of Theophylline Pharmacokinetic under the Effect of Roxithromycin in Rats by the MWNTs / Au / poly-L-lysine Modified Sensor,” *Int. J. Electrochem. Sci.*, vol. 12, pp. 330–346, 2017.

[129] A. K. Basu, A. N. Sah, A. Pradhan, and S. Bhattacharya, “Poly-L-Lysine functionalised MWCNT-rGO nanosheets based 3-d hybrid structure for femtomolar level cholesterol detection using cantilever based sensing platform,” *Sci. Rep.*, no. October 2018, pp. 1–13, 2019.

[130] E. Esmaeili, M. Soleimani, and A. Shamloo, “Dual improvement of DNA-directed antibody immobilization utilizing magnetic fi shing and a polyamine coated surface,” *RSC Adv*, vol. 6, pp. 111210–111216, 2016.

[131] J. Movilli, A. Rozzi, R. Ricciardi, R. Corradini, and J. Huskens, "Control of Probe Density at DNA Biosensor Surfaces Using Poly(," *Bioconjugate Chem.*, vol. 29, p. 4110−4118, 2018.

[132] A. Gupta, T. B. Rawal, C. J. Neal, H. A. Zeinabad, T. Cheng, and T. Lee, "Exploration of two-dimensional bio- functionalized phosphorene nanosheets (black phosphorous) for label free haptoglobin electro-immunosensing applications," *Nanotechnology*, vol. 29, p. 135101, 2018.

[133] E. B. Cooper, S. Gaudet, P. K. Sorger, and S. R. Manalis, "Electronic detection of DNA by its intrinsic molecular charge," *PNAS*, vol. 99, no. 22, 2002.

[134] J. Han, J. Wu, and J. Du, "Fluorescent DNA Biosensor for Single-Base Mismatch Detection Assisted by Cationic Comb-Type Copolymer," *Molecules*, vol. 24, pp. 574–584, 2019.

[135] J. Movilli, A. Rozzi, R. Ricciardi, R. Corradini, and J. Huskens, "Control of Probe Density at DNA Biosensor Surfaces Using Poly (L-Lysine)," *Bioconjugate Chem.*, vol. 29, p. 4110−4118, 2018.

[136] L. Shao-cong *et al.*, "Thin-core fiber-optic biosensor for DNA hybridization," *Optoelectron. Lett.*, vol. 14, no. 5, 2018.

[137] M.-J. Lin, C.-C. Wu, and K.-S. Chang, "Effect of Poly-L-Lysine Polycation on the Glucose Oxidase/Ferricyanide Composite-Based Second-Generation Blood Glucose Sensors," *Sensors*, vol. 19, p. 1448, 2019.

[138] X. Feng, N. Gan, H. Zhang, T. Li, Y. Cao, and F. Hu, "Ratiometric biosensor array for multiplexed detection of microRNAs based on electrochemiluminescence coupled with cyclic voltammetry," *Biosens. Bioelectron.*, vol. 75, pp. 308–314, 2016.

[139] X. Lu, Y. Xu, C. Zheng, G. Zhang, and Z. Su, "Ethylene glycol diglycidyl ether as a protein cross-linker : a case study for cross-linking of hemoglobin," *J Chem Technol Biotechnol*, vol. 81, no. August 2005, pp. 767–775, 2006.

[140] A. M. Debela, M. Ortiz, V. Beni, and C. K. O. Sullivan, "Surface functionalisation of carbon for low cost fabrication of highly stable electrochemical DNA sensors," *Biosens. Bioelectron.*, vol. 71, pp. 25–29, 2015.

[141] G. M. Bruce E. Babb and Dappen, "Patent Number: 4,468,467," 1984.

[142] M. M. Lounasvuori, M. Rosillo-lopez, C. G. Salzmann, D. J. Caruana, and K. B. Holt, "The influence of acidic edge groups on the electrochemical performance of graphene nanoflakes," *J. Electroanal. Chem.*, vol. 753, pp. 28–34, 2015.

[143] C. L. Manzanares-palenzuela, E. G. R. Fernandes, M. J. Lobo-castañón, and B. López-ruiz, "Impedance sensing of DNA hybridization onto nanostructured phthalocyanine-modi fi ed electrodes," *Electrochim. Acta*, vol. 221, pp. 86–95, 2016.

[144] I. Magriñá *et al.*, "Electrochemical genosensor for the direct detection of tailed PCR amplicons incorporating ferrocene labelled dATP," *Biosens. Bioelectron.*, vol. 134, no. January, pp. 76–82, 2019.

➢ List of publications:

1. **N. Ahmed**, S. AL-Madhagi, M. Ortiz, C. K. O'Sullivan, I. Katakis; *Direct electrochemical detection of enzyme labelled, isothermally amplified DNA*, analytical biochemistry (April 2020), published.

2. **N. Ahmed**, A. Fragoso, M. Ortiz, C. K. O'Sullivan, I. Katakis; Surface modification of screen-printed electrodes as functional elements of molecular diagnostics devices, sensors (2020), in preparation.

➢ List of conferences:

1) 6th early stage researchers' workshop instituto iMdea nanociencia ***(attendance)***, Madrid, Spain, 22-23 June 2016.

2) X international workshop in sensors and molecular recognition ***(poster):*** *Integrated Electrochemical Microfluidic System for Molecular Diagnostics*; **N. Ahmed** and I. Katakis, Universitat politecnica de valencia, Valencia, Spain, 7-8 July 2016.

3) XXI Tranfrontier meeting on sensors and biosensors (TMSB 2016) ***(poster):*** *Integrated Electrochemical Microfluidic System for Molecular Diagnostics*; **N. Ahmed** and I. Katakis, institute d´Estudis catalans, Barcelona, Spain, 29-30 September 2016.

4) The third diagnostics and developing world conference (DDW 2017) ***(poster):*** *Integrated Electrochemical Microfluidic System for Molecular Diagnostics in Resource Limited Environments*, S. AL-madhagi, **N. Ahmed**, O. Mayboroda, C. O'Sullivan, I. Katakis, Brunel university, London, UK, 23-25 January 2017.

5) VIII International congress on analytical nanoscience and nanotechnology (NYNA 2017) ***(poster):*** *Integrated Electrochemical Microfluidic System for Molecular Diagnostics*; **N. Ahmed** and I. Katakis, Barcelona, Spain, 3-5 July 2017.

6) XXI Transfrontier meeting on sensors and biosensors (TMSB 2017) ***(poster):*** *Integrated Electrochemical Microfluidic System for Molecular Diagnostics*; **N. Ahmed**, M. Ortiz, A. Fragoso. C. O'Sullivan, and I. Katakis, Montpellier, France, 21-22 September 2017.

7) 28th Anniversary World Congress on Biosensors **(oral presentation)**: *Integrated screen-printed electrochemical microfluidic platform for molecular diagnostics*; **N. Ahmed**, S. AL-madhagi, O. Mayboroda, M. Prodromidis, I. Katakis, C. O'Sullivan, Miami, FL, USA, 12-15 June 2018.

8) 11th Ibero american congress on sensors and XXIII Tranfrontier meeting in sensors and biosensors (TMSB 2018) ***(poster):*** *Integrated Electrochemical Microfluidic System for Molecular Diagnostics*; **N. Ahmed**, M. Ortiz, A. Fragoso, C. O'Sullivan, and I. Katakis,Barcelona, Spain, 17-21 September 2018.

9) XXIV Transfrontier meeting in sensors and biosensors (TMSB 2019) ***(oral presentation):*** *Hand-Held Molecular Diagnostic Device Based on Solid Phase Recombinase Polymerase Reaction (RPA),* **N. Ahmed**, A. Fragoso, and I. Katakis, Perpignan, France, 26-27 September 2019.

UNIVERSITAT ROVIRA I VIRGILI
A NOVEL ELECTROCHEMICAL PLATFORM BASED ON SCREEN PRINTED CARBON ELECTRODES (SPCES) FOR MOLECULAR DIAGNOSTICS
Nihad Kamal Ibrahim Ahmed

UNIVERSITAT ROVIRA I VIRGILI
A NOVEL ELECTROCHEMICAL PLATFORM BASED ON SCREEN PRINTED CARBON ELECTRODES (SPCES) FOR MOLECULAR DIAGNOSTICS
Nihad Kamal Ibrahim Ahmed

UNIVERSITAT ROVIRA I VIRGILI
A NOVEL ELECTROCHEMICAL PLATFORM BASED ON SCREEN PRINTED CARBON ELECTRODES (SPCES) FOR MOLECULAR DIAGNOSTICS
Nihad Kamal Ibrahim Ahmed


UNIVERSITAT
ROVIRA I VIRGILI